SBORNÍK IX. KONFERENCE PIGMENTY A POJIVA

KONFERENCE
PIGMENTY
A POJIVA

CONFERENCE PROCEEDINGS OF THE 9TH CONFERENCE ON PIGMENTS AND BINDERS

7.–8. listopad 2016
07–08/11/2016

Kongres hotel Jezerka, Seč, Česká republika
Congress hotel Jezerka, Seč, Czech Republic

ORGANIZÁTOR/ORGANISER:

CHEMAGAZÍN

Ústav chemie a technologie makromolekulárních látek,
Fakulta chemicko-technologická,
Univerzita Pardubice

www.pigmentyapojiva.cz

IX. KONFERENCE PIGMENTY A POJIVA
7.–8. listopad 2016 • Kongres hotel Jezerka, Seč

THE 9TH CONFERENCE ON PIGMENTS AND BINDERS
07–08/11/2016 • Congress hotel Jezerka, Seč, Czech Republic

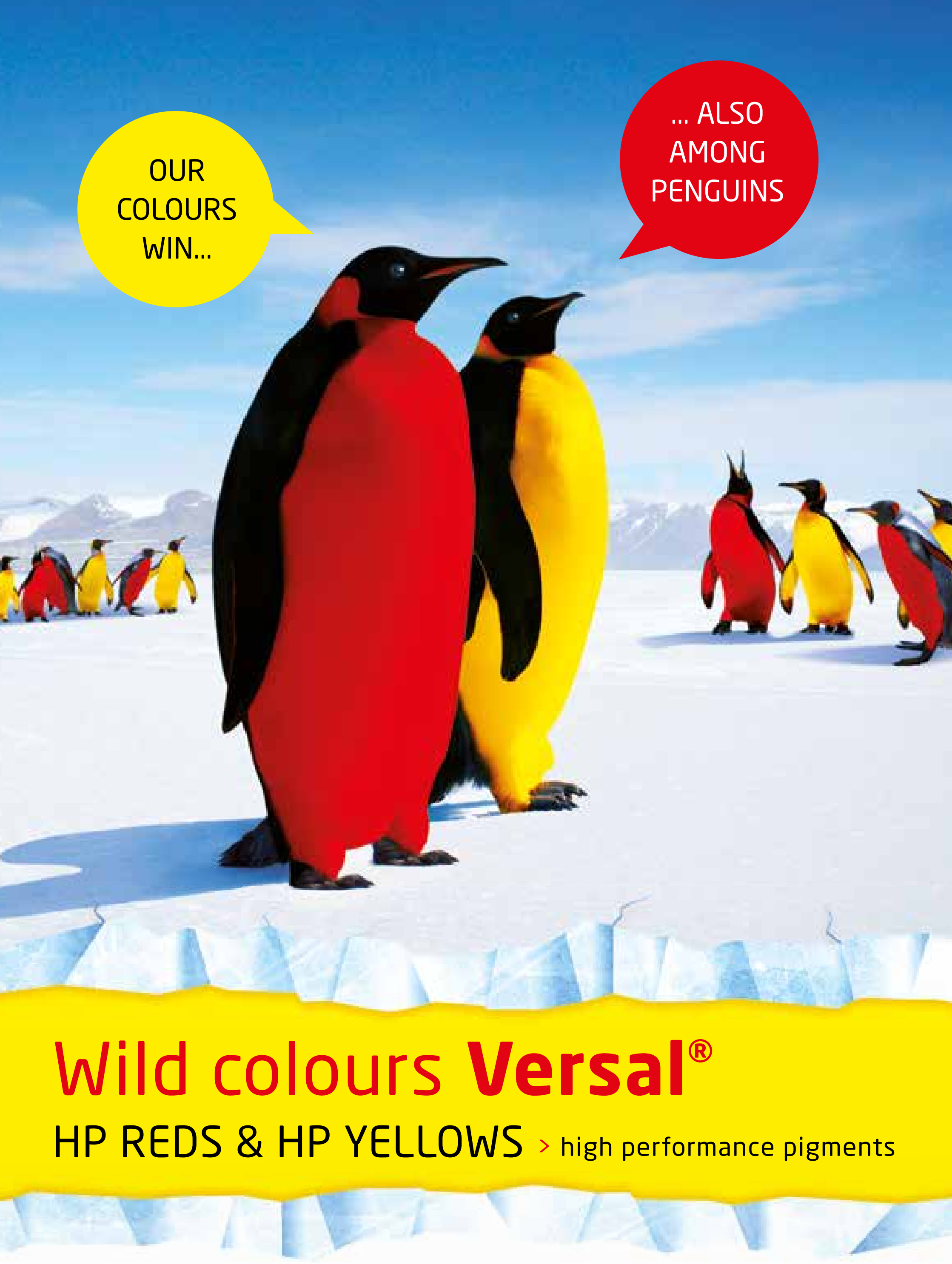
OUR COLOURS WIN...
... ALSO AMONG PENGUINS



ANAMET s.r.o. nabízí přístrojové vybavení pro laboratoře, výzkumná pracoviště i pro měření v provozu. Na český a slovenský trh dodáváme špičkové přístroje zahraničních firem (zastupujeme více než 30 firem). Pro veškerou dodávanou techniku zajišťujeme řešení na míru, záruční a pozáruční servis včetně dodávek náhradních dílů a spotřebního materiálu. V oblasti nátěrových hmot nabízíme přístroje těchto výrobců:

Konica Minolta Sensing vyrábí špičkové optické přístroje pro objektivní hodnocení barevnosti materiálů, kontrolu kvality displejů a světelných podmínek. Mezi nejprodávanější přístroje patří ruční spektrofotometry a tzv. displejmetry.

Dataphysics vyrábí přístroje na měření kontaktního úhlu, povrchového napětí a dalších parametrů spojených s jevy na površích či rozhraních látek všech skupenství.

Malvern Instruments vyrábí přístroje pro kontrolu materiálových vlastností jako je velikost částic, tvar částic, zeta potenciál, molekulová hmotnost polymerů či reologické vlastnosti.

LUM GmbH vyrábí analyzátory pro standardní i urychlené testování stability suspenzí a emulzí, dále umožňují stanovení distribuce velikosti částic. **Nový LUMiReader X-ray** využívá rentgenové záření pro sledování stability i velmi či velmi málo koncentrovaných disperzí – jako například barev a sedimentů pigmentů.

Bližší informace o produktech těchto firem vám sdělíme na našem stánku či je naleznete na webu www.anamet.cz.

Sborník/Conference proceedings

IX. KONFERENCE PIGMENTY A POJIVA
THE 9TH PIGMENTS AND BINDERS CONFERENCE

Vydavatel/Editor:
CHEMAGAZÍN s.r.o.

Organizátor/Organiser:
CHEMAGAZÍN s.r.o.,
Univerzita Pardubice, Fakulta chemicko-technologická,
Ústav chemie a technologie makromolekulárních látek

Kontakt/Contact:
CHEMAGAZÍN s.r.o.
Gorkého 2573, 530 02 Pardubice
www.chemagazin.cz

Všechny příspěvky uvedené v tomto sborníku byly recenzovány Vědeckým výborem konference. / All posts listed in this conference proceedings were reviewed by the Scientific Committee of the conference.

ISBN 978-80-906269-1-1

OBSAH/CONTENT

BUDOUCNOST ORGANICKÝCH PIGMENTŮ ZE SORTIMENTU SYNTHESIE S OHLEDEM NA LEGISLATIVU EU

THE FUTURE OF ORGANIC PIGMENTS IN SYNTHESIA'S ASSORTMENT IN VIEW OF THE EU LEGISLATION

IZÁK J.

Synthesia, a.s. – SBU Pigmenty a barviva

Summary

Company Synthesia is one of the last manufacturers of organic pigments and dyes in Europe. Synthesia has long-time experience in sales on the advanced markets in Europe and the USA. Synthesia provides customers with top quality technical service and significant legislative support as well. Synthesia has already registered 140 substances and raw materials according to REACH, mostly for the segment of organic pigments. We know and fulfil all obligations arising not only from REACH, but also from other related legislative requirements, such as CLP. Synthesia intends to produce and offer a stabilized and defined portfolio of organic pigments in the highest quality according to both EU legislation and end-users' requirements in the future.

Key words

Organic pigments, REACH, ETAD, registration

Synthesia aktivně pracuje na registracích REACH už od r. 2008. V současné době máme registrováno již více než 140 látek a surovin v souladu s požadavky REACH, především organických pigmentů a polotovarů (meziproduktů) pro jejich výrobu. Celkové náklady Sy zatím dosáhly téměř 90 mil. Kč. Nové informace získané při registracích byly zahrnuty do bezpečnostních listů a komunikovány směrem k zákazníkům. V poslední třetí fázi registrací, která potrvá do roku 2018, se Synthesia zaměřuje především na registraci organických barviv, ale je také dokončována registrace téměř všech zbývajících organických pigmentů.

ETAD

ETAD je sdružení výrobců barviv a pigmentů (viz zkratka anglického názvu = Ecological and Toxicological Association of Dyes and Organic pigments Manufacturers). Členy jsou všichni významní světoví výrobci organických pigmentů a hlavní hráči na trhu (BASF, Clariant, SUN Chemical atd.). Synthesia je členem ETAD od r. 2004.

Nařízení REACH a vliv na výrobu organických pigmentů

REACH (Registration, Evaluation, Authorization and Restriction of Chemicals) je nařízení EU platné od 1.6.2007. Upravuje výrobu a použití chemických látek a jejich potenciální vliv na lidské zdraví a životní prostředí. Nařízení REACH stanovuje regulace pro dovoz látek, materiálů a výrobků do EU. Základním předpokladem většiny postupů podle nařízení REACH je jednoznačná identifikace látky.

V rámci REACH Synthesia využila možnost předběžné registrace a do 1.12.2008 předregistrovala u Evropské chemické agentury (ECHA) všechny vyráběné organické pigmenty a polotovary v množství 1 t/rok a větším. Získala tak čas na přípravu kompletní dokumentace vyžadované pro registraci. Konkrétní termín řádné registrace záleží na vyráběném množství látky a na jejích očekávaných nebezpečných vlastnostech (viz tabulka č. 1).

Tab. 1. – Lhůty registrace pro předběžně registrované látky

Lhůta registrace	Specifikace látky
Nejpozději do 30.11.2010	Látky karcinogenní, mutagenní nebo toxické pro reprodukci, kategorie 1 nebo 2, v množství 1 t/rok a větším
	Látky vysoce toxické pro vodní organizmy s možností vyvolání dlouhodobých nepříznivých účinků ve vodním prostředí, v množství 100 t/rok a větším
	Ostatní látky v množství 1000 t/rok a větším
Nejpozději do 31.5.2013	Látky v množství 100 t/rok a větším
Nejpozději do 31.5.2018	Látky v množství 1 t/rok a větším

Díky dlouhodobé společné přípravě na REACH mohli členové ETAD založit už v první fázi sedm konsorcií a v druhé fázi pak dalších více než 10 konsorcií pro většinu organických pigmentů na trhu. Při zvažování variant postupu registrace Synthesia vybrala jako optimální strategii kombinaci vstupu do konsorcií a nákup dossierů od hlavního registranta. Výhodou vstupu do konsorcií je významná úspora nákladů, získání aktuálních informací a uplatnění vlastních testů. Nevýhodou je nutnost plateb ještě před termínem povinné registrace.

Tab. 2. – Členství Synthesie v konsorciích

Konsorcium	Pro látky	Hlavní registrant
P.Y. 74	PY 74	Clariant
Acetolone	PY 151, PY 154, PY 181, PO 36	Clariant
Monoazo Yellow	PY 1, PY 3, PY 111	Clariant
Monoazo Red	PR 4	SUN Chemical
Naphthol AS	PR 2, PR 170, PR 188	Clariant
Naphtholone	PR 176	Clariant
Metal Lakes I	PR 48:3, PR 57:1, PR 57:Sr	BASF
Metal Lakes II	PY 62, PY 168 / * PY 61	BASF / * Synthesia
Disazo Yellow	PY 93, PY 95, PY 128, PY 155 / * PY 94	BASF / * Synthesia
Disazo Red	PR 144, PR 166, PR 214, PR 242	BASF

U vybraných pigmentů PY 139, PY150, PY 183, PR 177, PB 15:1 a PG 7 je Synthesia účastníkem příslušných SIEF (Substance information exchange forums) a data byla nakoupena od hlavních registrantů. Synthesia je hlavním registrantem pro disazokondenzační žluť PY 94, monoazo lak PY 61 a možná bude pro monoazo žluť PY 4. Pro pigmenty PY 191, PY 192, PR 254 a PR 255, uváděné jako ELINCS látky, podala Synthesia samostatnou registraci s potřebnými testy. ELINCS látky (= European List of Notified Chemical Substances) jsou „nové“ látky, u kterých je po překročení výroby v množství nad 1 t/rok nutná okamžitá registrace.

Synthesia v prvních 2 fázích procesu registrace REACH do r. 2015 registrovala 29 pigmentů. U dalších 12 pigmentů probíhá proces registrace, který by měl být ukončen ještě v r. 2016. Vynaložené náklady na registraci pigmentů z palety Versal budou k 31.12.2016 činit více než 40 mil. Kč. V letech 2017–2018 počítáme s registrací dalších minimálně 15 pigmentů s náklady více než 12 mil. Kč. K 31.5.2018 budeme mít registrovány všechny pigmenty ze sortimentu Synthesie s produkcí nad 1 t/rok s výjimkou Versalového borda F2R (PR 12). Předpokládané celkové náklady na registraci organických pigmentů pro Synthesii přesáhnou 50 milionů Kč.

VÚOS, a.s.

Synthesia je schopna zajistit pro sebe, ale i pro další potenciální zájemce, dostatečnou kapacitu pro testování chemických látek, neboť je 100% vlastníkem společnosti VUOS, a.s., akreditované instituce na poli výzkumu a vývoje. CETA – Centrum pro ekologii, toxikologii a analytiku, součást VÚOS – má oprávnění pro ekologické, toxikologické a analytické zkoušení chemických látek. Tento útvar provádí prakticky všechny potřebné experimentální práce spojené s registrací REACH a v dalších oblastech (expertní, administrativa) spolupracuje.

SVHC látky a proces autorizace podle nařízení REACH

Látky vzbuzující velké obavy, tzv. SVHC látky (Substances of Very High Concern) jsou identifikovány v souladu s kritérii nařízení REACH (článek 57). Jedná se o látky:

- CMR (látky karcinogenní, mutagenní nebo toxické pro reprodukci) – látky, které splňují kritéria pro klasifikaci kategorie 1 a 2 podle Směrnice 67/548/EHS,
- PBT (látky persistentní, bioakumulativní a toxické) nebo vPvB (látky velmi persistentní velmi bioakumulativní) – látky, které splňují kritéria uvedená v příloze XIII Nařízení REACH.

Cílem procesu autorizace je SVHC látky postupně nahradit vhodnými alternativními látkami nebo technologiemi, a to v případě, že toto nahrazení je z hlediska finančního a technického možné.

Identifikace látky jako SVHC a její zařazení na kandidátský seznam látek (příloha č. XIV nařízení REACH) je prvním krokem procesu autorizace. Na aktuálním kandidátském seznamu dostupném na webových stránkách ECHA je uvedeno 168 látek. Limit obsahu SVHC látky v konečném výrobku je 1000 ppm (0,1 %). Žádný z našich organických pigmentů nespadá do kategorie SVHC látek a obsah nečistot u všech pigmentů splňuje stanovený limit.

Bezpečnostní list (BL)

Synthesia revidovala a aktualizovala bezpečnostní listy = Safety Data Sheets (SDS) pro všechny výrobky v souladu s Nařízením EU č. 830/2015. Přestože je Synthesia povinna zasílat BL pouze k nebezpečnému zboží, poskytuje zákazníkům BL ke každé dodávce, příp. na vyžádání.

CLP

Nařízení Evropského parlamentu a rady (ES) č. 1272/2008 definuje způsoby klasifikace, balení a označování látek a směsí. Nařízení CLP (Classification, Labelling and Packaging) vstoupilo v platnost v lednu 2009 a způsob klasifikace a označování chemických látek, který zavedlo, vychází z globálně harmonizovaného systému Organizace spojených národů (GHS). Nařízení CLP zajišťuje, aby nebezpečnost chemických látek byla sdělována pomocí standardních H a P vět a výstražných symbolů na štítcích a v bezpečnostních listech.

Všechny pigmenty ze sortimentu Synthesie jsou směsi. Synthesia plní všechny požadavky podle tohoto nařízení.

Závěr

Synthesia jako jeden z posledních výrobců organických pigmentů v Evropě hodlá nadále vyrábět a nabízet stabilizované a definované portfólio organických pigmentů v nejvyšší kvalitě tak, aby plnila jak požadavky legislativy EU, tak i požadavky svých zákazníků.

NÁVRH NA HARMONIZOVANOU KLASIFIKACI TIO$_2$ VE SVĚTLE REÁLNÝCH RIZIK

TIO$_2$ HARMONIZED CLASSIFICATION (CLH) PROPOSAL IN THE LIGHT OF REAL RISKS

PIKAL P., MIKULÍK P.

Precheza a.s. Přerov

Summary

Our paper deals with situation arisen from proposal to ECHA to classify TiO$_2$ as carcinogenic material. We describe probable sequence of further steps, what could be the results of whole process and what impact of each result would be on producers and consumers. We tried to consider, what are main sources and bases for such proposal and novelty of these sources.

Key words

TiO$_2$, carcinogenicity, EU legislation process

Úvod

Mezi všemi pigmenty má bílý pigment zvláštní postavení, neabsorbuje viditelné světlo a jeho optický účinek je tak dán výhradně rozptylem světla na částicích pigmentu. V historii se jako bílý pigment používalo několik látek – křída (uhličitan vápenatý), olovnatá běloba (2 $PbCO_3 \cdot Pb(OH)_2$), zinková běloba (ZnO), síran barnatý samotný nebo ve směsi se sirníkem zinečnatým a titanová běloba (TiO$_2$). Vzhledem ke svým vlastnostem (stabilitě, inertnosti, netoxicitě, vysoké barvivosti) je v současné době titanová běloba nejpoužívanějším bílým pigmentem

Objev výroby TiO$_2$ zanedlouho oslaví stoleté výročí. Vznikl při zpracování ilmenitové rudy, kdy TiO$_2$ byl chápán jako vedlejší produkt při získávání železa. Záhy se zjistilo, že TiO$_2$ může sloužit jako bílý pigment a po vyloučení olovnaté běloby kvůli toxicitě olova se TiO$_2$ stal základním bílým pigmentem se současným objemem produkce blízko 6 mil. tun ročně. TiO$_2$ pigment má vynikající koloristické vlastnosti zejména z důvodu vysokého indexu lomu (nejvyššího mezi komerčními bílými pigmenty). Po úvodním objevu sulfátové výroby, produkující převážně anatas, následoval objev chloridové technologie, která umožňuje pouze produkci rutilu, a objev možnosti vyrábět rutil i sulfátovou technologií.

Optické vlastnosti pigmentu jsou dány fyzikou interakce elektromagnetického záření s hmotou. Jelikož absorpce viditelného světla je v případě bílého pigmentu minimální o optických vlastnostech rozhoduje rozptyl a z teorie plyne, že pro látku s určitým indexem lomu existuje velikost částic poskytující maximální rozptyl. Této velikosti se všichni výrobci snaží přiblížit a pro TiO$_2$ činí přibližně 150–200 nm. Zde je nutné podotknout, že se jedná o rozměr určený z četnostního rozdělení (měření elektronovým mikroskopem). Pigment tak v žádném případě nespadá do kategorie nanomateriálů tak jak zní jejich doporučená definice (2011/696/EU).

Samozřejmě v procesu výroby nelze přesně kontrolovat velikost částic a tak je určitý podíl částic vždy nižší než 100 nm. Jedná se zhruba o 10–40 % počtu částic avšak z hlediska hmotnosti jde přibližně o jedno až dvě procenta. Přesto je možné konstatovat, že během 100 let výroby bylo nezáměrně vyprodukováno (a použito) okolo 2–5 mil tun TiO$_2$ s velikostí částic pod 100 nm. S hledáním dalších aplikačních možností (zejména pro katalyzátory a použití v kosmetice jako UV absorbéry) byly vyvinuty materiály záměrně vyráběné s vysokým měrným povrchem (až 300 m^2/g) a s primárními částicemi pod 100nm, ale jejich výroba je stále v úrovni okolo 1 % celkové produkce TiO$_2$. Z uvedených údajů plyne, že v případě TiO$_2$ se v žádném případě nejedná o nějaký nový materiál vzniklý v poslední době a že při všech studiích případné toxicity byly s pigmentovým materiálem testovány i částice pod 100 nm.

Komentář k návrhu klasifikace

Návrh klasifikace CLH byl podán na ECHA v květnu tohoto roku ze strany ANSES (francouzská vládní agentura pro bezpečnost potravin, životního a pracovního prostředí) a ačkoliv rozebírá řadu, dle názoru předkladatelů, možných negativních efektů TiO$_2$, navržená klasifikace se týká pouze inhalace částic, neboť jiný způsob podání nevedl k výsledkům, opravňujícím jakoukoliv klasifikaci. Návrh se také neopírá o nějaká nová zjištění, ale je založen na několika studiích provedených mezi lety 1985–2010 [2,3,4,5,6]. Ačkoliv autoři návrhu zmiňují i další studie, ve kterých nebyly nalezeny negativní efekty [například 7,8,9], jejich výsledky jsou zpochybněny, hlavně proto, že podle autorů návrhu nebylo použito dostatečné koncentrace TiO_2 či dostatečné doby sledování. Stejně tak autoři návrhu sice zmiňují epidemiologické studie [10,11,12], ale mají námitky k metodologii studií i k tomu že ve studiích nebyly údaje o velikosti částic.

Do 15. července 2016 bylo možné podat připomínky k tomuto návrhu. Komentář podalo i sdružení výrobců titanové běloby TDMA a navrhuje ponechat TiO_2 bez klasifikace; celkem bylo komentářů 514. Z hlediska podpory názoru TDMA, tedy žádná klasifikace lze komentáře rozdělit takto (Ano znamená podporu návrhu TDMA):

Tab. 1

	Neutrální	**Ne**	**Ano**
Firma	5	0	339
Jednotlivec	0	1	42
MSCA*	2	7	1
Veřejné společenství/ Asociace**	3	0	114

* *Member State Competent Authority – Obvykle organizace na úrovni Státního zdravotního ústavu*
** *Sdružení výrobců nebo profesní organizace (SCHP)*

Kromě zástupců některých členských států (MSCA) většina připomínek podporuje pozici TDMA, tedy ponechat TiO_2 bez klasifikace. Zjevně je tedy značný rozdíl mezi posouzením relevance návrhu u MSCA a zbytkem respondentů. Dokonce i individuální připomínky všechny až na jedinou podporují pozici TDMA. Většina připomínek podporujících stanovisko TDMA se týká odborných toxikologických záležitostí, případně je v připomínkách zmíněno, že za dobu používání nedošlo k žádným negativním zdravotním komplikacím.

Co se týče vyjádření TDMA, tak základní námitky jsou:

- Epidemiologické studie (~ 24000 pracovníků) neprokázaly vztah mezi exposicí TiO_2 a výskytem tumorů, přičemž v návrhu chybí nejnovější studie .
- Návrh se opírá o vznik tumorů pouze u krys (nikoliv u dalších laboratorních zvířat) při vysokém zahlcení plic nebo při přímé aplikaci aerosolu do dýchacích cest což není fyziologická cesta, která by se mohla vztáhnout na lidi.
- U krys řada studií prokázala, že reagují na zatížení nerozpustnými částicemi jinak (silněji) než jiná laboratorní zvířata, případně primáti nebo lidé.
- Nesouhlasí s tvrzením v návrhu ANSES, že klasifikace TiO_2 pro mutagenicitu je neurčitá (inconclusive). Řada studií, včetně projektu NanoGenotox poskytla negativní výsledky genotoxicity. Genotoxické studie nebyly posuzovány dle jejich relevance a spolehlivosti (ECHA pravidla).

Lze najít ale i připomínky jiného charakteru, například že zvířata byla držena na dietě 7500 mg/kg živé váhy/den což by pro 80 kg člověka znamenalo sníst každý den asi 600 g TiO_2. Současně i některé zmíněné inhalační studie, které vedly k znatelným efektům [3] byly prováděny za značně nestandardních podmínek s koncentrací prachu až 250 mg/m^3. Taková koncentrace prachu vede k extrémnímu snížení viditelnosti na hodnoty okolo 6 m, kdy na tuto vzdálenost již nelze rozeznat černý objekt na bílém pozadí [14]. Taková koncentrace je možná v případě havárií, je ale naprostým nesmyslem uvažovat s možností chronického působení. Obecně evoluce vyvinula překážky bránící částicím vstupu do plic, a pokud se tam již nějaké dostanou, existují mechanismy na jejich opětné odstranění z organismu. Pokud jsou tyto mechanismy přetíženy, může docházet k negativním efektům, ale při dodržení stávajících limitů (10 mg/m^3) nemůže být o přetížení řeč.

Další postup v řešení návrhu a možné varianty

Další postup je dán pravidly ECHA a EU. Risk Assessment Committee (RAC) má celkem 18 měsíců na vypracování posudku a doporučení (pokud nebude návrh stažen). Po vypracování posudku je návrh předán Evropské komisi, která má další čas (obvykle 3–9 měsíců) na zpracování posudku a pak následuje zařazení CLH návrhu do nařízení CLP, přílohy VI s požadavky na implementaci.

V rámci tohoto procesu jsou prakticky možné všechny varianty od klasifikace 1B až po žádnou klasifikaci. Akceptace návrhu a zařazení TiO_2 mezi karcinogeny 1B by znamenalo řadu problémů, které by mohly vést až k vytlačení průmyslu vyrábějícího a zpracovávajícího TiO_2 z Evropy. Konkrétní vlivy při klasifikaci 1B jsou přehledně uvedeny v následující tabulce č. 2.

Tab. 2

Aplikace	Legislativa	Vliv
Všechny	CLP Regulace (1272/2008/EC)	Značení TiO_2 a případných výrobků obsahujících TiO_2 v nadlimitní koncentraci (0,1 % u klasifikace 1B a 1 % u klasifikace 2)*
Všechny	Direktiva Carcinogens and Mutagens at Work (2004/37/EC)	Nahrazení TiO_2 při užití, pokud nelze je třeba zajistit výrobu v uzavřených systémech, pokud ani to nelze, je třeba snížit exposici
Všechny	Direktiva Waste Framework (2008/98/EC, 1357/2014, 2000/532/EC)	Odpad obsahující více než 0,1 % TiO_2 bude charakterizován jako nebezpečný (v případě klasifikace 2 se koncentrace zvyšuje na 1 %), a nebude tak možné ho recyklovat
Všechny	REACH (1907/2006/EC)	Zákaz přímého prodeje veřejnosti substancí klasifikovaných jako 1A a 1B a směsí obsahujících tyto látky v koncentracích nad specifikovaný limit
** U značení výrobků pak nezáleží na tom v jaké oblasti (inhalační, dermální, orální) byl přítomný karcinogenní materiál klasifikován*		

Samozřejmě v oblastech jako je kosmetika, potraviny, farmacie a další vyvstanou specifické problémy, jelikož případná klasifikace může vyústit v zákaz jejího používání. Všichni výrobci TiO_2 včetně Prechezy využijí následující období k jednání s kompetentními autoritami, aby podpořili naše stanovisko, tedy žádná klasifikace. Pokud přesto dojde ke klasifikaci 1B a následně k zařazení TiO_2 do přílohy VI nařízení CLP a přílohy XIV nařízení REACH přinese to velmi negativní dopady jak na výrobce tak na spotřebitele.

Závěr

Ačkoliv nedošlo k žádným novým zjištěním ohledně toxicity TiO_2 nebo jeho negativních vlivů na zdraví nebo životní prostředí, byl vyvolán proces vedoucí k možnému zařazení TiO_2 mezi 169 substancí označovaných jako SVHC, mezi karcinogeny do společnosti trichloropropanu, sloučenin kademnatých, chromanů a dalších látek. Stírá se tak rozdíl mezi látkami, které jsou skutečně a prokazatelně toxické a ostatními látkami. V návrhu nejsou uvedena žádná nová zjištění a opírá se o několik málo studií na zvířatech, které byly positivní pouze v případě velmi vysokého přetížení organismu a to pouze u krys. Další vývoj i konečný výsledek bude záviset na rozhodnutí kompetentních orgánů Evropské unie. V rámci tohoto procesu se vynasnažíme poskytnout všem nezkreslené, vědecky podložené informace.

Literatura

[1] Mie, G. (1908), „Beiträge zur Optik trüber Medien, speziell kolloidaler Metallösungen“. *Annalen der Physik*. 330 (3): 377–445.

[2] Heinrich U., Fuhst R., Rittinghausen S., Creutzenberg O., Bellmann B., Koch W., Levsen K., Chronic inhalation exposure of Wistar rats and two different strains of mice to diesel engine exhaust, carbon black, and titanium dioxide. *Inhalation Toxicology*. 1995; 7(4):533–56.

[3] Lee K.P, Trochimowicz H.J, Reinhardt C.F., Pulmonary response of rats exposed to titanium dioxide (TiO_2) by inhalation for two years. *Toxicology and applied pharmacology*. 1985 Jun 30; 79(2): 179–92.

[4] Pott F., Roller M., Carcinogenicity study with nineteen granular dusts in rats. *Eur J Oncol*. 2005; 10(4):249–81.

[5] Roller M., Carcinogenicity of inhaled nanoparticles. *Inhalation Toxicology.* 2009; 21(S1): 144–57.

[6] Xu J., Futakuchi M., Iigo M., Fukamachi K., Alexander D.B., Shimizu H., Sakai Y., Tamano S., Furukawa F., Uchino T., Tokunaga H., Nishimura T., Hirose A., Kanno J., Tsuda H., Involvement of macrophage inflammatory protein 1alpha (MIP1alpha) in promotion of rat lung and mammary carcinogenic activity of nanoscale titanium dioxide particles administered by intra-pulmonary spraying. *Carcinogenesis.* 2010 May; 31(5):927–35.

[7] Muhle H., Bellmann B., Creutzenberg O., Dasenbrock C., Ernst H., Kilpper R., MacKenzie J.C., Morrow P, Mohr U, Takenaka S, Mermelstein R. Pulmonary response to toner upon chronic inhalation exposure in rats. *Fundamental and applied toxicology.* 1991 Aug; 17(2): 280–299.

[8] Thyssen J., Kimmerle G., Inhalation studies with polyurethane foam dust in relation to respirátory tract carcinogenesis. *J Environ Pathol Toxicol.* 1978 Mar–Apr; 1(4):501–8.

[9] Yokohira M., Hashimoto N., Yamakawa K., Suzuki S., Saoo K., Kuno T., Imaida K., Lung Carcinogenic Bioassay of CuO and TiO(2) Nanoparticles with Intratracheal Instillation Using F344 Male Rats. *J Toxicol Pathol.* 2009 Mar; 22(1):71–8.

[10] Fryzek J.P., Chadda B., Marano D., White K., Schweitzer S., McLaughlin J.K., Blot W.J., A cohort mortality study among titanium dioxide manufacturing workers in the United States. *J Occup Environ Med.* 2003 Apr; 45(4):400–9.

[11] Boffetta P., Gaborieau V., Nadon L., Parent M.F., Weiderpass E., Siemiatycki J., Exposure to titanium dioxide and risk of lung cancer in a population-based study from Montreal. *Scand J Work Environ Health.* 2001 Aug; 27(4):227–32.

[12] Boffetta P., Soutar A., Cherrie J.W., Granath F., Andersen A., Anttila A., Blettner M., Gaborieau V., Klug S.J., Langard S., Luce D., Merletti F., Miller B., Mirabelli D., Pukkala E., Adami H.O., Weiderpass E., Mortality among workers employed in the titanium dioxide production industry in Europe. *Cancer Causes Control.* 2004 Sep; 15(7):697–706.

[13] Ellis, E.D. et al. (2010), Mortality among titanium dioxide workers at three DuPont plants, *J Occup Environ Med.* 52(3), 303–9

[14] William C. Hinds, *Aerosol Technology: Properties, Behavior, and Measurement of Airborne Particles*, 2nd Edition February 1999, ISBN: 978-0-471-19410-1

KLASIFIKACE SMĚSÍ DLE CLP Z POHLEDU AKUTNÍ TOXICITY

CLASSIFICATION OF MIXTURES IN TERMS OF ACUTE TOXICITY ACCORDING TO CLP

BUREŠOVÁ B.

SBLCore s.r.o.

Summary

Classification of mixtures in terms of acute toxicity according to CLP operates on an entirely different principle than the established classification according to DPD. Not only does CLP evaluate on percentage of substances in mixtures that are dangerous to human health, but also estimates acute toxicity of the substances in the mixture. Acute toxicity values are expressed as (approximate) LD50 (oral, dermal) or LC50 (inhalation) values or as acute toxicity estimates (ATE).

Key words

CLP, DPD, classification, substance, mixture, acute toxicity

FOTOKATALYTICKÉ SNIŽOVÁNÍ IMISÍ NO_X POMOCÍ FUNKČNÍHO NÁTĚRU S PORÉZNÍ STRUKTUROU

THE PHOTOCATALYTIC ABATEMENT OF NOX IMISSIONS USING COMMERCIAL FUNCTIONAL COATING WITH POROUS MORPHOLOGY

ZOUZELKA R.

J. Heyrovsky Institute of Physical Chemistry, v.i.i., Academy of Sciences of the Czech Republic,
Dolejskova 3, 18223 Prague 8, Czech Republic

Summary

Titanium dioxide is the most important photocatalysts used for purifying applications. It was the purpose of this study to investigate the photocatalytic activity of commercial Protectam FN® containing TiO_2 nanoparticles towards NO and NO_2. Experiments on concrete as a support for photocatalyst were carried out in two types of reactors with laminar and turbulent flow under "real world setting" conditions of temperature, relative humidity, irradiation and pollutant concentrations. The results showed that photocatalytic process significantly reduced both nitrogen oxides in the air. The decrease in the total concentration of nitrogen oxides on contact with the photocatalytic surface reached 20–50 %, i.e. at a concentration of 100 ppb the decrease in NO and NO_2 was 20–50 ppb. The nitrogen oxides were oxidized up to their highest oxidation state, nitric acid (or nitrates) and undesirable nitrous acid was not formed at all. The experimental study conducted showed that the photocatalytic oxidation on the surface of the photocatalytic Protectam FN® coating is an effective method for the removal of nitrogen oxides from contaminated air.

Key words

TiO_2, NO_x, imissions, photocatalysis, air purification

Introduction

Dangerous nitrogen oxides (NO_x) are among the most closely studied of emissions for their toxicity to human health. The major source of NO_x in Europe is the road transport emitting around 40 %, comprising a mixture of NO and NO_2 (Guerreiro et al., 2015). This implies that it is necessary to substantially reduce nitrogen oxides concentration.

This decrease of NO_x can be achieved using photocatalysis, on a photocatalytically active surface. When using the photocatalytic process, NO is gradually oxidized to nitric acid, which is eventually neutralized in the presence of alkali metal ions or alkali soil into various nitrates, depending on the substrate nature.

Although s number of studies into the the photocatalytic abatement of NO_x under laboratory under laboratory conditions have been published [1–3], there is a lack of studies under real outdoor conditions. For instance, in Antwerp an area of ten thousand square meters was covered with photocatalytic pavement blocks and the NO_x efficiency was monitored. Although the reduction of NO_x emissions was observed both in laboratory and outdoor measurements, it was difficult to draw sound conclusions because of a too short period of measurement [4]. In similar research in Bergamo, Italy, a section of a local street was covered with photocatalytic paving stones, while another untreated section was used as a reference. The NO_x concentration was monitored for two weeks. Compared to the reference section a reduction in NO_x concentration of 30–40 % was achieved [5].

Considering their various environmental applications, the main advantage of photocatalytic TiO_2-based coating is their applicability to the different construction materials used in buildings, street pavements, tunnels, etc. However, because of the difficult operating conditions, the long-term photocatalytic performance and mechanical durability of photocatalytic coatings is of the utmost importance. Despite this, there is a conspicuous lack of data regarding the performance of photocatalytic coatings over several years.

In this study, we compare the photocatalytic performance in the reduction of NO_x concentrations in the air of two commercial TiO_2-based products, Degussa P25 (industry standard) and Protectam FN®2 (FN2), both of which were coated on common construction materials. Photocatalytic activity was assessed according to ISO standard 22197-1:2007 and proposed by of the European Committee for Standardization (CEN). To obtain reliable data concerning the effect of weathering, the photocatalytic performance of two-years-aged samples taken from a sound barrier located at one of the busiest thoroughfare in Prague was evaluated against that of fresh samples.

Materials and methods

Deposition and characterization of photocatalytic P25 and FN2 coatings

The commercial coatings Protectam FN2 and Degussa P25 (water suspension) were applied on common construction materials (façade coating on plaster and concrete blocks, each 50 × 100 mm in size) by spraying, creating almost transparent film 5 to 10 micrometers thick, with a slightly whitish undertone. P25 was used as an industry standard.

The crystallinity of the films was characterized using a high-resolution X-ray diffractometer Siemens D5000 operated at 40 kV and 45 mA with Cu Kα radiation ($\lambda = 1.5406$ Å). The texture properties of the films were determined by the analysis of adsorption isotherms of Kr at 77 K measured with a Micrometrics ASAP 2010 volumetric adsorption unit. The optical properties of the coatings were obtained by Perkin-Elmer Lambda 19 equipped with an integration sphere (diffuse reflectance spectra), and by FT-IR Nicolet 6700 spectrophotometer (infrared transmission spectra). The surface morphology of the films was carried out by scanning electron microscope (SEM) using a Joel JSM-6700F and also examined by transmission electron microscopy (TEM) using a Joel JEM-2100 UHR microscope.

Photocatalytic test

The photocatalytic test itself was performed according to the following scheme. First the sample to be tested was cleaned by UV irradiation (2 mW/cm^2) for at least 5 h to decompose residual organic matter. The experiments were conducted simultaneously in two reactors – in a reactor with laminar and turbulent flow, where a high degree of turbulence was modelled. In both reactors the sample photocatalytic surface was 50 cm^2, the volume of air flow was 3 L/min. Instead of short-term experiments of in 3–5 hours in accordance with the usual standards, the experiments in the study were prolonged to 24 hours. During the photocatalytic experiment samples were irradiated with three black light fluorescence lamps (Philips BLB 15W) emitting dominantly at the wavelength of 365 nm. The distance between the lamps and the film was adjusted to achieve irradiation intensity of exactly 1.0 mW/cm^2.

Before the photocatalytic experiments, NO or NO_2 were always absorbed onto the surface of the photocatalyst so as to achieve balance (i.e. to prevent the loss of nitrogen oxides due to adsorption during the measurement of activity). Thus the removal of nitrogen oxides in this study was due solely to photocatalysis, not to physical adsorption onto the surface. The input NO concentration was 1.0 ppmv corresponds to 1226 µg/m^3. The study was also focused on the lower concentration of 0.1 ppmv (122,6 µg/m^3) that is commonly found in polluted air in certain locations. The input NO_2 concentration was 0.1 ppmv, which corresponds to 188 µg/m^3. The reason for choosing such a significantly higher concentration is the critical dispersion conditions that may occur.

Photocatalytic efficiency of FN2 samples exposed to real condition of polluted area in Prague

We performed certain measurements of photocatalytic effectiveness of 2-years-aged samples according to modified ISO norms and proposed norms of the European Committee for Standardization (CEN). The test wall was placed in the proximity of a high-traffic road (in Barrandov) along which about 30,000 cars pass every day. In this area the NO_x concentration is increased and often exceed the allowed daily NO_2 limit of 40 µg/m^3.

Samples of the surface of anti-noise barriers, which had served for two years as test surfaces for the FN2 coating, were taken for laboratory measurements of their effectiveness in cleaning the air of exhaust gas emissions from automobile traffic.

Results and discussion

Photocatalytic performance of FN2 coatings

The experimental study whose results showed that when we used photocatalysis it was possible to significantly reduce both nitrogen oxides in the air. The decrease in the total concentration of nitrogen oxides on contact with the photocatalytic surface (i.e. the decrease of the total NO and NO_2 concentration) is expressed by a deNO_x coefficient.

Photocatalysis at NO concentration of 0.1 ppm that corresponded to the real pollutant situation in the field, taking into account the critical situation, was an independent concentration process. That means that when contaminated air came into contact with the photocatalytically active surface, the same percentage decrease in nitrogen oxides concentration occurred as in the field. The conversion factor averaged 50 %. Because the deNO_x coefficient reached from 0.02 to 0.05 ppm depending on the substrate (plaster or concrete), at the initial NO concentration of 0.1 ppm the photocatalytic process removed 20–50 % of nitrogen oxides from the air. Measurements of the photocatalytic coatings applied on various substrates showed that the impact of the substrates commonly used in construction on the photocatalytic surface was significant. The chemical nature of the substrate influenced the measure as much and the deNO$_x$ coefficient for concrete was higher than for plaster.

Experiments with nitrogen oxides (NO$_2$) showed that it was possible to achieve a significant decrease in their concentration using photocatalysis. The impact of the substrates was also significant. Compared to concrete, plaster removed two times more NO$_x$ than plaster, i.e. around 40% of NO$_x$ at the initial concentration of 0.1 ppm decreased onto plaster surface, compared to 22 % onto concrete.

The comparison of the products Protectam FN2 with the pure photocatalyst Aeroxide TiO$_2$ P25 showed that the Protectam product had very high efficiency. For instance, the photocatalytic efficiency of Protectam FN2 coated on plaster (NO$_2$=0.1 ppm) was about 35% higher than that of P25.

Fig. 1 – Comparison of the photocatalytic activity of a fresh FN2 coating with that of 2 years-aged one on concreted in plug flow reactor. Inlet NO concentration of 0.1 ppm at RH50%.

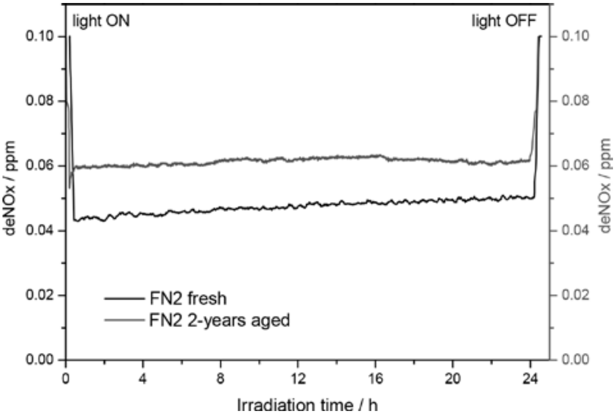

Conclusion

The results of the tests showed that even two years after they were applied to the surface of walls, FN2 photocatalytic coatings maintained exceptionally high effectivity. Tests showed that their effectiveness in removing NO$_x$ reached up to 20–40 %, i.e. at a concentration of 0.1 ppm the decrease in NO and NO$_2$ was 0.02–0.04 ppb. At concentrations of 30–40 µg/m^3 of NO$_x$ emissions where the wall is located, 300 m^2 of surface coated with FN2 coating is able to decrease NOx emissions.

References

[1] Lasek, J., Yu, Y., Wu, J.C.S., Removal of NO x by photocatalytic processes, *J. Photochem. Photobiol. C Photochem. Rev.*, 2013, 14, 29–52.

[2] Ohtani, B., Photocatalysis A to Z-What we know and what we do not know in a scientific sense, *J. Photochem. Photobiol. C Photochem. Rev.*, 2010, 11, 157–178.

[3] Sadanaga, Y., Matsumoto, J., Kajii, Y., Photochemical reactions in the urban air: Recent understandings of radical chemistry, *J. Photochem. Photobiol. C Photochem. Rev.*, 2003, 4,

85–104.

[4] Beeldens in: Symposium on Photocatalysis, Environment and Construction Materials, RILEM Publications SARL, Florence, Italy, 2007, p187–194

[5] Åkesson, B., Petters, S.M., 2013. Technical Report.

ANTIBAKTERIÁLNA MODIFIKÁCIA POLYOLEFÍNOV ÚČINKOM NÍZKOTEPLOTNEJ PLAZMY

ANTIBACTERIAL MODIFICATION OF POLYOLEFINS BY THE EFFECT OF LOW-TEMPERATURE PLASMA

NOVÁK I.[1], POPELKA A.[2], PRACHÁR J.[1], CHODÁK I.[1], ŽIGO O.[1]

1 Polymer Institute, Slovak Academy of Sciences, Slovakia
2 Center for Advanced Materials, Qatar University, P.O. Box 2713, Doha, Qatar

Summary

The surface of low-density polyethylene (LDPE) has been surface modified by low-temperature plasma, grafted by acrylic acid and subsequently were on the polymeric surface immobilized selected antibacterial compounds such as triclosan and chlorhexidine. This work has been studied the impact of selected antibacterial substances immobilized on low-density PE (LDPE) activated by low-temperature diffuse coplanar surface barrier discharge (DCSBD) plasma. The surface of LDPE modified using this multi-step method led to inhibition Escherichia coli and Staphylococcus aureus.

Key words

Antibacterial, low-temperature plasma, surface modification, low-density polyethylene

Introduction

LDPE infections causes, that this medical polymer represent main clinical complication [1–5]. Mentioned infections may cause implant failure, complex revision processes and implant removal, and all can lead to patient suffering, prolonged hospitalization and in some cases even death. Presence of hydrophobic and hydrophilic domains, charge the functional group densities, and their conformation play ascendant roles in affecting cell behaviour. Many problems trouble can be remove by surface modification of LDPE using appropriate method as well as low-temperature plasma when surface free energy is increasing due to introducing polar functional groups on treated surface and thus surface of LDPE is then more hydrophilic. Modification by plasma significantly impacts to adhesion improvement by removing surface contamination and to surface morphology changes through increased roughness due to etching. Antibacterial properties of polymers can be achieved by following: a) anti-infection agent mix in polymer; b) copolymerization anti-infection agent with monomer; c) surface treatment of medical polymer.

Experimental

Materials

LDPE BRALEN FB 2-17, Slovnaft Mol (Slovakia), containing no additives, the thickness of LDPE film was 20 µm, density = 0.918 g·cm^{-3}, mass flow rate (MFR at 190 °C, 2.16 kg) = 2 g per 10 min, Vicat softening temperature = 96 °C. This type of LDPE is suitable for food contact. The product complies with Food Contact Regulations and the grade is suitable for manufacturing of pharmaceutical packing-product. Triclosan, Irgasan, $C_{12}H_{7}Cl_{3}O_{2}$ (Fluka, Italy), chlorohexidine, imidodicarbonimidic diamide, $C_{22}H_{3}0Cl_{2}N_{10}$, Aldrich (Spain), acrylic acid (propenoic acid): $C_{3}H_{4}O_{2}$, extra pure, stabilized by 180 to 220 pm.

Plasma treatment

The LDPE foil activation was carried out by DCSBD equipment (made in Comenius University of Bratislava, Slovakia) under dynamic conditions at atmospheric pressure and laboratory temperature. The schematic representation with description of this system is given in Scheme 1. This treatment was realized at following settings: power supply = 200 W, plasma treatment time = 15 s, in air atmosphere and all samples were treated on both sides.

Antibacterials immobilization

LDPE grafted by PAA was immersed into solution of EDAC that acts as an activator of carboxyl groups, where *O-acylisourea* is produced and it has possibility to react with reducing agents. This way pre-prepared sample was then immersed into solution of triclosan and chlorhexidine (Scheme 1).

Scheme 1 – Multistep approach of biomolecule binding: 1. Plasma treatment, 2. Generation of radicals, 3. AA radical graft polymerization, and 4. Antibacterials deposition.

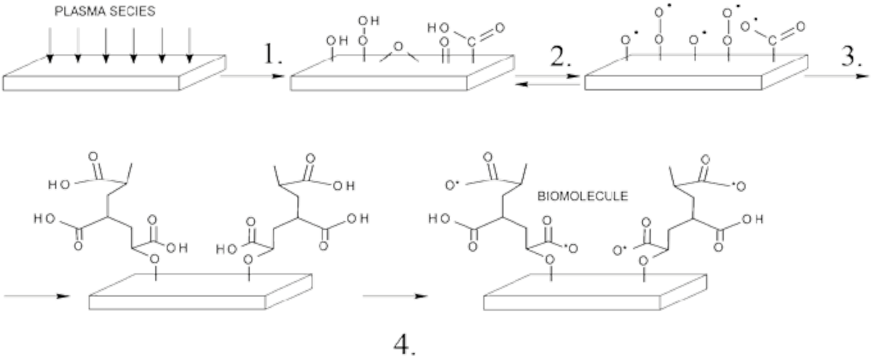

Surface wettability

The wettability of LDPE treated by multistep process via PAA plasma grafted and Antibacterials immobilization were carried out by the measurement of contact angle using sessile drop technique via Surface Energy Evaluation system (SEE system with CCD camera, Advex Instruments, Czech Republic). As testing liquids were used deionized water, ethylene glycol, glycerol, formamide, diiodomethane with volume equals 5 µl (elimination of influence of gravity) and a static contact angle was captured shortly after its creation when a thermodynamic equilibrium is reached between the three phases: solid, liquid, and gas. Surface energy (γ^{tot}), its polar acid-base (γ^{AB}), dispersive (γ^{LW}), electron-acceptor (γ^{-}) and electron-donor (γ^{+}) components were calculated by Acid-Base regression model using method of least squares.

Antibacterial tests

Bacterial adhesion and biofilm experiments were performed in vitro using gram-positive (*S. aureus* 3953) and gram-negative (*E. coli* 3954) bacteria. The circular shape specimens (d ≈ 8 mm) were cut from the pristine and modified LDPE samples. The bacterial adhesion was performed as follows, the test tubes with 10 mL of sterile water solution of utrient broth (Envitech, Czech Republic) were inoculated with given bacterial strain to reach ≈ 108 CFUmL^{-1} and left at room temperature for 30 min. Then, the specimens were inserted into the test tubes. After 24 h incubation the test tubes were opened and the specimens were carefully removed from the medium, rinsed with sterile distilled water to remove loosely adhered bacteria and placed into other test tubes containing 2 mL of sterile deionized water.

Results and Discussion

Surface wettability

Wetting can be defined by the degree to which it is wetted solid. When a drop is totally spread on solid surface and the contact angle approaches 0 deg, then the surface is a complete wetting. However, in many cases it is only a partial wettability (or non-wettability). To what extent will be a solid surface wetted can be evaluated by contact angle measurements. Wetting can be expressed relative strength of cohesion (liquid/liquid) and adhesion (solid/liquid) forces. Weak cohesion with strong adhesion due to the very low contact angle is close to full wettability. How solid/liquid interactions decrease and liquid/liquid interactions increase, then wettability decreases. The contact angles changes of testing liquid set, graft yield (*GY*), and surface free energy (γ^{tot}) and its components of antibacterial treated LDPE are shown in Table 1. The graft yield (*GY*) was calculated by the following equation: $GY[\%] = ((W_2 - W_1)/W_1).100\%$, where W_1 and W_2 represent the weight of the samples before and after surface treatment. The water contact angle (θ_w) of untreated LDPE (Sample 1) achieves the highest values from the all samples because it is polymer with hydrophobic and chemical inert surface. θ_w significantly decreased after plasma effect on Sample 1 when were introduced different functional groups coming from plasma species and therefore this treatment surface acquired more polar or hydrophilic character. The most decrease contact angle was observed in case polyacrylic acid (PAA) (Sample 3) which relates with its hydrophilic character. For investigation other the physicochemical parameters treated surface was used Lifshitz-Van der Waals/acid-base (*LW*/*AB*) theory whereby can be obtain γ^{tot} and its components such as non-polar *LW* (γ^{LW}) and polar AB (γ^{AB}) component. *LW* indicates the total dispersive Lifhitz-Van der Walls interaction and *AB* refers to the acid-base or electron-acceptor/electron donor interaction according to Lewis. Sample 3 in comparison with other samples whereas it excels by high polarity because it contains polar oxygen groups. Sample 4 and 5 showed the similar increase of surface free energy values thereby confirming an increase in wettability.

Table 1. – Surface properties LDPE treated by multistep modification process

Sample	θ_w [°]	θ_e [°]	θ_g [°]	θ_d [°]	θ_f [°]	γ^- [mN/m]	γ^+ [mN/m]	γ^{AB} [mN/m]	γ^{LW} [mN/m]	γ^{tot} [mN/m]	GY [%]
1	99.2	70.9	85.3	48.4	80.7	1.0	0.1	0.7	34.5	35.2	–
2	77.5	51.0	67.1	36.0	52.8	6.6	0.1	1.1	41.4	42.6	0.0
3	66.9	32.1	57.2	32.5	37.0	10.4	0.5	4.5	43.7	48.1	0.5
4	79.9	36.1	60.4	30.5	48.3	2.4	0.7	2.5	44.0	46.5	1.8
5	76.7	38.1	63.2	30.0	50.4	5.2	0.2	2.0	44.4	46.4	2.0

w=deionized water, e=ethylene glycol, g=glycerol, d=diiodomethane, f=formamide
**Sample 1: untreated LDPE; Sample 2: plasma-treated; Sample 3: acrylic-acid grafted; Sample 4: triclosan coated; Sample 5: chlorhexidine coated*

Antibacterial activity

Inhibition zone area was calculated from average diameter of inhibition zone, whereas area of the sample was not taken into account (Fig. 1). Untreated sample, plasma treated sample and sample grafted by PAA with chitosan together with glutarladehyde did not show any antibacterial activity against *E.coli* and *S. aureus* strains. Chitosan/pectin coated sample showed minor activity only against *S. aureus*, their inhibition zone move around 70 mm^2. The highest and most clear inhibition zones were given by samples grafted by PAA and coated by chitosan. Their levels were on average 35 mm^2 for *E.coli* and 275 mm^2 for *S.aureus*. PAA grafted sample showed no inhibition zone for *E.coli*, nevertheless same sample indicated antibacterial activity for *S.aureus*. This could be explained by high sensitivity of PAA brush and its ability to easily absorb impurities during manipulation. As it can be seen from results, only sample grafted by PAA and coated by chitosan demonstrated active antibacterial properties against both bacterial strains.

Conclusions

The contribution devoted to examining the impact of selected antibacterial agents, i.e. triclosan and chlorhexidine, bound to the surface of LDPE with acrylic acid by DCSBD plasma. The plasma effect was used grafting of acrylic acid to form the polymer via radical polymerization. The bounded acrylic acid created polymer brushes on the polymer surface that was capable of physical forces bind antibacterial agent's effective manner. Antibacterial effect of LDPE film pre-treated using this method was shown against *E. coli* and *S. aureus*.

Figure 1. – Antibacterial properties of LDPE against *S. Aureus* and *E. Coli*

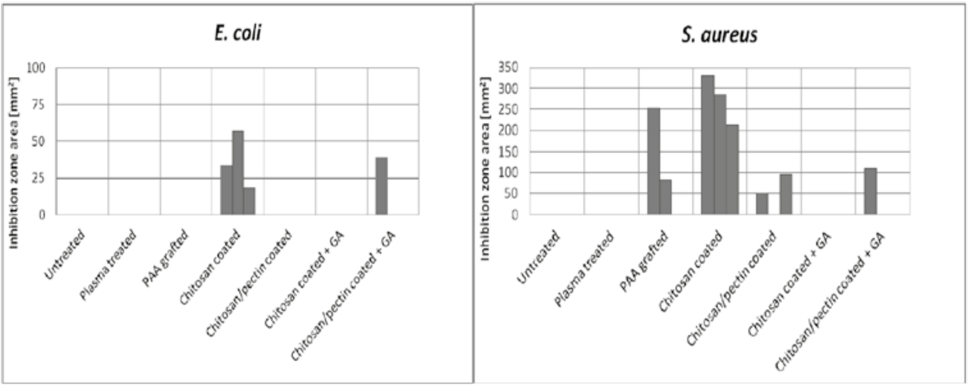

Acknowledgments

This work was supported by Slovak grant agency VEGA (grant No. 2/0199/14) and Slovak Research and Development Agency under the contract No. APVV-14-0518.

References

[1] ASADINEZHAD A., NOVÁK I., LEHOCKÝ M., BÍLEK F., VESEL A., JUNKAR I. et al., Polysaccharides Coatings on Medical-Grade PVC: A Probe into Surface Characteristics and the Extent of Bacterial Adhesion, *Molecules*, 2010, 15, p 1007–1027.

[2] BAZAKA K., JACOB M.V., CRAWFORD R.J., IVANOVA E.P., Plasma-assisted surface modification of organic biopolymers to prevent bacterial attachment, *Acta Biomaterialia*, 2011, 7, p 2015–2028.

[3] ELSABEE M.Z., ABDOU E.S., NAGY K.S.A., EWEIS M., Surface modification of polypropylene films by chitosan and chitosan/pectin multilayer, *Carbohydrate Polymers*, 2008,71, p 187–195.

[4] JOHN P. I., *Plasma Sciences and the Creation of Wealth*, Tata McGraw-Hill, New Delhi, Chapter 3, 2005.

[5] KENAWY E.R., WORLEY S.D., BROUGHTON R., The chemistry and applications of antimicrobial polymers: A state-of-the-art review, *Biomacromolecules*, 2007, 8, p 1359–1384.

NOVÉ POVRCHOVĚ AKTIVNÍ LÁTKY A SEKVESTRANTY ZALOŽENÉ NA ASPARAGOVÉ KYSELINĚ S ANTIKOROZNÍMI VLASTNOSTMI

NEW SURFACTANTS AND SEQUESTRANTS BASED ON ASPARTIC ACID WITH ANTICORROSIVE PROPERTIES

HRDINA R., BURGERT L., KALENDOVÁ A., VYTŘASOVÁ J., BROŽKOVÁ I., KREJČOVÁ A., BAYEROVÁ P., PINTO A.M.D.T., GENOVEZ C.M.

Summary

The lecture describes a new surfactants and sequestrants based on aspartic acid, and their preparation, which have a high surface activity, chelating properties, anticorrosion properties and are also biodegradable. Some surfactants tend to have antibacterial and antifungal properties. The prepared compounds are therefore suitable for cleaning surfaces of metal products, especially iron, and further as an additive in fluids in pipes such as cooling the engines of cars, solar panels, and the like.

Keywords

Surfactants, sequestrants, aspartic acid, anticorrosive properties, antimicrobial properties

ZNEHODNOCENÍ POVRCHOVÉ ÚPRAVY PRÁŠKOVOU BARVOU NA GALVANICKY ZINKOVANÉ OCELI VLIVEM NAVODÍKOVÁNÍ OCELI

DEPRECIATION OF POWDER COATING APPLIED ON ZINC ELECTROPLATED STEEL DUE TO HYDROGEN CHARGING OF STEEL

MINDOŠ L.

SVÚOM s.r.o.

Summary

This case study presents defects not associated with the actual electroplating process itself but with the additional coating procedure. A multi-coat system of zinc and powder coatings is relative frequently used type of surface treatment for various products. In powder coating many various defects forming pinholes or bubbles are a common problem. There are many reasons for these defects. This paper presents failure analysis methodology and the step-by-step approach to the particular case study.

Key words

Galvanizing, zinc coating, powder coating, pinholes, bubbles, hydrogen charging of steel

Introduction

Zinc electroplating is economic way of corrosion protection of wide spectrum of consumer articles and industrial steel products. Zinc electroplating may be applied in acid or alkaline baths. As it is electrochemical process in water conductive environments, there is risk of hydrogen diffusion of steel by hydrogen forming on cathode for both processes. Industrial application of zinc electroplated steel with organic coating dates to the ca second half of 20th century. There are used two basic types of paints for application of paint coatings in common praxis: traditional (liquid) paints – great development started together with chemical industry development (phenol formaldehyde resin finding – 1910, nitrocellulose manufacturing process – 1920, alkyd resins´ manufacturing process 1930) and powder coatings industrially applied more than 40 years.

In the last 15 years the world increasing of powder coating application is around 9 %. Thermoset powder coatings´ application has many advantages interesting for paint companies, mainly:

1) powder coatings are immediately prepared for application,

2) powder coatings decreased healthy risks for employees in painting shops,

3) powder coatings have very god properties of cured coatings,

4) powder coatings do not contain thinners, they emit near zero VOC.

Applied powder coatings melt at higher temperature where the chemical reaction and polymerisation occurred to leading a network-like structure and solid coatings´ forming. These coatings are used as decorative and protective applications. Decorative coatings have thickness in range 20–80 μm. The protective thermoset coatings have thickness from 60 μm to 80 μm [1]. The most common way of applying the powder coating to metal objects is to spray the powder using electrostatic guns. Other methods are immersion into the electrostatic fluidized bed and application by tribo gun, which charges the powder by (triboelectric) friction. Applied coatings are than cured at temperature 160–220 °C for ca 15–30 minute period [2]. Higher temperature obtains melting and flowing out of powder and its adhesion to metal surface. After cooling the powder coating creates solid, resistant and homogenous layer.

Powder coatings require suitable and proper surface preparation. Similarly as for traditional (liquid) paint coatings´ application the maximum attention shall be given to surface cleanliness; the anchoring profile is also very important factor. Type and degree of surface preparation are significantly affected by surface condition, substrate type, contamination type and requirements for final products. Principles of metal surface preparation are object of many studies, guidelines and technical standards.

Experimental methods

There were found an occurrence of many non-uniform blisters on evaluated steel components with duplex paint system; defects were evident by naked eye (see Figure 1).

Figure 1 – Non-uniform numerous occurrence of blisters in powder coating layer

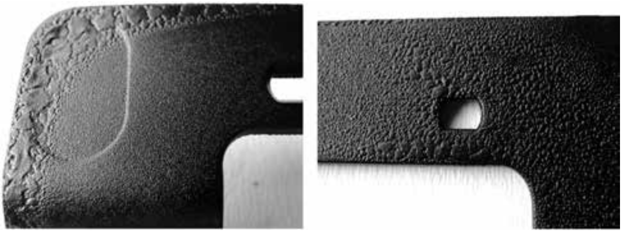

The powder coating was removed from a surface part and zinc coating was pickled to adjust thickness measuring gauge (see Figure 2). Thickness gauge was calibre to zero directly on steel surface. Coating thicknesses were measured:

- duplex system total average thickness 85.8 ± 14.6 µm,
- average zinc coating thickness 13.4 ± 2.8 µm,
- average powder coating thickness 85.8–13.4 = 72.4 µm.

Figure 2 – Partly removal of powder coating (left) and zinc pickled (right).

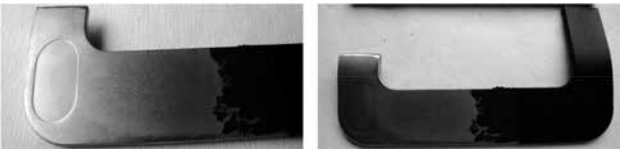

To identify the reason of defects in powder coating layer the surface treatment was tested by destructive adhesion test and by microscopic evaluation performed on segments removed from components. Failure analysis consists from macroscopic and microscopic evaluation of surface treatment and both coating layers. This way enables to obtain important information about defect creation reasons. Both layers (zinc and powder coating) and interface between them were evaluated separately. The cross sections of powder coating were studied by metallographic (optical) and electron scanning (SEM) microscopes. Cross-sections were documented at 100× to 8000× magnitudes.

Results and discussion

Figure 3 shows destructive adhesion tests of powder coating on zinc coated steel by cross-cut method on different component surface areas: on area without defects (left), on area partly coming to defects (middle) and finally on area with defects in surface treatment (right). These tests result in conclusion that the powder coating adhesion to zinc layer is excellent and the non-suitable preparation of zinc layer before powder coating application may be excluded.

Figure 3 – Adhesion tests of powder coating to zinc coated steel by cross-cut test according to EN ISO 2409. Powder coating adhesion may be estimated as degrees 0, 0 and 1, it means excellent to very good adhesion

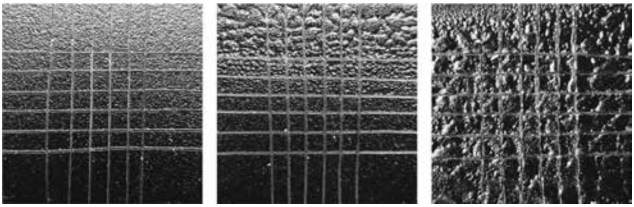

Figure 4 – Powder coating surface in area without blisters, noticeable texture, any occurrence of resin foam, 100x magnitude, bright field

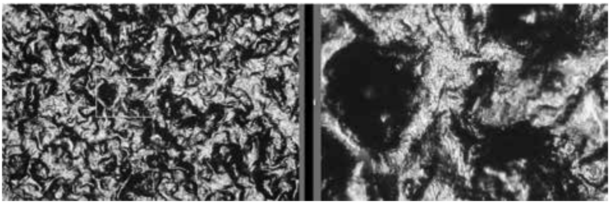

Figure 5 – Powder coating surface in area with blisters; left – detail of pore open to external powder coating layer surface; right - detail of blister bottom, where the resin intensive and fine foam is evident, 200x magnitude, bright field

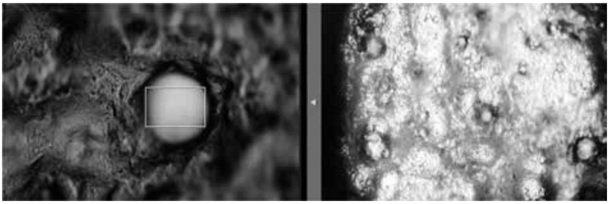

Figure 6 – Detail of defect bottom in electroplated zinc layer with steel surface, forming marks, 1000x magnitude, bright field

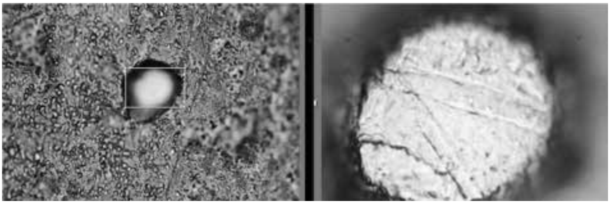

Figure 7 – Detail of porous structure on zinc layer surface, 1000x magnitude, bright field

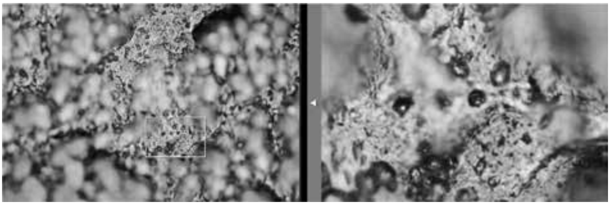

Figure 8 – Detail of bubble under powder coating layer formed by hydrogen penetration through zinc layer with ca 25 µm thickness. On zinc layer cross-section there are clearly evident ca 18 clusters of tiny pores, see red arrows. These pores´ clusters enable recombined hydrogen transport under layer of melted powder paint. Minimum 18 transport paths for hydrogen escape under powder paint layer are occurred on length shorter than 0,5 mm; 400x magnitude, bright field

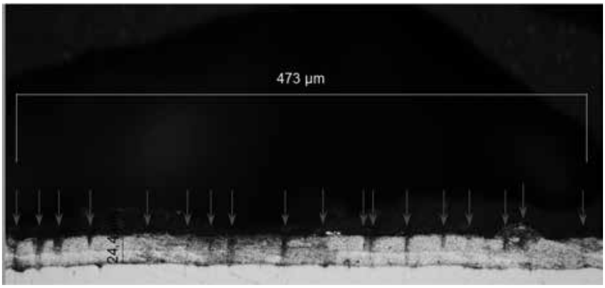

Figure 9 – 4 bubbles located practically on surface of zinc layer. Right – the residual powder coating layer on zinc layer after bubble swelling, 400x magnitude, bright field

Figure 10 – Detail (SEM) of zinc layer with numerous pores created by recombined hydrogen escape. On cross-section there are evident 2 zones where zinc layer is intensively pervaded by pores at total thickness. This way the transporting zones were formed for hydrogen escaping which swell the melted layer of powder coating during its curing, 8000x magnitude

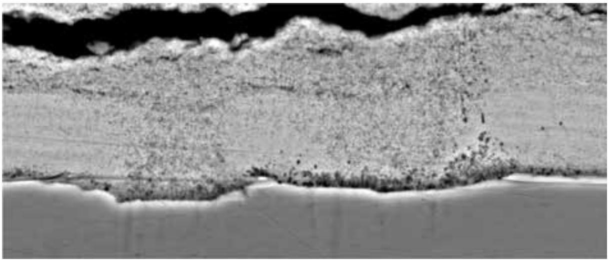

Conclusion

Duplex paint system, created by electroplated zinc coating and powder paint, is surface treatment type for protective and decorative properties of products with middle durability. Any defects in surface treatment reduce its protective and decorative value.

The hydrogen may introduce to steel during alkaline zinc plating and at subsequent thermal treatment adsorbed hydrogen diffuses and may form defects in zinc layer and also in powder coating layer. Presented study proves that the microscopic defects (pores) formed in electroplated zinc layer and macroscopic defects formed in powder coating layer after powder coating application as a results recombined hydrogen expansion. Microscopic evaluation of defects unequivocally proves the direct reason of defects´ occurrence. This failure analysis shall lead to avoid repeating occurrence of such problem.

Acknowledgement

This study was elaborated due to financial support of Ministry of Industry and Trade of the Czech Republic in the frame of project IP 06/2016.

Reference

[1] Patange G. D., *Performance of Paint Coating on Galvanized Steel in Coil Coating Line Steel World*, 34, 2009

[2] Belder E.G., Rutten H.J.J.,Perera D.Y., Cure characterization of powder coatings, *Progress in Organic Coating*, Volume 42, Issues 3–4, 2001, pp. 142–149

POVRCHOVÉ ÚPRAVY VOZIDEL – SPECIFIKA A FENOMÉNY

SURFACE TREATMENTS OF VEHICLES – SPECIFICS AND PHENOMENA

KOŠŤÁL M.

Summary

The article discusses some aspects of surface treatments of vehicles in the context of the specifics of the Czech market (discontinuity development in the period 1948–1989). It aims to outline the history of the development, technical terminology, education and training, linkages between industrial and refinish coating, types of paint shops, materials, technologies, coloristic and colorimetry. The author builds on 25-year-old domestic and foreign experience in the field of surface treatment of vehicles.

Key words

Surface treatments of vehicles – specifics of the CZ market, technical terminology, education and training, industrial and refinish rating, types of paint shops, materials, technologies, coloristic, colorimetry

Specifickým segmentem povrchových úprav je obor povrchových úprav vozidel (tzv. AUTOLAKŮ). Patří k vrcholům technologického vývoje. Cílem tohoto mého příspěvku je ve stručnosti uvést některé jeho fenomény, souvislosti a mystifikace, které mnohdy unikají naší pozornosti.

Historie

Doložitelná historie povrchových úprav sahá do doby 30 až 40 tis. let př.n.l. (první pigmenty). První laky (bezbarvé nebo probarvené) byly aplikovány před cca 4 tis. let př.n.l. zpočátku vesměs na přírodní bázi (teprve později se v rostoucí míře přecházelo na syntetické). V této prehistorické době se objevily už i předchůdci lakovacích a sušicích kabin (novodobě zavedených až v 50. letech min. stol.) ve formě sušících jam s filtrací mechanických nečistot a regulací relativní vlhkosti vzduchu. Vývoj dopravních prostředků a jejich povrchových úprav postupně vyvolal oddělení profese povrchových úprav vozidel od obecné lakýrnické profese a obecného lakýrnického školství. V naší zemi došlo k přerušení tohoto vývoje nejvýrazněji od 70. let min. stol. následkem tzv. železné opony, kdy byla navíc upřednostňována kvantita oproti kvalitě. Následky tohoto přerušení v určité míře pociťujeme dodnes.

Jaké ponaučení si z toho pro dnešek můžeme vyvodit:

a) základní materiály, technologické postupy a vybavení lakoven zůstaly v obecném principu po celou dobu převážně obdobné,

b) stěžejní podmínkou úspěšné aplikace (zejména finálního efektu) bylo a je precizní dodržování technologické skladby a technologické kázně (která se v současné době mnohdy porušuje),

c) přesto, že došlo k výraznému urychlení prací (z původních 100 nátěrových vrstev, jejichž provedení trvalo až 12 měsíců, dokážeme nátěrový systém aplikovat ve čtyřech až jedné technologické, resp. v osmi až jedné nástřikové vrstvě a časově v řádech několika hodin nebo pouhých minut), dochází mnohdy k nesprávné volbě nebo dokonce k vynechávání technologických vrstev a zkracování technologických časů,

d) výše zmíněné přerušení kontinuity vývoje povrchových úprav mělo a dosud má dopad do stavu terminologie, školství a praxe lakoven (přenášení „nešvarů“ z tohoto období) a je jednou z příčin řady nedorozumění, problémů a reklamací.

Terminologie

Dopadem již zmíněného přerušené kontinuity vývoje povrchových úprav došlo u nás i k zastavení vývoje odborné terminologie. Existuje sice čtyřjazyčná norma ČSN-ISO pro povrchové úpravy obecně, dodnes však chybí terminologie pro povrchové úpravy vozidel, které k vyjádření podrobností vyžadují nemálo dalších výrazů. To má dopad do kvality překladů dokumentace z cizích jazyků, které mnohdy postrádají jednoznačnost a jsou také příčinou řady nedorozumění, vad a reklamací.

Školství a vzdělávání obecně

Ve školském systému došlo v polovině 70. let ke sloučení oborů AUTOLAKÝRNÍK a MALÍŘ/NATĚRAČ (k obnově tohoto stavu došlo až od školního roku 2011/12). Chybí učebnice a kvalifikační příručky v obecné rovině (poslední vyšly v roce 1956 a 2004, další se připravují), které suplují výrobci a distributoři nátěrových hmot svými školícími systémy (formulovanými komerčně na své produkty).

Při řešení nedostatku kvalifikovaných lakýrníků má pomoci i systém získávání kvalifikací, který byl po čtyřletém vývoji a testování konečně spuštěn (na základě teoretických a praktických zkoušek je možné prostřednictvím autorizovaných subjektů získat dílčí kvalifikaci „PŘÍPRAVÁŘ“ nebo „FINÁLNÍ LAKÝRNÍK“ nebo výuční list „AUTOLAKÝRNÍK“). Předchází mu rekvalifikační nebo přípravné kurzy. Do standardů tohoto systému „Národního ústavu vzdělávání“ se podařilo již zmíněnou novou odbornou terminologii implementovat.

Partie konstrukce vozidel a návaznosti na povrchové úpravy

K pochopení veškerých souvislostí je potřeba prostřednictvím prostorových schematických znázornění a výčtu veškerých partií konstrukce jednotlivých typů vozidel seznámit se s veškerými vazbami na povrchové úpravy (lepení dílů, dutiny vč. jejich vyztužujících výplní, povlaky podlah, protihlukové vrstvy …) tak, jak se provádějí ve výrobě. Všichni opravárenští specialisté (mechanici, klempíři a lakýrníci) by je měli znát, aby mohli kvalitně volit a provádět postupy při opravách poškození a vad nátěrového systému.

Povrchové úpravy vozidel průmyslové a opravárenské

Mnohdy uniká pozornosti, že povrchové úpravy vozidel se dělí na průmyslové (PAL) a opravárenské (OAL). Obě tyto podskupiny autolaků mají řadu shodných i odlišných specifik. Pro jejich srovnání je vhodné vzájemně specifikovat ekvivalenty (např. fosfátování-ošetřování povrchu fosfátovými odrezovači apod.).

V oblasti PAL např. pracujeme s teplotami sušení 40 nebo 60 ˚C nebo také kolem 190 ˚C, v oblasti OAL s současné době už pouze s teplotami sušení 40 nebo 60 ˚C. Opravárenské autolaky jsou charakterizované speciálními materiály a postupy, ale především používáním míchacích zařízení, pomocí kterých je možné v lakovnách s minimálními skladovými zásobami operativně míchat širokou škálu barevných odstínů (pododstínů) vrchních laků. I když v sériových výrobách vozidel mnohdy dominuje robotizované nanášení nátěrových hmot, má zde prostor i jejich ruční nanášení (na výrobních linkách nebo opravárenských pracovištích). V oblasti OAL pracujeme pouze s ručním nanášením nátěrových hmot (pneumatickým, vysokotlakým, elektrostatickým nebo výjimečně štětcem); lidský faktor je zde nadále důležitý a nenahraditelný (identifikace defektů, znalost a volba správných postupů, zručnost při nanášení, přesnost očí).

Typy autolakoven

Autolakovny se dělí na výrobní (malo, středně a velkosériové), opravárenské nebo kombinované. Podle potřeb používají autolaky průmyslové nebo opravárenské nebo jekombinují (pak je potřeba příslušné technologické skladby předem odzkoušet). Ekologická legislativa definuje, ve kterých z nich je (ne)možné používání podlimitních (tzv. ekologických)nebo nadlimitních nátěrových hmot.

Možnosti využití autolaků v jiných segmentech pú

Specifické technologie pro povrchové úpravy vozidel lze pro jejich estetické efekty a barevnou stálost využít i v jiných segmentech povrchových úprav (helmy, trezory, kytary, stavební konstrukce, atd.). V některých případech jsou ale nutné potravinářské atesty.

Materiály

Široká škála nátěrových hmot, komponentů a přísad umožňuje provádět prvotní úpravu téměř všech druhů kovových, plastových a dalších materiálů nebo povlaků tak, aby byla zajištěna jejich soudržnost a antikorozní ochrana, dále pak různé varianty technologických skladeb podle potřeb. U opravárenských autolaků je charakteristická jejich vysoká vydatnost (nízká spotřeba), rychlá aplikace a krátké doby schnutí. Umožňují např. provést při teplotě prostředí 20˚C za jednu směnu nanesení více pruhů různých barevných odstínů (konturovací pásky je možné lepit na „čerstvý“ vrchní lak už za 0,5–1 hodinu, aniž dojde po jejím odtržení k poškození vrchního laku).

K jedné z mystifikací oboru autolaky patří např. tvrzení, že každý produkt s obchodním názvem ZÁKLADOVÝ PLNIČ (grundfüller …) zajišťuje plnohodnotnou antikorozní ochranu kovu. Výrobní firmy nátěrových hmot však dodávají dvě verze (s antikorozními pigmenty s dostatečným nebo jeho sníženým obsahem pojiva), což je nutné jednoduše otestovat přímo v lakovně podle (ne)nasákavosti příslušného naneseného a vyschlého produktu, jelikož tento fakt většinou z technologických (technických) listů výrobců zřejmý není, zavání to tudíž klamáním spotřebitele a způsobuje mnohá nedorozumění a reklamace.

Technologcké postupy a skadby

Pomineme-li velkosériovou výrobu vozidel, kde se pracuje převážně robotizovaně a při vysokých teplotách schnutí, pak nám zbývá aplikace průmyslových nebo opravárenských autolaků při teplotách nanášení a schnutí 20, 40 nebo 60 ˚C. Ty nám dávají možnost operativní volby různých variant technologických skladeb v souladu s požadovanými kritérii pro povrchovou úpravu vozidla nebo jeho dílu (prvotní úprava, tloušťka nátěrového systému a jeho estetický efekt, otěruvzdornost, životnost, atd.). Umožňují nám operativně aplikovat i různá dekoratérská řešení (např. náhradu samolepek lakováním).

Koloristika a kolorimetrie

K fenoménům autolaků patří koloristika a kolorimetrie. U povrchových vozidel je vyžadována vysoká přesnost. Od roku 1913 je registrováno cca 180 tis. barevných kódů, pro které bylo formulováno cca 1,7 mil. barevných odstínů a pododstínů. To znamená, že pro každý z nich v průměru existuje více jak 9 variant (u nejsložitějších z nich jich je dokonce kolem 160). Příčinou vzniku takového počtu barevných variant je, že ve výrobě při každé sérii dochází k odchylkám mezi jednotlivými šaržemi vrchních laků a na cestě od výstupu ze sériové lakovací linky ke konečnému odběrateli dochází až k osmi opravám vrchního laku. Např. zhruba 40 % osobních automobilů je během této cesty opravováno tzv. rozstřikem (na jednom se mnohdy na různých částech karosérie vyskytuje více znatelných barevných odchylek).

V sériových výrobách se používá cca 150 tvarů a velikostí metalických zrn, které výrobci opravárenských autolaků imitují prostřednictvím kombinací cca osmi z nich. Složitější barevné odstíny navíc obsahují perleťové pigmenty. Fenoménem jsou syntetické pětivrstvé pigmenty o velikosti 0,1 μm, které umožňují neefektivnější „flip-flop“ efekt (rychlé změna struktury a barev pod různými úhly pohledu).

Opravárenští autolakýrníci jsou postaveni před náročný úkol – v krátkém čase musí operativně řešit opravu defektu v perfektní shodě s barevným odstínem vozidla. K tomu nestačí pouhé provedení měření spektrofotometrem, ale je potřeba z jeho nabídky prostřednictvím ručně nastříkaných vzorků hledat nebo případně dotónovat akceptovatelnou variantu.

Pokud součástí technologie konkrétního výrobce autolaků jsou rozsáhlé ručně stříkané vzorkovnice, které jsou ve shodě s příslušnými recepturami v každé výrobní šarži pigmentových bází, obejde se lakýrník bez spektrofotometru. Ve všech případech je ale konečnou instancí kontrola okem pod různými druhy osvětlení. Pokud lakýrník není s těmito principy seznámen nebo není ochoten je akceptovat, dochází k řadě iluzí a mystifikací, které se pak šíří po celém trhu.

Závěr

Tento příspěvek vychází z mých pětadvacetiletých praktických zkušeností v oboru povrchových úprav vozidel a vzhledem k omezenému prostoru její stručný nástin. Podrobně je (a bude) uvedena v učebnicích (příručkách), které byly nebo budou vydány.

ANTIKOROZNÍ VLASTNOSTI KŘEMIČITOWOLFRAMOVÉ A FOSFOWOLFRAMOVÉ HETEROPOLYKYSELINY V NÁTĚROVÝCH FILMECH

ANTICORROSIVE PROPERTIES OF SILICOTUNGSTIC ACID AND PHOSPHOTUNGSTIC HETEROPOLYACID IN THE PAINT FILMS

NECHVÍLOVÁ K.[1], KALENDOVÁ A.[1], STEJSKAL J.[2]

1 Department of Chemistry and Materials Technology, FCHT, Univerzity of Pardubice
2 Institute of Macromolecular Chemistry AS CR, Department of Conducting Polymers, Prague

Summary

The aim of this work was to provide an initial characterisation of heteropolyacids and examine their behaviour and properties as pigments in paints using different concentrations of the pigment and filler. Solvent-based epoxy-ester resin served as the binder. The paints were applied to steel and glass panels for mechanical and corrosion resistance testing. The organic coatings were exposed to a corrosive atmosphere with NaCl. This test was completed with electrochemical measurement. The parameters examined included the paint film's mechanical and anticorrosion efficiency. The environments in which the new coatings are most efficient were also sought.

Key words

Heteropolyacids, epoxy-ester resin, organic coatings

Introduction

Metal corrosion is a topic that has been known from the times mankind started using iron (and steel) not only for day-to-day uses [1]. Global (39 countries) raw steel production was 1.548 billion tonnes in 2013 and even more, 1.598 billion tonnes, in 2015; iron production was then 1.155 billion tonnes. The most recent data for 2016 (as of 22 August) are 930 billion tonnes of steel and 670 billion tonnes of iron (data from the World Steel Association [2]). Iron and steel can be used efficiently and economically only if their surface is protected against the ambient corrosive effects [3]. Organic coatings represent an option to protect the metal surfaces against corrosion. Such coatings consist (as a minimum) of a binder, a filler, and a pigment which co-determines the properties of the system [4].

In the present work we used heteropolyacids (HPAs) as the anticorrosion pigments. Heteropolyacids are compounds that were used only once in paints [5]. Generally speaking, a heteropolyacid is a polyacid that is obtained by condensation of an inorganic acid involving two (or more) different metals [6], hydrogen, oxygen, a metal or non-metal. Acids of this type are known for their potential repeatable use as acid catalysts in chemical reactions [7]. HPAs are complex protic acids with universal structures and physico-mechanical properties [5, 8]. They are economically attractive and environmentally friendly [9] crystalline substances that are very well soluble in polar solvents, exhibit a very high acidity [8, 10] and possess tunable redox properties, whereby they are interesting both as acids and as redox catalysts [12–14]. Hydrated HPAs such as phosphotungstic heteropolyacid (PTA) and silicotungstic heteropolyacid (STA) have been known for over a century but it was not until 1979 that the HPA hydrates were found to exhibit exceedingly high proton conductivity [15]. Proton conductivity is a manifestation of hydrogen bonds of various strengths due to the water molecules of the x-hydrate [16]. The behaviour of molybdophosphoric type HPAs in paints was described by Xu, who applied this HPA to a steel substrate, exposed it to a corrosive environment and analysed the protective film's composition. The components included mainly complex compounds such as $Fe_n[PMo_xO_y]$ and $M_n[PFeMo_xO_y]$ where M = K, Na [17].

Experimental part

Preparation of the heteropolyacids

Polyaniline base was prepared by the oxidation of 0.2M aniline hydrochloride with 0.25M ammonium peroxydisulfate in aqueous medium followed by the deprotonation of the solids with 1M ammonium hydroxide and drying. Polyaniline base (30 g) was reprotonated by suspension in the solutions of phosphotungstic or tungstiosilic acid (30 g of heteropolyacid dissolved in 300 ml of water) for 24 h. The resulting polyaniline salts then were collected by filtration, rinsed with ethanol, and left to dry in air.

Pigment characteristics, paint preparation and application

Some properties of the HPA pigments were determined pycnometrically (AccuPyc II 1340 Pycnometer, USA) as per ISO 787-10. The critical pigment volume concentration (CPVC) was calculated based on linseed oil consumption (ISO 787-5) per 100 g of the pigment by using the mortar-and-pestle method (CSN 67 0531). A concentration series was then set up based on the known CPVC value. The pigment particle shape and morphology (Fig. 1a: STA; Fig 1b: PTA) were examined on an electron microscope (JEOL – JSM 5600 LV, Japan). The paint systems were dispersed in a ball mill (Ballotini, 3.4 mm diameter) and filtered. The homogenised binder/pigment systems contained the pigment at volume concentrations PVC = 0.5, 1; 3 and 5 wt%. $CaCO_3$ was used as the filler to keep the Q coefficient constant at Q = 10. Two coatings, viz. the non-pigmented epoxy-ester resin and the coating with the filler only, served as the reference systems in this study.

The paints were applied to clean and degreased glass panels and steel panels (Q-LAB Corporation, UK) by using a box ruler. The dry film thickness was 80 ± 5 µm.

Fig. 1 – SEM photographs of the pigments: a - STA (2µm scale); b - PTA (10 µm scale)

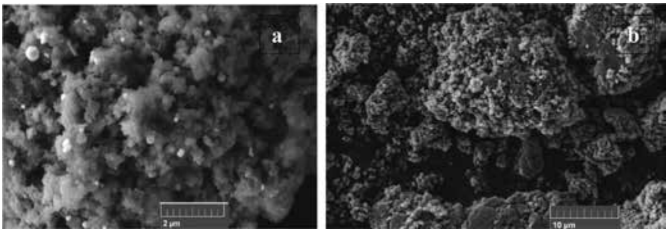

The specific electric conductivity (χ) and pH of a 10% pigment suspension in redistilled water were measured during 21 days as per ISO 789-9 and ISO 787-14. The suspension was filtered and a steel panel was submerged in the suspension and allowed to stay there for another 15 days. The data provided the corrosion loss of the material (XM/%). The hot-water-soluble and cold-water-soluble contents were also determined (ISO 787-8 and 787-3).

Physico-mechanical tests

The physico-mechanical tests were performed on steel panels 76 mm x 75 mm x 0.8 mm size (Q-LAB Corporation, UK).

Film resistance to impacts was evaluated by the falling weight method as per ISO 6272. The 1000 g weight was allowed to fall freely on the painted steel panel's averse and reverse sides, and the largest height at which the paint film still remained intact was recorded.

The cupping test, during which a steel ball 20 mm in diameter was indented into the painted panel, was carried out as per ISO 1520. The lowest depth at which the paint film was damaged was recorded.

Film adhesion to a steel substrate was evaluated by the cross-cut method described in ISO 2409. A cutting tool with the blades 2 mm apart was used to cut a square lattice having a defined area through the paint film down to the substrate. Adhesion was evaluated on the 0 to 5 scale where 0 denotes the highest film resistance.

The bending test using a cylindrical steel mandrel was performed by following ISO 1519. The largest mandrel diameter at which the paint film cohesion failed was recorded.

The arithmetic mean of the data obtained was calculated as the paint films' physico-mechanical efficiency parameter.

Corrosion tests

The coated steel panels 152 mm x 102 mm x 0.8 mm size (Q LAB Corporation) were subjected to an accelerated corrosion test. A vertical cut 7 cm long was made through the paint film to the substrate metal of all the samples tested. The corrosion effects in the cut area were then evaluated.

The samples were exposed to a salt fog atmosphere with 100% relative humidity for 1500 hours and 2184 hours. The test chamber was run in 12-hour cycles, a cycle comprising 6 hours of exposure to the salt fog solution (pH 6.5 – 7.2) at 35 °C ± 2 °C; 2 hours of exposure at 23 °C ± 2 °C; and 4 hours in condensed moisture at 42 °C ± 2 °C.

The following corrosion effects were evaluated as per ISO 4628-2 to 4628-5 after removing the panels from the chamber: blister formation on the entire paint film surface (ASTM D 714-78), degree of corrosion in the test cut (ASTM D 1654-92) and degree of steel substrate surface corrosion after removing the paint film (ASTM D 610-85). The paint's anticorrosion efficiency in the test environment was expressed through the arithmetic mean of the scores.

Results and discussion

It should be noted that the non-pigmented epoxy-ester resin (nEP) itself exhibits excellent physico-mechanical properties and provides an outstanding mechanical resistance (= 100%) in all the tests. Figs. 2a-d demonstrate that a weight falling from 100 cm left the specimens previously exposed to $(NH_4)^2SO_4$ for 672 hours intact.

Fig. 2 – Impact test of the paint films: a) nEP; b) reference $CaCO_3$; c) STA (1 wt%); d) PTA (3wt%)

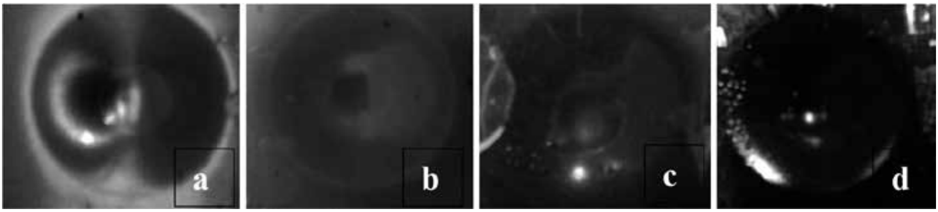

However, nEP on its own is unable to protect the substrate metal against corrosion, and so the HPAs were added to improve the paint's corrosion resistance. The various heteropolyacids differ mainly in the extent of linseed oil absorption. For instance, PTA can absorb up to 30 g/100 g pigment more oil (Table 1). This difference is mirrored in the CVPC, where PTA does not allow the system to be filled to the same level as STA.

Tab.1 – Characterisation of the pigments and fillers

CPV[a)] [wt%]	Density at 23°C [g/cm³]	Oil absorp. (linseed oil) [g/100g]	CPVC[b)] [wt%]	Solubility in water[c)] at 23°C [%]	Solubility in water[c)] at 100°C [%]	XM pig.[d)] after 35 days [%]	XM film[e)] after 35 days [%]
STA (Silicotungstic heteropolyacid)							
0.5	1.593	73.1	44.4	0.744	0.96	20.95	0.1
1							0.18
3							0.18
5							1.64
PTA (Phosphotungstic heteropolyacid)							
0.5	1.513	104.0	37.2	0.429	0.429	36.07	0.18
1							0.91
3							0.18
5							1.46
$CaCO_3$ - Omyacarb							
Q = 10	2.725	46.9	67.9	0.611	0.611	38.25	0.36

a) Critical pigment volume concentration calculated by linseed oil consumption
b) Determination of water soluble matter for pigments (CSN EN ISO 787-3 and 787-8)
c) Corrosion losses of steel panels submerged in aqueous extracts of the powdered pigments, in 35 days
d) Corrosion losses of steel panels submerged in aqueous extracts of the free paint films, in 35 days

The aim of the study was to characterise the pigments and ascertain if they are well suited for use as agents for anticorrosion protection of steel. They are substances of acid nature (Table 2) – pH on day 21 was 4.78–5.4. When a homogenised mixture of the HPA and $CaCO_3$ was added to the coating system, the pH of the aqueous extract of the free paint film increased to nearly approach the neutral region, depending on the pigment volume concentration. The system with the highest PVC = 5 wt% was an exception, where the filler proportion was not that appreciably high and the initial pigment nature predominated. Furthermore, the steel panel weight losses in the two types of aqueous extracts were determined in 36 days of submersion. The lowest weight loss, mere 0.01%, was observed in the aqueous extract of the film with STA at CPV = 0.5 wt%. This concentration also provided the highest corrosion protection in the salt fog atmosphere, and the electrochemically measured corrosion rate was in the order of 10E-12. The optimum PTA pigment concentration was PVC = 3 wt%, at which the corrosion loss was lowest, viz. 0.18%, and the anticorrosion protection efficiency highest, viz. 89%. This system proved to be the most efficient also in the long run, on exposing the samples to the same environment for as long as 2184 hours. The efficiency of the remaining systems decreased as much as to 62%. While the system with an HPA retains its protective properties if exposed to the corrosive environment for 1500 hours or less, its long-term protective properties are not adequately good. A comparison of the paint films is shown in Fig 3 (3a, 3b: in 1500 hours; 3c, 3d: in 2184 hours).

Fig. 3 – Panels exposed to the salt solution atmosphere, photographs before and after removing the paint films. a) STA 5 wt%; b) PTA 3 wt% after 1500 h of exposure; c) STA 5wt%; PTA 3wt%) after 2184 h of exposure

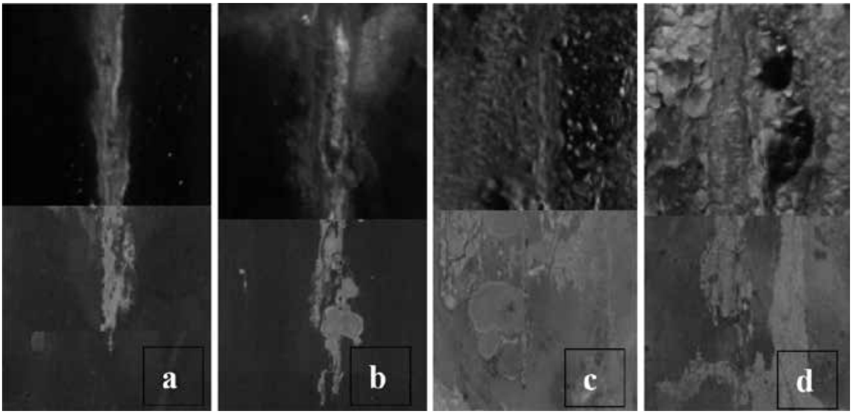

Table 2 also lists the proton conductivity data of the HPAs, decreasing with increasing pigment volume concentrations for the free pain films. The conductivity increased appreciably during the experiment in the case of the powdered pigments. Paint film blistering decreased with decreasing conductivity, the paint film adhesion, however, increased, whereby the paint film was losing adhesion to the substrate metal. The foregoing applies to the STA system. As to the PTA system, PVC = 3 wt% appears to provide the best results: no blistering took place, substrate metal corrosion was lowest, 0.03%, and no adhesion loss was observed.

The novel paint systems are suitable for C5-I type environments (ISO 12944-2 and ISO 7253) at a medium to long lifetime. This is industrial atmosphere or indoor atmosphere with elevated humidity.

Tab. 2 – Corrosion characteristics of the paint systems with HPAs

CPV [wt%]	**OFME$^{e)}$ after 30d [%]**	**Anticor. efficiency**		**Corr. rate$^{f)}$ [mm.year^{-1}]**	**pH$_{pig.}$**	**pH$_{film.}$**	**$\chi_{pig.}$**	**$\chi_{film.}$**
		NaCl$_{1500h}$ [%]	**NaCl$_{2184h}$ [%]**		**at 7/21 day [± 0.01 %]**		**at 7/21 day [± 0.5 % µS.cm^{-1}]**	
STA (Silicotungstic heteropolyacid)								
0.5	100	83	62	69.0 E-12	4.44/4.78	6.57/6.68	475/1219	537/621
1	100	77	63	69.0 E-12		6.58/6.73		433/498
3	100	76	66	12.0E-11		6.46/6.37		405/376
5	100	78	66	12.0E-11		4.99/4.10		84/111
PTA (Phosphotungstic heteropolyacid)								
0.5	100	67	62	36.0E-11	4.73/5.4	6.54/6.75	1022/1380	675/774
1	100	49	62	75.0E-11		6.48/6.97		765/841
3	100	89	72	16.0E-11		5.91/6.20		312/295
5	100	62	68	88.0E-11		4.87/4.97		104/114
$CaCO_3$ - Omyacarb								
Q = 10	100	79	69	59.0E-12	7.5/7.71	6.47/6.90	174/295	962/1021
Non-pigmented epoxy ester resin								
–	100	42	48	58.0E-12	–	3.81/3.75	–	91/139

e) Paint films' overall physico-mechanical efficiency (average of the scores; %)
f) Corrosion rate measured by the electrochemical method (VSP-300, France)

Conclusions

New heteropolyacid-based coating materials were prepared. Two heteropolyacids, viz. silicotungstic heteropolyacid and phosphotungstic heteropolyacid, were tested and compared with reference paint systems containing either the binder (epoxy-ester resin) alone or the binder and $CaCO_3$ serving as the filler. The performance of the paint systems was inferred from the comparison. The two HPAs-differ in the optimum pigment volume concentration, which is PVC = 0.5 wt% for STA and PVC = 3 wt.% for PTA. The mechanism of their protective function is not fully understood yet; some authors suggest that it consists in the formation of complex compounds of the phosphate, silicate and tungstate types. Studies to precisely identify the protective function and composition of the corrosion products are under way or planned.

Acknowledgment

Authors acknowledge SEM analysis provided by Center of Materials and Nanotechnologies with financial support by the grants LM2015082 and CZ.1.05/4.1.00/11.0251 from the Ministry of Education, Youth and Sports of the Czech Republic.

References

[1] R.Z. zand, K. Verbeken, A. Adriaens, Influence of the cerium concentration on the corrosion performance of ce-doped silica hybrid coatings on hot dip galvanized steel substrates, *Inter. J. Electrochem. Sci.*, 2013, 8, p548–563

[2] World Steel Association, Belgium (www.worldsteel.org)

[3] P.P. Deshpande, N.G. Jadhav, V.J. Gelling, D. Sazou, Conducting polymers for corrosion protection: a review, *J. Coat. Technol. Res.*, 2014, 11, p473–494.

[4] A. Kalendova, P. Rysanek, K. Nechvilova, Investigation of the anticorrosion efficiency of ferrites

$Mg_{1-x}Zn_xFe_2O_4$ with different particle morphology and chemical composition in epoxy-ester resin-based coatings, *Prog. Org. Coat.*, 2015, 86, p147–163.

[5] K.P. Han, J.L. Fang, A protective coating P-Mo-V heteropolyacid on steel, *Journal of Electron Spectrospocy and Related Phenomena*, 1997, 83, p92–93.

[6] I.V. kozhevnikov, Catalysis by heteropoly acids and multicomponent polyoxometalates in liguid-phase reactions, *Chem. Rev.*, 1998, 98, p171–198.

[7] M. Noritaka., M. Makoto, Heterogeneous Catalysis, *Chemical Reviews*, 1998, 98, p199–217.

[8] M.-Y Huang, X.-X. Han, Ch.-T. Hung, J.-C. Lin, P.-H.Wu, J.-C. Wu, S.-B. Liu, Heteropolyacid-based ionic liquids as efficient homogeneous catalysts for acetylation of glycerol, *Journal of Catalysis*, 2014, 47, p42–51.

[9] K. Nikoofar, Silicotungstic acid (H4SiW12O40): An efficient Kegging heteropoly acid catalyst fot the synthesis of oxindole derivates, *Arabien Journal of Chemistry,* 2014 – IN PRESS (http://dx.doi.org/10.1016/j.arabjc.2014.07.008)

[10] H.-J. Kim, Y.-G. Shul, H. Han, Synthesis of heteropolyacid (H3PW12O40)/SiO_2 nanoparticles and their catalytic properties, *Applied Catalysis A: General*, 2006, 299, p46–51.

[11] M. Chakrabarty, A. Mukherji, R. Mukherjce, S. Arima, Y. Harigaya, A Keggin heteropoly acid as an efficient catalyst for an expeditious, one-pot synthesis of 1-methyl-2-(hetero)arylbenzimidazoles, *Tetraherdon Letters*, 2007, 48, p5239–5242.

[12] P. Staiti, Proton conductive membranes based on silicotungstic acid/silica and polybenzimidazole, *Materials Letters*, 2001, 47, p241–246.

[13] F.J. Berry, G.R. Derrick, J.F. Marco, M, Mortimer, Silica – supported silicotungstic acid: A study by X-ray photoelectron spectroscopy, *Materials Chemistry and Physics*, 2009, 114, p1000–1033.

[14] J.H. Choi, T.H. Kang, J.H. Song, Y. Bang, I.K. Song, Redox behavior and oxidation catalysis of $H_nXW_{12}O_{40}$ (X = Co^{2+}, B^{3+}, Si^{4+}, and P^{5+}) Keggin heteropolyacid catalysts, *Catalysis Communications*, 2014, 43, p155–158.

[15] J. Sun, D.R. MacFarlane, M. Forsyth, Characterization of a proton conductor based on silicotungstic acid, *Electrochemia Act*a, 2001, 46, p1673–1678.

[16] J. Mosa, A. Durán, M. Aparicio, Epoxy-polystyrene-silica sol-gel membranes with high proton conductivy by combination of sulfonation andtungstophosphoric acid doping, *Journal of Membrane Science*, 2010, 36), p135–142.

[17] Y.D. Xu, *Journal East China Inst. Chemical Technology*, 1981, 2, p13.

VLIV TVARU ZINKOVÝCH ČÁSTIC NA KOROZNÍ VLASTNOSTI ORGANICKÝCH POVLAKŮ OBSAHUJÍCÍCH VODIVÝ POLYMER

EFFECT OF ZINC PARTICLE SHAPE ON THE ANTICORROSION PROPERTIES OF ORGANIC COATINGS CONTAINING ZINC AND A CONDUCTIVE POLYMER

KOHL M., KALENDOVÁ A.

Faculty of Chemical Technology, Institute of Chemistry and Technology of Macromolecular Materials,
University of Pardubice, Studentská 95, 53210 Pardubice, Czech Republic

Summary

The aim of this work was to prepare organic coatings containing a conductive polymer and either spherical or lamellar zinc particles and to evaluate their mechanical and corrosion resistance. Polyaniline phosphate was used as the conductive polymer. This substance was prepared by oxidative polymerisation of aniline in 1 M phosphoric acid using ammonium peroxodisulphate as the oxidant. The oil number and density were determined for the pigment and the critical pigment volume concentration was calculated by using the data. Once the basic characteristics of the pigment had been established, the organic coatings were formulated. The organic coatings contained polyaniline phosphate at pigment volume concentrations 1%, 5% and 10%, to which zinc – spherical in one concentration series and lamellar in another series – had been added in amounts such that the total pigment volume concentration was constant and equal to the critical pigment volume concentration. The organic coatings were subjected to mechanical and corrosion tests. Mechanical tests included the impact test, bending test, cupping test and adhesion test. Corrosion was assessed in an accelerated cyclic test in salt spray atmosphere.

Key words

Spherical zinc, lamellar zinc, conductive polymer, polyaniline, coating

Introduction

Zinc powder is used as an anticorrosion pigment in paints, in which it constitutes what is called a sacrificed electrode [1, 2]. Spherical zinc particles are typically used in corrosion protection applications, although lamellar particles are sometimes also used. Lamellar particles exhibit a lower tendency to settle and are capable of sorbing larger amounts of the binder than the spherical particles, which implies that they are able to attain a lower pigment volume concentration (PVC) in the paint [3]. As another asset, the lamellar pigment extends the travelling path of the liquid medium diffusing from the surface to the substrate; reflect ultraviolet radiation, thereby protecting the binder from degradation; and, also importantly, plays the role of reinforcement improving appreciably the paint film's mechanical properties [4].

Zinc coatings protect the steel substrate cathodically only during the first phase of the corrosive action. Slowly, the pores in the coating are sealed by the zinc corrosion products such as zinc oxides, zinc hydroxide and basic zinc carbonates, whereby the coating becomes impermeable for the incoming components of the corrosive medium. Hence, the zinc particles are soon coated with zinc corrosion products, electric conductivity decreases and this type of protection ceases to exist: cathodic protection transforms to barrier protection. The neutralisation and filtration mechanisms also play a role in addition to the barrier mechanism [5].

So it can be reasonably assumed that the long-term protective effect of a non-damaged zinc coating is based on the filtration effect. As the aggressive electrolyte penetrates through the paint layer, zinc corrodes spontaneously and takes up oxygen (playing the role of the depolariser) as well as the agents stimulating ion corrosion (H^+, Cl^-, SO_4^{2-}). Ultimately, only the non-aggressive aqueous solution can reach the steel surface. The emerging corrosion products also enhance the barrier effect in the coating and facilitate neutralisation of the electrolyte penetrating through the film from the outside [6–9].

Experimental part

Polyaniline phosphate synthesis

The polyaniline phosphate (PANI-H_3PO_4), was prepared by oxidative polymerisation in dilute phosphoric acid by using ammonium peroxodisulphate as the oxidant. The synthesis is depicted in Fig. 1.

Fig. 1 – Synthesis of the polyaniline phosphate

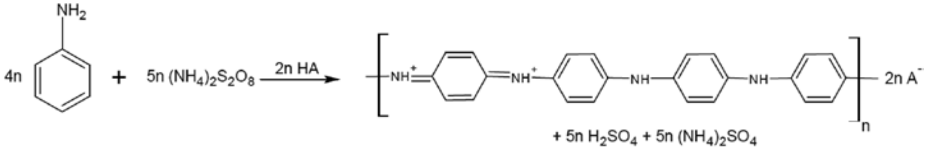

Pigment parameter determination

Pigment density was determined by using a Micromeritics AutoPycnometer 1320. Oil absorption was measured by the "pestle – mortar" method based on Czech Standard CSN 67 0531. The data were used to calculate the critical pigment volume concentration (CPVC). Microphotographs of the pigment particles were obtained on a JEOL–JSM 5600 LV electron microscope (Japan) and used to deduce the pigment particle shape. The mean particle size (d50) was determined on a Mastersizer 2000 (Malvern Instruments Ltd., UK).

Formulation and preparation of the organic coatings

In the present study, two series of organic coatings was prepared by using polyaniline phosphate at volume concentrations 1%, 5% and 10% and by completing the total pigment volume concentration to the critical level (critical pigment volume concentration, CPVC) with spherical zinc (series 1) or with lamellar zinc (series 2). A Dissolver type system was used at 4000 rpm/40 minutes to prepare the paints. Once prepared, the paints were applied to steel panels (standard S-36 low-carbon steel panels, Q-Lab Corporation) and the dry film thickness (DFT) was measured with a magnetic gauge as per ISO 2808. An artificial vertical cut was made through the paint films for the accelerated corrosion tests. The cut was 80 mm long and 0.5 mm deep and was made in accordance with EN ISO 12944–6 by using a cutting tool complying with ISO 2409 (tool for single cuts).

Mechanical properties of the paints

The paints were subjected to tests providing information on the paint film elasticity and strength. Surface hardness of the paint films was also measured, viz. with a Persoz pendulum system in accordance with ISO 1522. Adhesion of the films to the substrate was assessed on cutting a lattice into the films as per ISO 2409, by using a special cutting blade with cutting edges 2 mm apart. The impact strength of the paint films applied to steel panels was determined by letting a 1000 g weight fall onto the panels from different heights and recording the largest height (in mm) at which the film integrity remained undisturbed (ISO 6272). The paint film resistance to cupping was evaluated by measurement on an Erichsen cupping tester. The result is the steel ball indentation depth (in mm) at which the film integrity remained undisturbed, as specified in ISO 1520. The test aimed at evaluating the paint film resistance to bending consists in bending the painted panels over mandrels of different diameter and recording the largest diameter (in mm) at which the paint film integrity is disturbed, as specified in ISO 1519.

Corrosion test procedures

The organic coatings were applied to steel panels and subjected to an accelerated cyclic corrosion test in a neutral salt spray atmosphere (ISO 9227). The exposure of the samples in a testing chamber was performed in 12-h cycles divided into three parts: 6 h of exposure to a mist of 5 %-solution of NaCl at a temperature of 35 °C; 2 h of exposure at a temperature of 23 °C; and 4 h of humidity condensation at a temperature of 40 °C. The samples were evaluated after 720 h of exposure. The corrosion effects after completion of the test were evaluated as specified in the above ISO standards. Blistering on the paint film surface and in the test cut was assessed by comparing with the photographs of standards included in the ASTM D 1654–92 standards. Corrosion on the metal plane was evaluated (after stripping the paint film down) by comparison with the photographs of standards included in the ASTM D 610-85 standard. Corrosion in the test cut was evaluated by measuring the distance to which corrosion propagated from the cut to its sides.

Results and discussion

Pigment specification

The pigments' densities and oil numbers were determined and the data were used to calculate the critical pigment volume concentrations. Accurate knowledge of this parameter is imperative for obtaining correct formulations. The mean particle sizes were measured and were found nearly identical for spherical zinc and PANI-H_3PO_4, while the lamellar zinc particles were nearly twice as large. The pigment particle shapes were evaluated from microphotographs (Fig. 2) taken on an electron microscope.

Tab. 1 – Characteristics of the pigments

Pigment	**Density [g/cm^{-3}]**	**Oil absorption [g/100g]**	**CPVC [%]**	**Particle size [μm]**
spherical zinc	7,14	6,4	67	5,8 ± 0,1
lamellar zinc	6,55	23,3	38	13,0 ± 0,1
PANI-H_3PO_4	1,54	50,2	55	6,8 ± 0,1

Fig. 2 – Scanning electron micrographs: a) spherical zinc; b) lamellar zinc; c) PANI-H_3PO_4

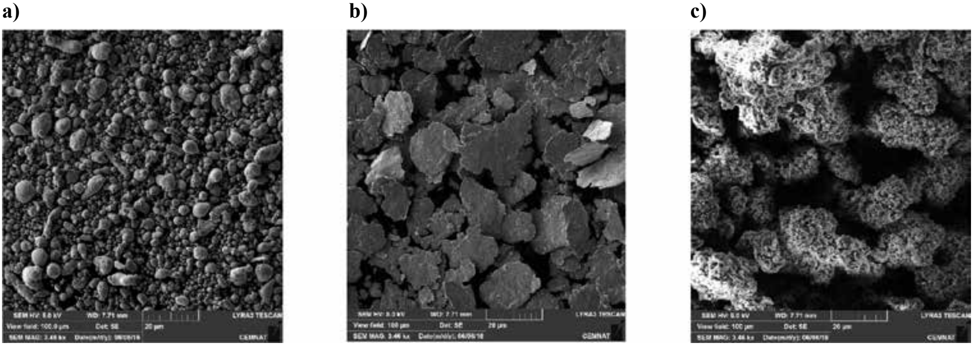

Mechanical properties of the organic coatings

Mechanical properties of the organic coatings were evaluated by using 4 tests (Tables 2 and 3). The data demonstrate that the organic coatings with lamellar zinc particles attained a mechanical resistance level nearly twice as high as the coatings pigmented with spherical zinc. This can be explained so that the lamellar particles laminate, i.e. reinforce, the binder, their elasticity can play a role even at a low binder content, thereby imparting a mechanical resistance to the coating. Spherical zinc lacks this ability due to its spherical particle shape. Furthermore, the data demonstrate that the coatings' mechanical resistance increases with increasing PANI-H_3PO_4 volume concentration. In other words, the use of PANI-H_3PO_4 as a pigment in zinc coatings was beneficial in all the formulations. This pigment (PANI-H_3PO_4) was used here to increase the organic coatings' adhesion and resilience. This effect is contributed to by the anions derived from phosphoric acid, which make up for the positive charge at the chain of this conductive polymer and improve coating adhesion to the substrate metal.

Tab. 2 – Mechanical test results for organic coatings containing PANI–H_3PO_4 and spherical zinc (DFT = 110 ± 10 μm)

$PVC_{PANI\text{-}H_3PO_4}$ [%]	**Cupping test [mm]**	**Impact test [cm]**	**Adhesion test [dg]**	**Bend test [mm]**
0	4.0	30	1	10
1	4.1	30	1	8
5	4.4	35	1	6
10	4.5	35	1	6

Tab. 3 – Mechanical test results for organic coatings containing PANI–H_3PO_4 and lamellar zinc (DFT = 120 ± 10 µm)

$PVC_{PANI\text{-}H_3PO_4}$ [%]	Cupping test [mm]	Impact test [cm]	Adhesion test [dg]	Bend test [mm]
0	4.9	45	0	8
1	5.7	45	0	6
5	6.2	50	0	6
10	6.5	50	0	< 4

Corrosion properties of the organic coatings

The results of the accelerated corrosion test, which was terminated after 720 hours, are listed in Tables 4 and 5. The tables show that the corrosion resistance was lower for the coatings with spherical zinc particles than for coatings with lamellar zinc particles. The superiority of the latter is due to the larger surface area of the lamellar particles, facilitating contact between the pigment particles. Owing to this contact, electric conductivity of the paint film with lamellar zinc particles is higher than that of the paint film with spherical zinc particles, in which the zinc particle contact area is very small. Moreover, owing to their shape, the lamellar particles in the coating are able to make up an efficient physical barrier against the penetrating corrosive medium (barrier protection mechanism). This fact can also be seen in the microphotographs of sections of organic coatings containing either spherical or lamellar zinc particles (Fig. 3).

Fig. 3 – Microphotographs of sections of organic coatings containing either spherical or lamellar zinc particles

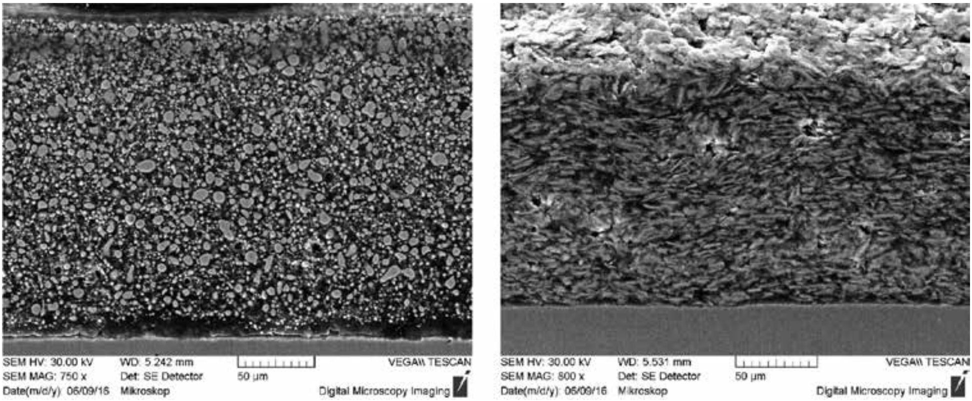

Organic coating pigmented with spherical zinc (PVC = CPVC)

Organic coating pigmented with lamellar zinc (PVC = CPVC)

PANI-H_3PO_4 had a beneficial effect by increasing the organic coatings' corrosion resistance. This conductive polymer was used to improve electric contact between the zinc particles, which is a prerequisite for electrochemical reaction of zinc. Furthermore, use is made of the polyaniline salt's ability to capture electrons and use them to transform to the polyaniline base [10].

Tab. 4 – Corrosion test results for organic coatings containing PANI – H_3PO_4 and spherical zinc (DFT = 90 ± 10 µm)

$PVC_{PANI-H_3PO_4}$ [%]	Blistering		Corrosion	
	In a cut [dg]	Metal base [dg]	Metal base [%]	In a cut [mm]
0	2 D	2 D	50	2.0–2.5
1	4 D	2 MD	33	1.0–1.5
5	4 D	4 MD	16	1.0–1.5
10	4 D	4 MD	16	1.0–1.5

Tab. 5 – Corrosion test results for organic coatings containing PANI – H_3PO_4 and lamellar zinc (DFT = 90 ± 10 µm)

$PVC_{PANI-H_3PO_4}$ [%]	Blistering		Corrosion	
	In a cut [dg]	Metal base [dg]	In a cut [dg]	Metal base [dg]
0	2 MD	2 MD	33	1.5–2.5
1	4 MD	4 M	1	0.5–1.0
5	4 MD	4 M	0.3	0.5–1.0
10	4 MD	4 M	0.3	0.5–1.0

Conclusion

The results of the mechanical tests and corrosion tests show that organic coatings pigmented with PANI-H_3PO_4 and containing lamellar zinc particles can attain higher mechanical and anticorrosion efficiencies than coatings without the conductive polymer or coatings with spherical rather than lamellar zinc particles. The improved mechanical resistance can be explained in terms of the reinforcing ability of the lamellar zinc particles, the improved anticorrosion resistance, in terms of the good electric contact between the zinc particles provided by the larger contact area of the lamellar particles. Moreover, the coatings with lamellar zinc constitute a better physical barrier separating the substrate metal from the corrosive environment. It was confirmed that PANI-H_3PO_4 improves both the mechanical properties and the corrosion resistance of the zinc-pigmented organic coatings.

Acknowledgment

Authors acknowledge SEM analysis provided by Center of Materials and Nanotechnologies with financial support by the grants LM2015082 and CZ.1.05/4.1.00/11.0251 from the Ministry of Education, Youth and Sports of the Czech Republic

References

[1] A. Kalendová, Effects of particle sizes and shapes of zinc metal n the properties of anticorrosive coating, *Progress in Organic Coatings*, 2003, 46, p324.

[2] J. Havlík, A. Kalendová, D. Veselý: Electrochemical, chemical and barrier action of zinc dust/anticorrosive pigments containing coatings, *Journal of Physics and Chemistry of Solids*, 2007, 68, p1101.

[3] L. Hochmannová, Spherical and lamellar zinc dust, *European Coating Journal,* 2002, 3, p36.

[4] A. Kalendová, A. Kukačková, P. Tamchynová, K. Rašková, Nátěrové systémy pro korozní ochranu kovových materiálů, výběr pojiv a pigmentů, *Acta Mechanica Slovaca*, 2003, ISSN 1335–2393, p97.

[5] J. Vogelsang, Ochrana oceľových konštrukcií zinkovými epoxidovými nátermi, *European Coatings Journal*, 2000, 4, p86.

[6] P. Spathis, I. Poulios, The corrosion and photocorrosion of zinc and zinc oxide coating, *Corrosion Science*, 1995, 37, p673.

[7] H. Marchebois, S. Touzain, S. Joiret, J. Bernard, C. Savall, Zinc-rich powder coatings corrosion in sea water: influence of conductive pigments, *Progress in Organic Coatings*, 2002, 45, p415.

[8] H. Marchebois, S. Joiret, C. Savall, J. Bernard, S. Touzain, Characterization of zinc-rich powder coatings by EIS and Raman spectroscopy, *Surface and Coatings Technology*, 2002, 157, p151.

[9] A. P. Yadav, H. Katayama, K. Noda, H. Masuda, A. Nishikata, T. Tsuru, Surface potential distribution over a zinc/steel galvanic couple corroding under thin layer of electrolyte, *Electrochimica Acta*, 2007, 52, p3121.

[10] E. Armelin, M. Martí, F. Liesab, J. I. Iribarren, C. Alemán, Partial replacement of metallic zinc dust in heavy duty protective coatings by conducting polymer, *Progress in Organic Coatings*, 2010, 69, p26.

ŠTÚDIUM VLASTNOSTÍ ŠPECIÁLNYCH ADHEZÍV

INVESTIGATION OF SPECIAL ADHESIVES PROPERTIES

FLORIÁN Š., NOVÁK I., ŽIGO O.

Ústav polymérov SAV, Dúbravská cesta 9, 845 41 Bratislava, Slovensko

Summary

For preparation of electrically conductive adhesives two kinds of electroconductive fillers have been used: non-regular spherical metallized basalt particles and metallized fibres of wollastonite. Polymeric composites containing polyvinylacetate and/or epoxide matrix and electroconductive filler have been prepared. Higher electrical conductivity of the composites was reached using metallized wollastonite fibres in comparison with metallized basalt particles.

Key words

Electrically conductive composite, special adhesives, metallized paricles, silver-coate filler

Úvod

V elektrotechnickom priemysle sa využíva viac ako 500 druhov lepidiel [1, 2]. Ako príklad použitia elektrovodivých lepidiel možno uviesť náhradu technológie reaktívneho pájkovania čipov k súboru prívodov pri výrobe mikroelektronických súčiastok lepením, lepenie sa používa aj pri konštrukcii rozmerných čipov mnohobitových pamätí, pričom napr. pamäťový prvok s kapacitou 1 Mb má lepený čip [3]. Použitím izotrópnych elektricky vodivých adhezív na báze polymérnej matrice plnenej elektrovodivým plnivom možno v niektorých prípadoch nahradiť spájkovanie elektronických prvkov spájkou Sb/Pb [3–6].

Cieľom príspevku bolo skúmanie vplyvu polymérnej matrice a typu metalizovaných elektrovodivých častíc na elektrické a fyzikálno-mechanické vlastnosti elektrovodivých tlakovo-citlivých kompozitných adhezív

Experimentálna časť

Pokovenie plniva, metódy merania: Elektricky vodivé plnivá sa pripravili sa bezprúdovým pokovením vybraných druhov častíc plniva. Ako vodivý komponent bolo použité striebro.Elektricky vodivé kompozity boli pripravené mechanickým primiešaním častíc pokrytých strieborným povlakom do epoxidovej alebo polyvinylacetátovej matrice v stanovenom hmotnostnom pomere. Meranie vnútorného elektrického odporu kompozitných adhezív sa uskutočnilo s použitím vysoko a nízkonapäťového stabilizovaného zdroja jednosmerného napätia, pikoampérmetra Tesla BM 545 a meracieho prípravku s kruhovými meracími elektródami. Meranie fyzikálno-mechanických vlastností kompozitov sa uskutočnilo na univerzálnom testovacom zariadení Instron 4301.

Použité materiály: Epoxidový oligomér ChS Epoxy 513 (Spolchemie, ČR), tvrdidlo Telalit 410, (Chemotex, ČR), polyvinylacetátová vodná disperzia Duvilax LS 50 (Duslo, SR). Bolo použité elektrovodivé plnivo na báze postriebreného čadiča (AGM), pričom boli nepravidelné sférické častice čadiča pokryté vrstvou striebra s hrúbkou 0.2 μm, veľkosť častíc čadiča < 40 μm, koncentrácia Ag = 12 hmot. %, Wollastonit Nyglos 4 (Nyco Minerals, USA) – anorganický kremičito-vápenatý minerál na báze $CaSiO_3$ s ihličkovitou kryštalickou štruktúrou, dĺžka vlákien bola 44 μm, hrúbka vlákien wollastonitu bola 4 μm, postriebrený wollastonit mal hrúbku pokrytia striebrom 0.2 μm. Elektricky vodivé plnivá sa pripravili sa bezprúdovým pokovením vybraných druhov častíc plniva. Ako vodivý komponent bolo použité striebro.Elektricky vodivé kompozity boli pripravené mechanickým primiešaním častíc pokrytých strieborným povlakom do epoxidovej alebo polyvinylacetátovej matrice v stanovenom hmotnostnom pomere. Meranie vnútorného elektrického odporu kompozitných adhezív sa uskutočnilo s použitím vysoko a nízkonapäťového stabilizovaného zdroja jednosmerného napätia, pikoampérmetra Tesla BM 545 a meracieho prípravku s kruhovými meracími elektródami. Meranie fyzikálno-mechanických vlastností kompozitov sa uskutočnilo na univerzálnom testovacom zariadení Instron 4301.

Výsledky a diskusia

Pri výbere časticových materiálov pre pokovenie bola zohľadnená:

– veľkosť častíc, ktorá do značnej miery ovplyvňuje jednak výsledné mechanické vlastnosti kompozitu a jednak spotrebu striebra pri ich pokovovaní. Boli porovnané vlastnosti kompozitu formulovaného na báze pokoveného plniva na báze čadiča s nepravidelnými sférickými časticami s označením PČ a postriebreného vláknitého plniva wollastonit Nyglos 4, ktorý má jeden rozmer – dĺžku vlákien – približne rovnakú ako je rozmer častíc PČ:

– tvar častíc, ktorý je dôležitým parametrom z hľadiska perkolačnej schopnosti plniva. Boli porovnané vlastnosti kompozitov obsahujúcich pokovené častice čadiča nepravidelného sférického tvaru s kompozitmi obsahujúcimi pokovené bifilné – vláknité plnivo (wollastonit).

Pri výbere modelových polymérnych matríc boli zohľadnené kritériá ich dostupnosti, ceny a typu. Boli vybraté dva bežné typy polymérnych matríc – disperzná a dvojzložková reaktívna.

Závislosť elektrickej vodivosti kompozitu na báze polymérnej matrice Duvilax LS 50 na type postriebrených častíc a ich objemovom % v kompozite je na obr. 1. Podľa obr. 1 tvar kriviek vodivosti v závislosti na objeme zakomponovaného plniva má pre obidve študované plnivá podobný trend. Podstatne sa však líšia hodnoty vodivosti kompozitov pri rovnakých objemoch plniva. Vláknité plnivo na báze wollastonitu vykazuje významne vyššiu vodivosť v oblasti plnenia 15 až 30 obj.% plniva v porovnaní s plnivom AGM. Podobnú závislosť získame aj v prípade matrice ChS Epoxy 513/Telalit 410 (Obr. 2). Podľa obr. 2 tvar kriviek vodivosti v závislosti na objeme zakomponovaného plniva má pre obive študované plnivá podobný trend, hoci rozdiely vo vodivosti v oblasti obsahu 15 až 30 obj. % plniva sú výraznejšie v prípade matrice Duvilax LS 50. Podstatný vplyv na vodivosť kompozitov má typ použitého plniva, hlavne tvar jeho častíc. Dosiahnutie vyššej vodivosti v prípade použitia plniva Wollastonit môžeme pravdepodobne pripísať tomu, že vláknité toto plnivo má vzhľadom na svoju geometriu viac možností k vzájomnému kontaktu v kompozite ako je to v prípade čadičového plniva PČ. Zaujímavé je porovnanie hodnôt medze pevnosti skúmaných kompozitov pri dosiahnutí elektrickej vodivosti 1 S/cm. (Tab. 1). Zatiaľ čo pri použití plniva wollastonit má kompozit s elektrickou vodivosťou 1 S/cm medzu pevnosti približne 26 MPa, táto hodnota pre plnivo AGM klesá až na 15 MPa. Na druhej strane má kompozit na báze wollastonitu nižší modul pružnosti E pri približne rovnakej hodnote RPP.

Záver

V predloženej práci bol študovaný vplyv tvaru a koncentrácie elektricky vodivých plnív v polymérnej matrici na elektrické a fyzikálno-mechanické vlastnosti výsledných elektrovodivých kompozitných adhezív: Pri príprave elektrovodivých adhezív boli použité dva typy elektrovodivých plnív s rôznou geometriou častíc: nepravidelné sférické častice resp. častice s vláknitou štruktúrou a dva typy polymérnych matríc: polyvinylacetátová disperzia a dvojzložkový epoxidový systém, Boli stanovené elektrické charakteristiky elektrovodivých kompozitov na báze komerčných adhéznych matríc Duvilax LS 50 a ChS Epoxy 513. Bolo zistené, že pri použitím vláknitého elektrovodivého plniva wollastonit sa dosahuje vyššia elektrická vodivosť kompozitu ako v prípade použitia nepravidelných sférických čadičových častíc plniva AGM v celom rozahu plnenia. Na dosiahnutie vodivosti 1 S/cm je potrebné použiť o 30 obj.% menej wollastonitu v porovnaní s plnivom AGM. Boli stanovené materiálovo-kohézne charakteristiky pripravených elektrovodivých kompozitov. Bolo zistené, že epoxidový kompozit na báze plniva wollastonit dosahuje o cca 70 % vyššiu medzu pevnosti pri pretrhnutí v porovnaní s kompozitom na báze plniva AGM.

Obr. 1 – Závislosť elektrickej vodivosti polymérneho kompozitu na type postriebrených častíc, polymérna matrica Duvilax LS 50

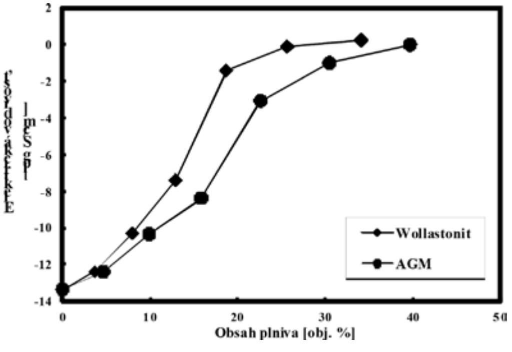

Obr. 2 – Závislosť elektrickej vodivosti polymérneho kompozitu na type postriebrených častíc, polymérna matrica ChS Epoxy 513 : Telalit 410 = 4 : 1

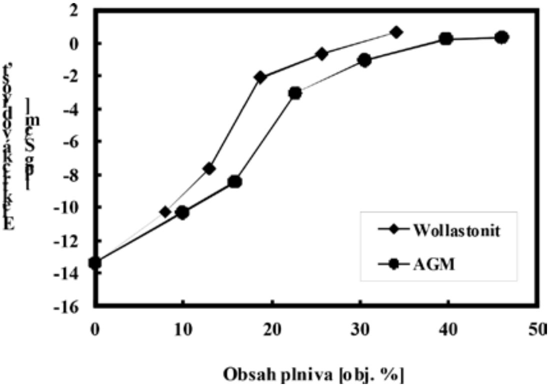

Tab. 1 – Parametre kohéznej pevnosti pri vodivosti 1 S/cm, polymérna matrica ChS Epoxy 513/Telalit 410

Typ Ag plniva Parameter	Wollastonit	AGM
MPP [MPa]	26	15
RPP [%]	1,2	1,2
E [MPa]	1450	2200

Poďakovanie

Príspevok bol podporený Vedeckou grantovou agentúrou Ministerstva školstva, vedy, výskumu a športu SR a SAV, grant VEGA č. 2/0199/14 a Agentúrou na podporu výskumu a vývoja, grant APVV-14-0518.

Použitá literatúra

[1] D.M. Sun, M.Y. Timmermans, Y. Tian, A.G. Nasibulin, E.I. Kauppinen, S. Kishimoto, T. Mizutani, Y. Ohno, Flexible high-performance carbon nanotube integrated circuits, *Nat. Nanotechnol.*, 2011, 6, p 156–161.

[2] T. Sekitani, U. Zschieschang, H. Klauk, T. Someya, Flexible organic transistors and circuits with extreme bending stability, *Chem. Mater.*, 2010, 9, p 1015–1022.

[3] J. H. Ahn, H.S. Kim, K.J. Lee, S. Jeon, S.J. Kang, Y. Sun, R.G. Nuzzo, J.A. Rogers, Heterogeneous three-dimensional electronics by use of printed semiconductor nanomaterials, *Science*, 2006, 314, p 1754–1757.

[4] H. Jiang, K.S. Moon, Y. Li, C.P. Wong, Surface functionalized silver nanoparticles for ultrahigh conductive polymer composites, *Chem. Mater.*, 2006, 18, p 2969–2973.

[5] Y. Li, K.S. Moon, C.P. Wong, Electronics without lead, *Science*, 2005, 308, p 1419–1420.

[6] I.D. Rosca, S.V. Hoa, Method for reducing contact resistivity of carbon nanotube-containing epoxy adhesives for aerospace applications, *Compos. Sci. Technol.*, 2011, 71, p 95–100.

TiO_2 FOTOKATALÝZA – VLASTNOSTI, VYUŽITELNOST, BEZPEČNOST, STANDARDIZACE A MÝTY

PHOTOCATALYSIS OF TIO_2 – PROPERTIES, APPLICABILITY, SAFETY, STANDARDIZATION PROCESS AND MYTHS

PROCHÁZKA J., ŠEFL P.

Advanced Materials-JTJ

Summary

Advanced Materials-JTJ have demonstrated long-term function of FN® Photocatalytic Coatings in variety of medical and environmental applications over the past eight years. Long-term protection against viruses and bacteria has been developed for hospital facilities as well as schools and public places reducing the risk of airborne infection as much as 70%. Protective self-cleaning coating against dirt and microorganisms has been tested over two year in a busy highway junction in Prague for environmental function of air depollution from exhaust gases with an excellent efficiency reaching 40% per pass after two years in this very exposed environment. These useful properties enable us to reduce the hospital acquired diseases, risk of infection in schools and work places, and lower the civilization impact on environment.

Introducing photocatalysis into daily life is however slower than it could have been. Environmental activists with part of academic sector make good living on spreading hysteria about nanoparticles without ever providing any realistic measure or a proof of any particular harm in real conditions unfortunately slow down the process. Lobby protecting the traditional markets also support the groups. Lately, instead of improving our environments and saving life, health and wealth of people, the government bodies introduce new laws and regulations based on the irrelevant reviews of the above groups, which either kill some applications of photocatalysis or make them extremely expensive.

Examples will be provided.

Key words

FN® photocatalytic coatings, air purification, protective coatings, selfcleaning coatings, decontamination, depollution, environmental applications

Advanced Materials-JTJ během posledních osmi let demonstrovali dlouhodobé využití fotokatalytických Funkčních nátěrů (FN®) pro ochranu povrchů proti špíně a mikroorganismům, elektivní čištění vzduchu v interiérech a antibakteriální účinnost, která, jak předvedl známý odborník na hygienu RNDr. Erich Pazdziora je poprvé v historii schopna poskytnout dlouhodobou ochranu pacientů i personálu v nemocničních zařízeních.

Velmi podstatnou funkcí fotokatalytického povrchu je jeho schopnost čistit vzduch od exhalací a zlepšovat tak znečištění vytíženého prostředí. Před dvěmi lety naše firma ošetřila zvukové bariéry u frekventované komunikace na Barrandově a po této době vystavení všem vlivům počasí a exhalátů z dopravy je její účinnost pro dekontaminaci vzduchu prakticky nezměněna. Tento reálný pokus ukazuje na perfektní použitelnost fotokatalytických nátěrů FN pro dekontaminaci vzduchu a zlepšení životního prostředí. Presentované výsledky mají zásadní charakter a ověřila je Akademie věd a VŠCHT

Podle údajů ministerstva životního prostředí žije na území se zhoršenou kvalitou ovzduší 51 % obyvatelstva ČR a toto teritorium představuje 22 % rozlohy ČR. V posledních 5 letech byly uzákoněny nové imisní limity, závazné v celé EU, které však ve většině evropských měst nejsou dodržovány. International Agency for Research on Cancer (IARC), součást World Health Organization (WHO), klasifikovala v květnu 2012 spaliny z dieslových motorů jako karcinogení pro člověka (Group 1). Direktiva EU 1999/30/ES zároveň požaduje výrazné snížení emisí oxidů dusíku a to již od ledna 2010 ve všech členských zemích EU a nedávné snížení povolených koncentrací benz(A)pyrénu pod 2ppb reaguje na jeho vysokou nebezpečnost nejenom v ovzduší, ale také ve spodních vodách.

Pro dekontaminaci vody na fotokatalytických nátěrových produktech FN, Advanced Materials-JTJ se svými partnery provedly rozsáhlou škálu laboratorních a praktických experimentů s odstraňováním nebezpečných látek z vody pomocí fotokatalýzy. Konkrétní rozklady pesticidů, antibiotik a dalších nebezpečných látek a využitelnost pro dekontaminaci životního prostředí budou presentovány v této sekci.

Ochrana povrchů a životního prostředí pomocí multifunkčních nátěrů přináší nové kvality a možnosti, které pomáhají zlepšit kvalitu našeho života, stejně jako zmírnit civilizační dopady na životní prostředí.

Proti uvedení této moderní technologie do praxe však tradičně postupují nejrůznější síly, které technický pokrok buďto zdržují, nebo, jak si ukážeme na příkladech, jsou schopny jej kompletně znemožnit. Nejsou to jenom militantní aktivisté, kteří se často opírají o zcela nevěrohodné důkazy a zpravidla ani nehledí na absurditu svých tvrzení, ale další zájmovou skupinou, která působí proti novým technologiím je část akademické sféry, jenž si ze zpochybňování bezpečnosti nanomateriálů a šíření hysterie dělá vynikající živnost. Nelze ani přehlídnout zájmové lobby, které budou vždy chránit své zavedené technologie a vystupovat proti lepším řešením dokud se jejich investice nevrátí. Aktivity předešlých skupin vedou k tomu, že státní správa následně dělá paradoxní kroky, které na základě neoddůvodněných obav, bez seriózních expertních komisí a bez žádného praktického podložení, vedou k legislativním změnám, které dlouhodobě znemožňují využití výhod, které nám fotokatalytická technologie nabízí nebo je zásadním způsobem prodražují.

Praktické příklady z oblasti hygieny, kosmetiky, výroby pigmentů a barev budou diskutovány.

METODY STANOVENÍ FOTOKATALYTICKÉ ÚČINNOSTI RŮZNÝCH TYPŮ POVRCHŮ

METHODS OF PHOTOCATALYTIC ACTIVITY ASSESSMENT ON VARIOUS TYPE OF SURFACES

BAUDYS M.[1,2], KRÝSA J.[2]

1 Technoparc Kralupy UCT Prague, Žižkova 7, 27801 Kralupy nad Vltavou

2 Department of Inorganic Technology, University of Chemistry and Technology Prague (UCT),
Technická 5, 16628 Praha 6

Summary

The objective of this paper is to summarize methods of photocatalytic activity assessment which can be applied on various types of surfaces. Beside standard ISO methods in gas phase the paper is focused on the application of model inks which can be used as rapid indicators of photocatalytic activity. The principle is in irreversible reduction of dye in ink which occurs on photocatalytic surface only. This method can be applied on water based acrylic paint containing 8% of photocatalyst anatase. During weathering in QUV photocatalytic activity increases (increase of rate of photocatalytic oxidation of acetaldehyde and also rate of reduction of ink containing Acid Violet 7). This increase can be explain by the degradation of polymer paint on the surface resulting in increase of TiO_2 particles available for photocatalytic reaction which was proved by EDS EDAX analysis.

Key words

Photocatalysis, TiO_2, model inks, self-cleaning, ISO test, acetaldehyde.

Introduction

Semiconductor photocatalysis is a promising method for the decomposition of various compounds, either pollutants dissolved in water (dyes, pesticides, drugs, etc.) or pollutants present in air (NO_x or VOC). Another application are self-cleaning surfaces which via the combination of photocatalytic activity and photoinduced superhydrophilicity are not so much susceptible to soiling and help to keep such surface clean [1]. Typical example of such surfaces are photocatalytic facade paints, recently also paints for indoor use, which claim to improve air quality, appear on the market.

The principle of photocatalysis is given by adsorption of UV light by photocatalyst particle (mostly TiO_2 of anatase modification) which leads to generation of hole – electron pairs. Most of the photogenerated holes and electrons recombine into heat, only smart portion of separated reactive species reach the surface of the photocatalyst where they can participate in redox reactions. Holes (or ·OH radicals) have high oxidation potential and are able to oxidized even stable organic compounds. Comparing to other advanced oxidation processes, the main advantage of photocatalysis is that except UV light and photocatalyst we don't need to add into system other reagent [2].

Commercial widespread of photocatalytic materials provoked the need of photocatalytic testing using standards method. Thus the goal of this paper is to introduce various methods of photocatalytic activity assessment which can be applicable on various commercial products such as photocatalytic glass, paints, ceramics etc. [3, 4].

ISO standard methods

To assess the photocatalytic ability of pollutants removal from air, there are several ISO standard methods differing with the type of pollutant, concentration and total gas flow. The summary of ISO standard method is in Table 1. Popular method is based of removal of NO_x, because the supply NO gas is very quickly oxidized to NO^-_3 (due to the relatively low oxidation potential of NO to NO_3^- = 0,957 V vs. NHE compared to the potential of valence band hole (3V)). The photocatalytic oxidation of NO to NO_3^- proceeds via following reaction (eq. 1–3). Potential accumulation of nitric acide caused production of NO_2 (eq. 3) which is more toxic than the inlet NO. This can lead to steady state, when the amount of NO removal is given by the rate of NO_2 production [5, 6].

Tab. 1 – Parameters of standard ISO method

Standard **Pollutant**	ISO 22197-1 NO	ISO 22197-2 acetaldehyde	ISO 22197-3 toluene	ISO 22197-4 formaldehyde
Initial concentration [ppm]	1	5	5	1
Total flowrate [dm³/min]	3	1	0.5	1
Intensity of UV light [mW/cm²]	1	1	1	1
Test time [hours]	5	3	3	3
Analysis	chemiluminiscence analyser	GC	GC	GC

$$4NO + O_2 + 2H_2O \xrightarrow{h\nu,\, TiO2} 4HNO_2 \qquad \text{(eq. 1)}$$

$$2HNO_2 + O_2 \xrightarrow{h\upsilon,\, TiO2} 2HNO_3 \qquad \text{(eq. 2)}$$

$$2HNO_3 + NO \xrightarrow{h\upsilon,\, TiO2} 3NO_2 + H_2O \qquad \text{(eq. 3)}$$

The typical time dependence of concentration in case of NO_x test is illustrated on Fig. 1. The amount of photodegraded NO_x is than proportional to the difference of integrated area above the NO curve and the area under NO_2 line. Photocatalytic activity is than expressed as the amount of NO_x removal during 5 hour test using formula 4, where n_{ads} is the amount adsorbed on the test piece, n_{des} is amount desorbed by the test piece and n_{NO} and n_{NO_2} is equal to integrated areas above NO curve and under NO_2 curve respectively.

$$n_{NO_x} = n_{ads} + n_{NO} + n_{NO_2} + n_{des} \qquad \text{(eq. 4)}$$

Fig. 1 – Example of thew concertation profile of NO, NO_x and NO_2 during the photocatalytic experiment

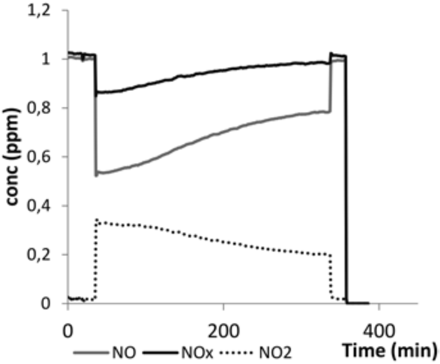

Another example of ISO standard are methods using organic compounds such as formaldehyde, acetaldehyde, and toluene. This methods are performed on the same apparatus as a NO_x test, the difference is in analysis which is realized by gas chromatography. Photocatalytic activity is than expressed as the amount of degraded pollutant in a last hour of the test [7]. An example of removal of acetaldehyde on photocatalytic coating is shown on Fig. 2. In case of sample containing pure anatase (particle layer prepared by sedimentation of TiO_2 suspension) we can see high conversion of acetaldehyde removal (conversion about 90 %). In case of sample of an acrylic paint (8 wt. % of anatase photocatalyst) the decrease of acetaldehyde concentration is negligible. This is not surprising because active particles are covered by the binder. After exposition in QUV panel simulating accelerated weathering effect the thin polymer film on the paint surface degrades which results in an increase of surface-exposed concentration of TiO_2 particles. The increase of surface concentration was proofed using EDAX EDS analysis. After exposition in QUV panel Ti surface concentration increases form 43 % (unexposed paint) to 55 % (after QUV exposition) [8].

Fig. 2 – Concentration of acetaldehyde during the photocatalytic experiment

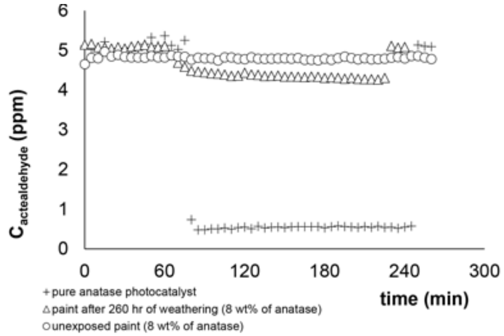

Model inks

Unlike ISO standard methods (in gas phase), model inks represent inexpensive rapid method of photocatalytic activity assessment. The method is based on irreversible color change of dye in ink which occurs on the photocatalytic surface. Ink consists of dye (the reduction of dye is connected with change of color), hydroxyethylcelulose (binder) and the excess of glycerol which acts as a sacrificial electron donor. Most of photocatalytic processes are connected with the low quantum yields (most of photogeneration carriers recombine thus only small portion of adsorbed photon are converted to oxidation species). In model ink, due to the presence of glycerol (which is oxidized by holes to glyceraldehyde), the charge separation is efficient and the reduction of dye, which is connected with color change, is very quick and takes few seconds. From the practical point of view it is important to say, that the reduction method based on smart inks is equivalent to methods based on oxidation processes [9].

Fig. 3 – An example of discoloration of ink containing dye Acid Violet 7 on photocatalytic paint (top) and on reference sample (bottom)

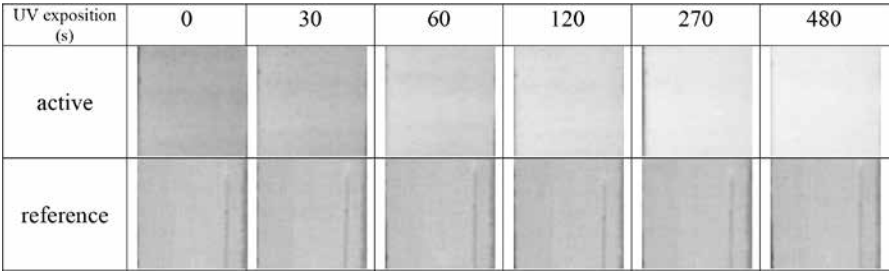

The advantage of model ink is in low demand on laboratory equipment. Color change of model ink is periodically recorded using hand held scanner and photocatalytic activity is than expressed as a time of irradiation needed to 90 % of overall color change (Ttb90).

On the Fig. 4 there is illustrated a correlation between the rate of photocatalytic reduction (reduction of model ink containing Acid Violet 7) and the rate of photocatalytic oxidation of acetaldehyde according to the ISO 22197-2 standard. We can see that after exposition in QUV panel (260 hr) the rate of photocatalytic reduction and the rate of photocatalytic oxidation increases, so both methods gives similar results. The increase of photocatalytic activity can be explained by the increase of surface-exposed concentration of TiO_2 particles during weathering test.

Fig. 4 – Photocatalytic activity of acrylic paint (containing 8% of anatase photocatalyst) as a function of exposition in QUV, comparison of two methods of photoactivity evaluation

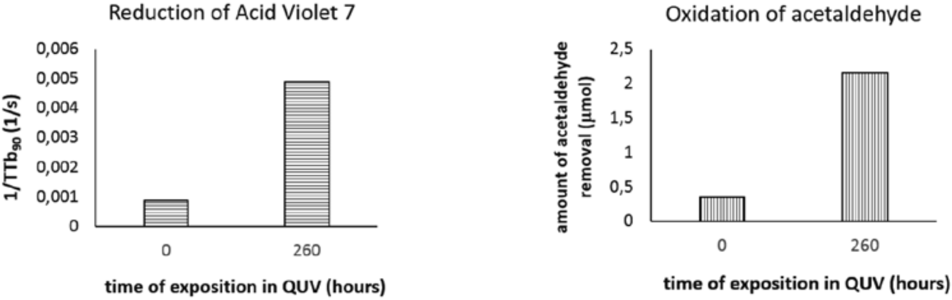

Conclusions

Model inks can be used as a rapid method for photocatalytic assessment of various surface paints, glass, and ceramics. Compared to oxidative bleaching of dyes, due to the presence of glycerol which improves charge separation and reduce recombination losses, the color change of ink on photocatalytic surface is very quick, take few seconds. This method is in good agreement with an ISO standard oxidation method in gas phase (oxidation of acetaldehyde) as was proved by the photoactivity evaluation of photocatalytic paint during accelerated weathering test.

References

[1] S. Banerjee, D.D.Dionysiou, S.C.Pillai, Self-cleaning applications of TiO_2 by photo-induced hydrophilicity, *Appl. Catal. B:Enviromental,* 2015, 176, p396

[2] A. Fujishima, T.N. Rao, D.A. Tryk, Titanium dioxide photocatalysis *J. Photochem. And Photobiol C:Chemistry,* 2000, 1, p 1

[3] A. Mills et all. A simple, inexpensive method for the rapid testing of the photocatalytic activity of self--cleaning surfaces, *J. Photochem and Photobiol A: Chemistry,* 2013, 272, p18.

[4] A. Mills et all Photocatalytic activity indicator inks for probing a wide range of surfaces, *J. Photochem and Photobiol A:Chemistry,* 2014, 290, p63

[5] ISO 22197-1:2007, Fine ceramics, advantage technical ceramics – test method for air-purification performance of semiconducting photocatalaytic materials – part 1: removal of nitric oxide, ISO, Geneva, 2007.

[6] A. Mills et all., Overview of the current ISO test for photocatalytic materials, *J. Photochem and Photobiol: A: Chemistry* 2012 237 p7

[7] ISO 22197-2:2011 Fine ceramics, advantage technical ceramics – test method for air-purification performance of semiconducting photocatalaytic materials – part 2: removal of acetaldehyde, ISO Geneva, 2011

[8] M. Baudys et. all, Weathering test of photocatalytic facade paints containing ZnO and TiO_2. *Chemical Engineering Journal* 2015, 261, p83

[9] J. Krýsa et all, Quantum yield measurements for the photocatalytic oxidation of Acid Orange 7 (AO7) and reduction of 2,6-dichlorindophenol (DCIP) on transparent TiO_2 films of various thickness, *Catal. Today* Volume 240, Part A, 2015, 240, p132

IČ REFLEKTIVNÍ KOMPLEXNÍ ANORGANICKÉ PIGMENTY TOMATEC

IR REFLECTIVE COMPLEX INORGANIC COLOUR PIGMENTS TOMATEC

KUMM R., ZOUHAR D.

Grolman s.r.o.

Summary

The paper describes structure, properties and potential application of Tomatec complex inorganic colour pigments. CICPs are highly stable pigments concerning heat, UV and chemicals, they are relatively easy to disperse and show wide compatibility in various paints and coatings systems and plastics. Thanks to their structure, IR reflective grades are capable of reflecting solar irradiation in IR spectra, thus keeping the irradiated surface relatively cool, although the visible colour is dark. This effect then affects various parameters in the end application, such as energy savings, formaldehyde emissions, fire retardancy, dilatation, aging, etc. Measurements of reflective curves, variety of available colours is presented.

Key words

CICP pigment, IR Reflective, surface temperature, camouflage paints, heat buildup reduction, Tomatec

HANSENOVY PARAMETRY ROZPUSTNOSTI

HANSEN SOLUBILITY PARAMETERS

BANDŽUCH J.
SYNPO, a.s.

Summary

The paper deals with determination of Hansen solubility parameters some raw materials designed for coatings production. There is discussed possibilities utilization of measured values in practice.

Key words
Hansen solubility parameters, coatings

Hansenovy parametry rozpustnosti (HSP) byly vyvinuty dr. Charlesem Hansenem (1938), jako cesta k predikci zda se bude jedna látka rozpouštět v druhé a budou tak tvořit spolu roztok. Poprvé byly publikovány v roce 1967.

HSP jsou založeny na myšlence, že podobný se rozpouští (mísí) v podobném. Tj. obdobné molekuly jsou charakterizovány podobnými vazbami. Na základě této úvahy lze podle dr. Hansena charakterizovat každou molekulu třemi parametry (v MPa$^{1/2}$):

δ_d – energie z disperzních sil mezi molekulami. Jedná se obecně o van der Waalsovy interakce mezi všemi molekulami. S ohledem na skutečnost, že jsou všudypřítomné, máme tendenci je ignorovat. Nicméně pro jejich účinnost si stačí připomenout známý „Gekoní“ efekt, který umožňuje tomuto zvířeti chodit i po svislých plochách.

δ_p – energie z disperzních sil mezi molekulami. V tomto případě jde o přitažlivost mezi molekulami na základě existujících dipólů. Tyto síly jsou významné téměř ve všech molekulách s výjimkou některých uhlovodíků a fluorovaných uhlovodíků.

δ_h – energie z vodíkových vazeb mezi molekulami. Jedná se o velmi významné síly, vždyť jen díky nim je voda kapalná.

Tyto tři hodnoty mohou pak být využity jako souřadnice v 3D prostoru. Pak lze konstatovat, že nejbližší dvě molekuly budou „mísitelné“.

Vzdálenost mezi dvěma body v 3D Hansenově prostoru se pak vypočte:

$(R_a)^2 = 4(\delta_{d2} - \delta_{d1})^2 + (\delta_{p2} - \delta_{p1})^2 + (\delta_{h2} - \delta_{h1})^2$

Poté lze na základě 3D energetické sféry látky R_0 definovat tzv. relativní energetický rozdíl dvou látek RED.

$RED=R_a/R_0$

Pro RED < 1… látky jsou mísitelné

Pro RED = 1 … látky jsou omezeně mísitelné

Pro RED > 1… látky jsou nemísitelné

Stanovení Hansenových parametrů rozpustnosti

Z důvodu relativní jednoduchosti byla použita metoda doporučovaná dr. Hansenem, která se zakládá na sledování snášenlivost různých typů látek, u kterých známe jejich parametry rozpustnosti, s látkou měřenou. Z tohoto důvodu byl vytvořen soubor rozpouštědel (z větší části běžně používaných látek), který (včetně hodnot jednotlivých parametrů rozpustnosti) uvádí následující tabulka 1.

Tab. 1 – Soubor použitých rozpouštědel

Rozpuštědlo	δ_d (Mpa$^{1/2}$)	δ_p (Mpa$^{1/2}$)	δ_h (Mpa$^{1/2}$)
Xylen	17,8	1	3,1
Aceton	15,5	10,4	7,0
Toluen	18,0	1,4	2,0
Ethylenglykolmonobutylether	16	5,1	12,3
2-Propanol	15,8	6,1	16,4
n-Butylacetát	15,8	3,7	6,3
Isobutylalkohol	15,1	5,7	15,9
Diethylenglykolmonobutylether	16	7	10,6
N,N-Dimethylformamid	17,4	13,7	11,3
Propylenglykolmonomethylether acetát	15,6	5,6	9,8
Propylenglykolmonomethylether	15,6	6,3	11,6
Glycerol	17,4	11,3	27,2
Dipropylenglykolmonomethylether	15,5	5,7	11,2
Diacetonalkohol	15,8	8,2	10,8
Propylenglykol	16,8	10,4	21,3
Diethylenglykomonoethylether	16,1	9,2	12,2
Ethylenglykolmonobutylether acetát	15,3	7,5	6,8
2,2,4-Trimethyl-1,3-Pentandiol Monoisobutyrát	15,1	6,1	9,8
Methylisobutylketon	15,3	6,1	4,1
Heptan	15,3	0	0
N-Methyl-2-Pyrrolidon	18	12,3	7,2
n-Butylpropionát	15,7	5,5	5,9
Rhodiasolv RPDE	17,21	6,26	9,16
Rhodiasolv DIB	15,9	2,4	7,1
o-Dichlorobenzen	19,2	6,3	3,3
Propylenkarbonát	20	18	4,1
Acetonitril	15,3	18	6,1
Nitromethan	15,8	18,8	6,1
Diethylether	14,5	2,9	4,6
Voda	18,1	17,1	16,9

Těmito rozpouštědly jsme se snažili pokrýt co nejširší rozsah jednotlivých parametrů rozpustnosti a zároveň se vyhnout použití velmi drahých či vyloženě toxických látek. Rozmístění jednotlivých látek v Hansenově třírozměrném prostoru je pak zobrazeno v obrázku 1.

Obr. 1 – Rozmístění použitých rozpouštědel v Hansenově 3D prostoru

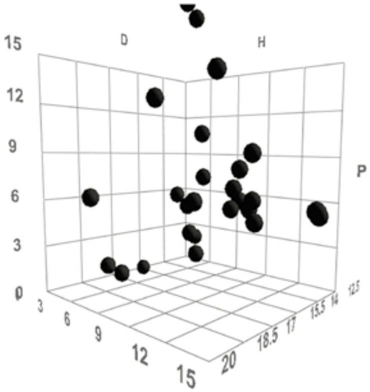

Postup stanovení parametru rozpustnosti touto metodou byl následující. Do zkumavky byl odvážen cca 1 g zkoumané látky a následně bylo přidáno cca 5 g látky o známém parametru rozpustnosti. Zkumavka byla uzavřena a směs látek byla homogenizována. Poté byla zkumavka vložena do stojánku v laboratoři. Po 24 hodinách byly vzorky vyhodnoceny vizuálně následujícím způsobem – pokud vznikl homogenní roztok, bylo rozpouštědlo „dobré“, pokud nevznikl homogenní roztok, bylo rozpouštědlo „špatné“. Pomocí takto získaného výsledného „skóre“ byly stanoveny HSP počítačovým programem HSPiP (Hansens parameters in Practice). Výsledky stanovení jsou uvedeny v tabulce 2.

Tab. 2 – Hodnoty HSP stanovené u pojiv

Látka	δ_d (Mpa$^{1/2}$)	δ_p (Mpa$^{1/2}$)	δ_h (Mpa$^{1/2}$)	δ (Mpa$^{1/2}$)
Laropal A81	22,9	0,04	14,6	27,2
SFD 2	14,0	8,2	1,4	16,3
S621	15,7	6,2	6,3	–

Obdobně bylo provedeno stanovení HSP některých aditiv a dalších látek používaných ve výrobě nátěrových hmot. Výsledky jsou uvedeny v tabulce 3 a jejich grafické znázornění v 3D Hansenově prostoru pak na obrázku 2.

Obr. 2 – Hodnoty HSP u některých aditiv umístěné v 3D Hansenově prostoru

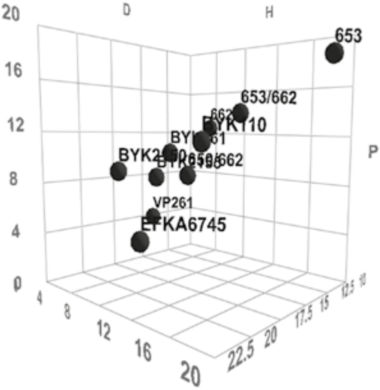

Tab. 3 – Hodnoty HSP u některých aditiv

Látka	δ_d (Mpa$^{1/2}$)	δ_p (Mpa$^{1/2}$)	δ_h (Mpa$^{1/2}$)	δ (Mpa$^{1/2}$)
TEGO 650	18,5	6,5	9,4	21,8
TEGO 651	11,9	15,1	19,6	27,4
TEGO 653	12,2	18,2	19,7	29,5
TEGO 662C	12,2	12,5	6,0	18,4
VP261	15,6	4,4	2,7	16,5
DisperByk 2150	19,6	9,0	5,1	22,2
DisperByk 161	16,5	10,4	6,7	20,6
BYK 110	18	11,5	12,7	24,9
LOVOCOAT FORM	17	0,04	9,2	19,3
LOVOCOAT STABLE	17,9	15,4	16,3	28,7
DisperBYK110	17,1	10,6	6,7	21,2
ASIL 200	18	12,3	7,2	–
FORM/STABLE 3/2	17,2	10,9	8,9	22,3
DISPERBYK 2155	17,3	8,4	6,1	20,2
ACEMAT TS100	17,2	10	9	21,8
EFKA 6745	20,7	4,4	9,8	23,3

Stejným způsobem byly také stanoveny hodnoty HSP pro pigmenty. Zde však bylo vyhodnocení daleko složitější. Ideální by bylo měření rychlosti sedimentace měřené látky v jednotlivých rozpouštědlech. Protože tento způsob měření nebylo možné v našich podmínkách realizovat, vyhodnocení bylo provedeno podle kritérií uvedených v tabulce 4.

Tab. 4 – Vyhodnocování HSP u pigmentů

Parametr	Hodnocení
1	Kompletně dispergováno (homogenní disperze)
2	Dispergováno, ale nehomogenní
3	Velmi nehomogenní
4	Zbotnáno, ale pigment sedimentuje
5	Totálně odděleno (sedimentováno)

Kdy hodnoty parametru 1a 2 byly považovány za vyhovující (snášenlivý systém), hodnoty 3 až 5 za nevyhovující (nesnášenlivý systém). V tabulce 5 jsou uvedeny hodnoty HSP některých změřených pigmentů.

Tab. 5 – Hodnoty HSP u některých pigmentů

Látka	δ_d (Mpa$^{1/2}$)	δ_p (Mpa$^{1/2}$)	δ_h (Mpa$^{1/2}$)	δ (Mpa$^{1/2}$)
RKB 2	19,3	9,5	21,4	30,3
RGU	20,4	13,7	14,7	28,7
ASG V	16,5	8,6	5,1	19,3
SICOTAN Gelb	18,0	0	7,8	19,6
IRGALITE Yellow	19,0	10,7	6,3	22,7
FEPREN	22,6	1,9	15,4	27,5
Červeň DP3G	23	6,9	15,7	–
MONARCH 120	20,9	12,5	11,4	26,9
BAYFERROX 3920	19,1	5,3	13,8	24,1
PALIOTEL ORANGE	23,2	10,4	14,6	29,3
HOSTAPERM VIOLET	17,5	11	8,8	22,4
HELIOGEN GRUN	19,6	14,6	7,7	25,6
VERSÁL ŽLUŤ 2GXD	19	12,2	7,3	23,7
LITHAL ECHTTMARRON	20,6	8,4	5,6	22,9

V následujícím obr. 3 jsou zobrazeny tyto hodnoty v 3D Hansenově prostoru. Na obr. 4 je pro ilustraci uvedeno umístění modři ASG v 3D Hansenově prostoru včetně znázornění sféry R0 pro tuto látku.

Obr. 3 – Hodnoty HSP u některých pigmentů umístěné v 3D Hansenově prostoru

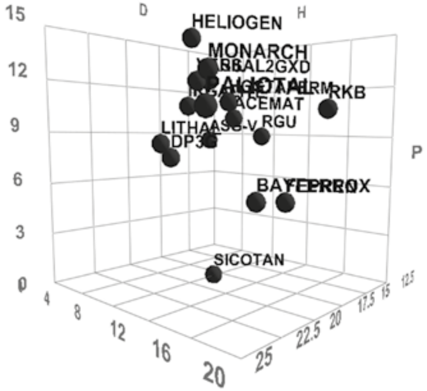

Obr. 4 – Modř ASG v 3D Hansenově prostoru

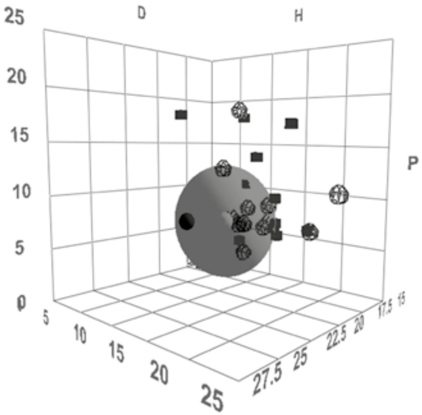

Závěr

Pomocí této relativně jednoduché a levné metody (pomocí parametrů rozpustnosti) lze charakterizovat suroviny používané pro výrobu nátěrových hmot. Možnosti využití parametrů rozpustnosti jednotlivých látek lze v oboru nátěrových hmot podle mého názoru spatřovat v následujících oblastech:

– Sledování kvality (respektive rozptylu vlastností) u problematických surovin, které nelze bez použití velmi náročných analytických metod analyzovat (hodnotit jejich kvalitu).

– Výběr vhodných rozpouštědel, případně jejich směsí, pro daný polymer, tak, aby bylo možno matematicky (nikoli empiricky) zajistit dobrou kompatibilitu systému a zároveň zabezpečení dobré adheze na substrát a ovšem i možnost náhrady ekologicky či senzoricky nevyhovující rozpouštědla rozpouštědly lépe vyhovujícími požadavkům.

– Výběr vhodných rozpouštědel a dispergačních aditiv pro daný systém pojivo – rozpouštědlo – pigment (plnivo).

Poděkování

Tato přednáška byla vypracována s podporou MPO – projekt FR-TI3-57.

SOUČASNÉ KLÍČOVÉ VÝZVY VÝROBCŮ 2K POLYURETHANOVÝCH NÁTĚRŮ NA KOV (A JEJICH MOŽNÁ ŘEŠENÍ POMOCÍ MODERNÍCH POLYISOKYANÁTOVÝCH TECHNOLOGIÍ)

KEY CHALLENGES FACING FORMULATORS OF 2K PU METAL COATINGS TODAY (AND POSSIBLE SOLUTIONS USING MODERN POLYISOCYANATE TECHNOLOGIES)

CORNICK M.

Market Development Manager, Vencorex

Summary

The presentation deals with using different aliphatic polyisocyanate technologies in the hardener component of 2K polyurethane coating formulations, in order to solve technical challenges that face the formulators of such coatings systems.

Key words

Aliphatic isocyanate, low VOC, high solids, drying time, corrosion resistance

Polyurethane coatings are used in a variety of applications today, including: coatings on metal for the automotive, engineering and transportation industries, coatings on wood for the construction and furniture industries, and coatings on plastic for electronic goods. Aliphatic polyisocyanates (as opposed to their aromatic counterparts) in particular are used as cross-linkers in those application areas where a high degree of UV, weathering, and chemical resistance is required.

The performance requirements coming from the applications where such coatings are used are becoming increasingly challenging. Therefore the formulator of such coatings must be aware of all of the tools that can potentially be used in order to meet such technological challenges.

This presentation examines three such challenges that face formulators working in the area of coatings for metal substrates, and proposes possible routes via. aliphatic polyisocyanate technologies to solve such challenges.

The challenges that are considered in this presentation are:

- Increased regulation on VOC / demand for high solids
- Increasing demands on product / process efficiency
- Increasing demands on product performance (better impact strength, adhesion and corrosion resistance)

With regard to the demand for low VOC / high solids coatings, the presentation shows that the viscosity of the polyisocyanate that is used can directly influence the VOC level in the final coating formulation, as seen in the figure below –

Fig. 1 – VOC of coating formulation as a function of viscosity of hardener

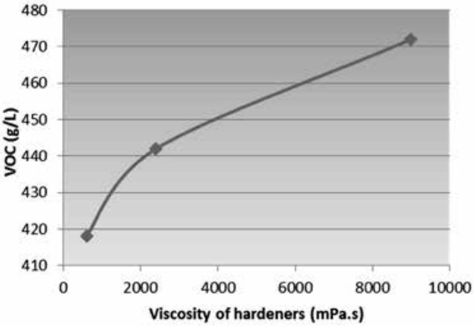

The presentation then goes on to discuss the options for using lower viscosity polyisocyanates, e.g. to replace “traditional” hexamethylene diisocyanate biuret hardeners with hexamethylene diisocyanate trimer hardeners, and the potential to use lower molecular weight polyisocyanates, in order to achieve reductions in the VOC level of the final coating formulation.

With regard to the demands on product / process efficiency, the presentation looks at the drying time of coatings and shows how it is possible to increase the drying speed of a formulation based on a hexamethylene diisocyanate trimer hardener by partially replacing this material with an isophorone diisocyanate trimer hardener, as seen in the figure below –

Fig. 2 – Dust free time for coatings containing various mixtures of HDI and IPDI trimers

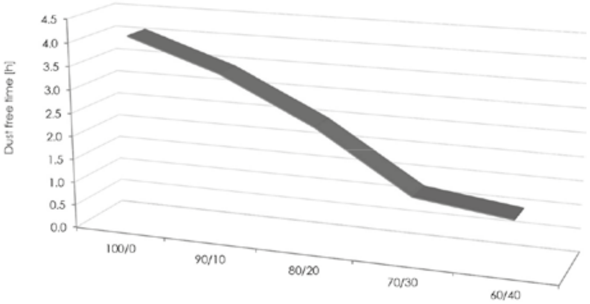

The presentation also looks at the advantages and disadvantages in drying speed and performance that can be obtained by using higher functionality polyisocyanate hardeners.

In the section on increasing demands on product performance, the presentation looks at a number aspects, such as impact resistance, adhesion and corrosion resistance. Here an innovative polyisocyanate technology is introduced exhibiting a high degree of flexibility and hydrophobicity, combined with an ultra-low viscosity, which has been proven to give some advantages in different formulations, with regard to these aspects.

Fig. 3 – Impact resistance of coating with / without inclusion of flexible polyisocyanate

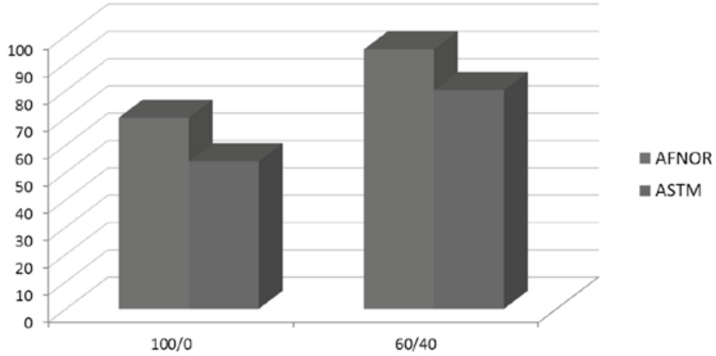

Acknowledgements

P. Barbeau, A. Jomier, R. Klucker, S. Nabet and P. Olier; all from Vencorex.

ECOS ND15, NOVÝ KOBALTOVÝ URYCHLOVAČ SUŠENÍ OXIDAČNĚ VYTVRZOVANÝCH POVLAKŮ

ECOS ND15, A NOVEL COBALT BASED ACCELERATOR FOR THE DRYING OF OXIDATIVELY CURING COATINGS

SCHOLLAERT T.

UMICORE SPECIALTY MATERIALS, BELGIUM

Summary

Since decades cobalt carboxylates have been used as primary catalysts for the cross-linking of oxidatively curing coatings.

Current cobalt-based products, used as driers in inks and coatings or as accelerators for curing unsaturated polyester resins and gel-coats, are increasingly under pressure due to the uncertainty on their hazard classification and REACh implementation. Indeed, some inorganic cobalt salts are yet classified as lung carcinogen category 1B (EU Regulation). If cobalt carboxylates would get classified as carcinogenic by inhalation then the future use of these products will be restricted.

Umicore has developed an innovative cobalt based accelerator, proven to be much less hazardous than current cobalt carboxylates. A unique chemistry embeds cobalt into a polymer structure, assuring minimal bioavailability and hindering any toxicological effect while safeguarding an excellent performance.

The innovation resides in a combination of metal and alkyd chemistry, resulting in a 'safety-by-design' compound. The presentation will give more details on the chemistry, toxicology assessment and performance of the novel accelerator.

Keywords

ECOS ND15, cobalt replacement, REACh implementation, toxicity, inks, paints, coatings, unsaturated polyester

VLIV TECHNOLOGIE MLETÍ NA VLASTNOSTI PIGMENTU

THE IMPACT OF GRINDING TECHNOLOGY ON THE PROPERTIES OF PIGMENTS

RESCH P.

Fryauf Filmix s.r.o., zastoupení firmy NETZSCH Feinmahltechnik GmbH

Technologie zjemňování částic je jedním ze zásadních parametrů, který ovlivňuje vlastnosti pigmentů. Tyto technologie přitom zaznamenávají rychlý vývoj a postupy, které byly obvyklé včera, již nemusí platit zítra. V praxi to například může znamenat, že i při důsledném sledování běžných kvalitativních vlastností pigmentů se může pigment chovat v recepturách jinak pouze kvůli změně technologie mletí. Jak v pozitivním, tak v negativním slova smyslu.

Následující přednáška vybírá nejobvyklejší technologie mletí pigmentů, k nimž přiřazuje charakteristické vlastnosti, které můžeme pro tu či onu technologii očekávat.

Sledovanými veličinami jsou:

- Dosažitelná jemnost mletí
- Tvar (šíře) distribuční křivky částic
- Tvar částic
- Tepelné namáhání částic
- Další specifika jednotlivých systémů

Porovnáváme následující technologie:

- Kulové mlýny / suché perlové mlýny
- Kolíkové mlýny
- Úderové mlýny se vzdušným tříděním
- Tryskové mlýny
- Perlové mlýny

KULOVÉ MLÝNY / SUCHÉ PERLOVÉ MLÝNY

Obr. 1 – Kulový mlýn

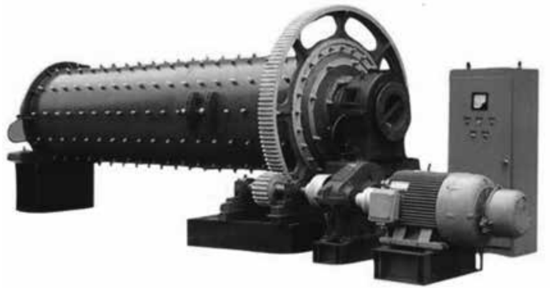

Obr. 2 – Suchý perlový mlýn SpheRho

Dosažitelná jemnost mletí: desítky až stovky mikrometrů. Tvar distribuční křivky: velmi široká, možné upravit následným vzdušným tříděním. Tvar částic: téměř nemožné ovlivnit, protože vkládanou energii do mletí není téměř možné regulovat, poněkud lepší u suchého perlového mlýnu. Tepelné namáhání částic: poměrně malé, protože celková energie vztažená na jednotku objemu je nízká ve srovnání s ostatními mlecími systémy.

KOLÍKOVÉ MLÝNY

Obr. 2 a 3 – Kolíkové mlýn Condux

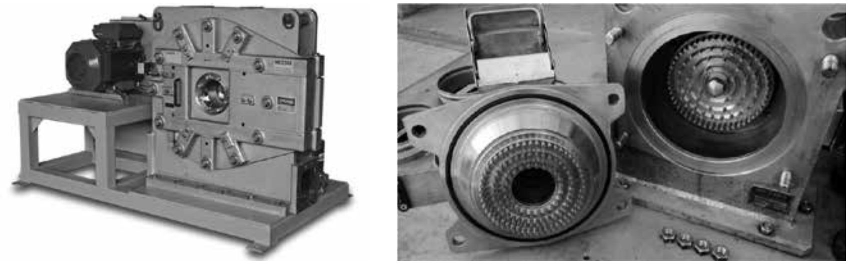

Dosažitelná jemnost mletí: desítky až stovky mikrometrů, obvykle pouze desaglomerace, nikoli mletí primární částice. Tvar distribuční křivky: poměrně široká Tvar částic: obvykle se jedná o desaglomeraci, mlýn tedy neovlivňuje zásadně tvar částic. Tepelné namáhání částic: teplotní spád vstup – výstup obvykle 10–20°C, snadná možnost chlazení plynem.

ÚDEROVÉ MLÝNY SE VZDUŠNÝM TŘÍDĚNÍM (TŘÍDÍCÍ MLÝNY)

Obr. 4 – Třídicí mlýn CSM

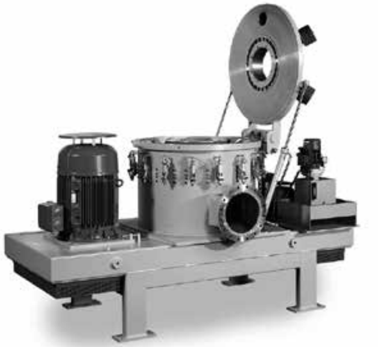

Dosažitelná jemnost mletí: desítky, výjimečně i jednotky mikrometrů. Tvar distribuční křivky: úzká. Tvar částic: tvar částic lze částečně ovlivnit energií vkládanou do mlecího procesu. Tepelné namáhání částic: velmi snadná možnost chlazení plynem. Ostatní: jednoduchá možnost přidávání aditiv (tekutých i kapalných).

TRYSKOVÉ MLÝNY

Obr. 5 – Tryskový mlýn CGS

Obr. 6 – Tryskový mlýn ConJet

Dosažitelná jemnost mletí: jednotky mikrometrů, tryskové mlýn s parou stovky nanometrů. Tvar distribuční křivky: velmi úzká (nejužší ze sledovaných systémů). Tvar částic: tvar částic lze velmi dobře ovlivnit energií mletí. Tepelné namáhání částic: velmi snadná možnost chlazení plynem. Ostatní: jednoduchá možnost přidávání aditiv (tekutých i kapalných), tryskové mlýny s parou dokáží odvádět z materiálu vodu.

PERLOVÉ MLÝNY

Obr. 7 – Perlový mlýn Alfa

Obr. 8 – Perlový mlýn LME

Dosažitelná jemnost mletí: desítky mikrometrů až jednotky nanometrů. Tvar distribuční křivky: v závislosti na vedení technologického procesu poměrně široká až úzká. Tvar částic: tvar částic lze velmi dobře ovlivnit energií mletí. Tepelné namáhání částic: velmi snadná možnost chlazení. Ostatní: možnost přidávání aditiv, velmi flexibilní a univerzální systém.

ANALÝZA PIGMENTŮ METODAMI VIBRAČNÍ SPEKTROSKOPIE

PIGMENT ANALYSIS BY MEANS OF VIBRATIONAL SPECTROSCOPY

PÁSZTOR J., ŠEC K., LINDNEROVÁ MUDROŇOVÁ K.

Nicolet CZ s.r.o., Křelovická 970, 104 00 Praha

Summary

Vibrational spectroscopy is a very powerful tool for characterization of chemical compounds in all states. This method is also suited for polymorph analysis since the differences between various crystal structures are very well noticeable in measured spectra.

In this study we present the basic principles of vibrational spectroscopy using the case of analysis of different polymorphs of metal oxides, e.g. TiO_2 *(anatase and rutile), which is commonly used in paints, and detection of dangerous CdS (cadmium yellow) in coloured polymers. Furthermore, the approach of spectral bands decomposition using the Omnic (TQ Analyst) software is presented.*

Key words

Pigments, FT-IR, Raman spectroscopy, Omnic

Úvod

Vibrační spektroskopie (Ramanova a infračervená spektroskopie) je nedestruktivní metoda analýzy, která využívá neelastického rozptylu záření (Ramanova spektroskopie) a absorpci infračerveného záření (infračervená spektroskopie – FT-IR). Tyto dvě metody jsou vzájemně komplementární. Získaná spektra jsou unikátní nejen pro každou chemickou látku, reagují i na drobné změny v okolí molekul a je pomocí nich možné rozlišit i jednotlivé polymorfy látky. [1]

Svou nezastupitelnou roli má vibrační spektroskopie mimo jiné také v oblasti analýzy pigmentů a pojiv, kde se hojně využívá řada jejích výhod. Některé v průmyslu hojně využívané látky mají tendenci v přírodě i ve výrobě zaujímat více krystalových struktur, tzv. polymorfů. Ty mají rozdílné optické vlastnosti [2], což je pro některé průmyslové aplikace zásadní.

Experiment

Prvním z praktických příkladů studovaných látek je oxid titaničitý (TiO_2), který se v přírodě vyskytuje ve třech formách (rutil, anatas a brookit) a má široké použití jako barvivo v potravinářství, kosmetice či jako pigment do nátěrových hmot. Již malá změna poměru jejich zastoupení se projeví viditelnou změnou vlastností povrchu, a proto je rozlišení polymorfů esenciální nejen pro chemický průmysl, ale také pro biomedicínské aplikace. [3]

Dalším prezentovaným příkladem je analýza řady různých typů pigmentů (např. sulfidu kademnatého CdS – kadmiové žluti) a korozních složek pomocí měření ve vzdálené infračervené oblasti (FIR). V neposlední řadě budou pomocí praktických příkladů představeny možnosti infračervené spektroskopie při odhalování zakázaných a nebezpečných látek v pigmentovaných polymerech a forenzní aplikace vibrační spektroskopie při analýze laků vozidel z místa činu.

Výsledky a zpracování experimentálních dat

Výsledky získané pomocí Ramanových a FT-IR spektrometrů je dále možné zpracovat pokročilými matematickými metodami. Lze provádět nejen kvalitativní, ale také kvantitativní analýzu, kterou je navíc možné automatizovat. Pro posuzování kvantity a kvality vzorku se používá program TQ Analyst, v kterém je možné kalibrační modely vytvářet.

Obr.1 – IR spektra kadmiové žluti, kalcitu a podezřelého polymeru.

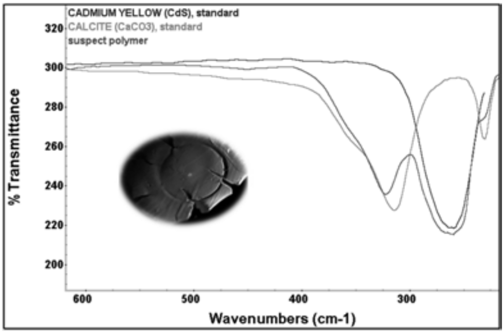

Závěr

Vibrační spektroskopie je elegantním nástrojem pro identifikaci neznámých látek, verifikaci materiálů i analýzu různých polymorfů téže látky. Díky metodám vzorkování je možné měřit vzorky všech skupenství, ve spojení s mikroskopií lze navíc analyzovat objekty o velikosti od několika mikrometrů, a tak vibrační spektroskopie nachází uplatnění ve vědě, průmyslu i forenzních aplikacích.

Literatura

[1] M. Nicol, M. Y. Fong: Raman Spectrum and Polymorphism of Titanium Dioxide at High Pressures, *The Journal of Chemical Physics*, 54, 7, 1971.

[2] L. Kernazhitsky, V. Shymanovska, T. Gavrilko, V. Naumov, L. Fedorenko, V. Kshnyakin, J. Baran: Room temperature photoluminescence of anatase and rutile TiO_2 powders, *Journal of Luminescence*, 146, 199–204, 2014.

[3] M. Gaintantzopoulou, S. Zinelis, N. Silikas, G. Eliades: Micro-Raman spectroscopic analysis of TiO_2phases on the root surfaces of commercial dental implants, *DentalMaterials*, 30, 861–867, 2014.

LUMiFrac® – TECHNOLOGIE PRO ODSTŘEDIVÉ TESTOVÁNÍ ADHEZE

LUMiFrac® – CENTRIFUGAL ADHESION TESTING TECHNOLOGY

DUDÁK M.

ANAMET s.r.o.

Summary

New Centrifugal Adhesion Testing Technology provides wide range of forces which may be used for testing adhesion, cohesion, shear and bond strength of paints and other surface treatments. This technology facilitate quick testing of up to 8 samples simultaneously to provide good statistical results. Results for various applications will be presented such as warm-curing epoxy-adhesives, optical coatings on plastics, metal coatings on glass and polymer coatings on metals. This technology typically helps to resolve questions of optimum mixing ratio and curing temperature.

Key words

Centrifugal tester; adhesion, cohesion and shear strength, surface coatings

GPC-MALS VS. A4F-MALS: STANOVENÍ MOLEKULOVÉ HMOTNOSTI SAMOSÍŤUJÍCÍCH AKRYLÁTOVÝCH POJIV NA BÁZI EMULZNÍCH KOPOLYMERŮ

GPC-MALS VS. A4F-MALS: MOLAR MASS DETERMINATION OF SELF-CROSSLINKING ACRYLIC BINDERS BASED ON EMULSION COPOLYMERS

MACHOTOVÁ J.[1], PODZIMEK Š.[1,2], ZGONI H.[2,1]

1 Institute of Chemistry and Technology of Macromolecular Materials, Faculty of Chemical Technology,
University of Pardubice, Studentska 573, 532 10 Pardubice, Czech Republic
2 SYNPO, Ltd., S. K. Neumanna 1316, 532 07 Pardubice, Czech Republic

Summary

Self-crosslinking core-shell latexes were synthesized by the emulsion polymerization of acrylic monomers. The molar mass of copolymers forming the shell layer was gradually reduced by isooctyl 3-mercaptopropionate included in the synthesis of the shell layers. The molar mass distribution of latex particles was determined using size exclusion chromatography and asymmetric flow field flow fractionation, respectively, both separation methods being coupled with a multi-angle light scattering detector. Whereas SEC-MALS was found to be convenient for the characterization of low molar mass shell copolymers without crosslinked structure, A4F-MALS was proved as a very efficient technique for the characterization of high molar mass copolymers and core-shell microgels.

Keywords

Emulsion polymerization, core-shell latex, keto-hydrazide crosslinking, molar mass distribution, A4F, chain transfer

Introduction

Currently, the self-crosslinking acrylic latexes based on diacetone acrylamide (DAAM) and adipic acid dihydrazide (ADH) crosslinking system have been studied extensively [1,2]. The reaction between the carbonyl functionalities of DAAM and hydrazide groups of ADH proceeds rapidly at ambient temperature and is favored by the loss of water and the simultaneous decrease in pH arising from the evaporation of ammonia or amines during the film forming process [3].By introducing the self-crosslinking chemistry in emulsion polymers, the physical and chemical integrity of latex films is enhanced, while the film formation process may be complicated due to suppressed inter-diffusion and entanglement of polymer chains during the particle coalescence stage [4,5].

Polyacrylate latexes synthesized by emulsion polymerization are naturally branched or even crosslinked inside each particle and form branched structures or even microgels during the synthesis [6,7] as a consequence of the coupling of propagating branches generated through chain transfer to a polymer [8,9]. Typical problems connected with utilization of these latexes are often related to film-forming properties of originally discrete polymer particles. In order to obtain a high-quality film, the polymer chains must inter-diffuse at the interfaces between the particles. This is, of course, not a problem for linear polymers of low glass transition temperature (T_g) but the coalescence of lightly crosslinked microgels results in interfaces that remain weaker than the particles and a lightly crosslinked network is not continuous, which typically leads to worse final coating properties [10]. A simple way to control the crosslinking or branching during the emulsion polymerization of acrylic monomers is to use a chain transfer agent (CTA) during the polymerization. This strategy is widely used in emulsion polymers to control the level of crosslinking in each particle [11,12]. Hence, the desired film properties can be tuned by varying the molar mass of emulsion copolymers.

As the precise control of latex copolymer particles structure from the point of view of the molar mass and its distribution may be particularly important in the case of self-crosslinking latexes, there is a strong need in the characterization and control of the molecular architecture of these polymers. The combination of size exclusion chromatography (SEC) with a multi-angle light scattering (MALS) detector has been numerously shown as a powerful technique for the determination of molar mass distribution of various synthetic and natural polymers. However, SEC may fail in case of polymer samples containing ultra-high molar mass fractions or branched macromolecules that can be degraded by shearing forces in SEC columns or elute abnormally due to the anchoring of branched chains in the pores of column packing; and also carboxylic groups typically added to stabilize aqueous dispersion of final latex particles may contribute to enthalpic interactions between macromolecules and column packing. Asymmetric flow field flow fractionation (A4F) can be used as an alternative separation technique with several advantages over traditionally used SEC. The main differences of A4F compared to SEC are the lack of stationary phase and significantly reduced operating pressure (typically around 10 bar). The lack of stationary phase completely eliminates the abnormal SEC elution of branched polymers and strongly reduces the possibility of enthalpic interactions as the surface of the semipermeable membrane is several orders of magnitude smaller than that of packed SEC column. As a matter of fact, polymers interacting with SEC column packing, ultra-high molar mass polymers and branched polymers belong to key application areas of A4F.

In our present work, we concentrated on the comparison of the molar mass determination of structured emulsion microgels by means of SEC-MALS and A4F-MALS analytical systems. The object of our interest focused on latexes based on DAAM and ADH crosslinking system. As these latexes are usually composed of core-shell particles with DAAM repeat units incorporated into the polymer backbone of the shell layer, the molar mass of the shell layer was systematically varied by a chain transfer agent and its effect on end-use coating properties was explored in particular.

Experimental

Latex preparation and characterization

Water dispersions of structured microgel particles were synthesized comprising a variable content of acrylic monomers (see Table 1). The core/shell weight ratio of the samples was 2/3, which means a shell thickness about 26 % of the particle diameter. The nature of acrylic monomers forming core and shell phases was chosen to achieve a calculated Tg of approximately 6–8 °C. A slight cross-linking inside the latex particle core was introduced by a controlled amount of AMA. The level of isooctyl 3-mercaptopropionate CTA included in synthesis of each of the shell layers was systematically varied. The shell layer included a constant amount of DAAM repeat units to provide ketone carbonyl functionalities for interfacial crosslinking by reaction with ADH added during latex formulation. To improve the colloidal stability of latexes and to ensure the acid catalysis of keto-hydrazine crosslinking reaction, carboxyl functionalities were introduced into the structure of core and shell layers by copolymerization with a constant amount of MAA into all the prepared copolymers.

The latexes were produced in a 700 ml glass reactor by the semi-continuous non-seeded emulsion polymerization under nitrogen atmosphere at 85 °C. This procedure ensured relatively homogeneous latex particles of statistical copolymers. The reactor charge was put into the reactor and heated to the polymerization temperature. Then the monomer emulsion was fed into the stirred reactor at feeding rate about 10 ml/min in two steps (1. core preparation, 2. shell preparation). After that, during 2 hours of hold period the polymerization was completed. The latex was cooled to room temperature and filtered to remove any coagulum. The pH was adjusted to 8.5 with ammonia solution. To produce self-crosslinking latexes of structured microgel particles, a 10 wt.% aqueous solution of ADH, in the amount corresponding to the molar ratio ADH:DAAM = 1:2, was added to the aqueous core-shell microgel dispersion with agitation.

Tab. 1 – Composition of self-crosslinkable latexes based on structured microgels

Sample	**Composition of monomer feeds [wt.%] MMA/BA/MAA/AMA/DAAM/CTA**	
	Core	***Shell***
L0	48.5/48.5/1.5/1.5/0/0	47.5/47.5/1.5/0/3.5/0
L0.1	48.5/48.5/1.5/1.5/0/0	47.45/47.45/1.5/0/3.5/0.1
L0.75	48.5/48.5/1.5/1.5/0/0	47.12/47.13/1.5/0/3.5/0.75
L1.5	48.5/48.5/1.5/1.5/0/0	46.75/46.75/1.5/0/3.5/1.5
L2.5	48.5/48.5/1.5/1.5/0/0	46.25/46.25/1.5/0/3.5/2.5

Molar mass determination

An instrumental setup of A4F-MALS consisted of an A4F system Eclipse 3+ (Wyatt Technology Corporation), a HELEOS MALS photometer and an Optilab rEX refractive index (RI) detector (both Wyatt Technology Corporation). The review of theoretical principles as well as the details of the A4F instrumentation can be for example found in the recent reference [28]. Both MALS and RI detectors operated at 658 nm. The instrumental set-up was completed with a Waters 2487 dual wavelength Absorbance detector that was set to the operating wavelength of 254 nm. A long channel with a wide 350 mm spacer and a regenerated cellulose 5 kDa membrane was used for the A4F separation using linear cross flow gradient from 3 mL/min to 0.1 mL/min within 15 min, followed by 30 min isocratic step at 0.1 mL/min and 10 min at zero mL/min. Elution and focusing steps (2 min each) preceded the injection + focusing step (3 min) that was followed by additional 10 min focusing. That means the elution started at 17 min.

An instrumental setup of SEC-MALS consisted of a set of two PL gel Mixed-B 300 mm x 7.5 mm columns (Agilent, USA), an Agilent 1100 Series HPLC pump and the same detectors as used for A4F. Tetrahydrofuran (THF) was used as the mobile phase for both SEC and A4F experiments at SEC flow rate and A4F detector flow rate of 1 mL/min. Samples of latexes without ADH were injected as solutions in THF in the volume of 100 µL and the concentration of about 0.2 % w/v. All prepared solutions were filtered with 0.45 µm filter before the injection into SEC columns or A4F channel. The data acquisition and processing were carried out by ASTRA 6 software (Wyatt Technology Corporation). The MALS data were processed using Berry light scattering formalism. The *dn*/*dc* of copolymers was calculated based on the *dn*/*dc* values of parent homopolymers and the weight fractions of monomers in a given copolymer. The calculation of molar mass was performed assuming chemical homogeneity of the prepared copolymers. Although this assumption may not be completely fulfilled it must be taken in order to get molar mass from the MALS detector.

Results and discussion

Molar mass determination of shell copolymers

Molar mass distribution curves of pure shell copolymers determined using SEC-MALS and A4F-MALS techniques are presented in Fig. 1 and the number-average, weight-average and z-average molar masses (M_n, M_w, M_z, respectively) of shell copolymers obtained from SEC-MALS and A4F-MALS are shown in Tables 2,3. It can be seen clearly that increasing the CTA content in the composition of monomer feeds resulted in a shift of molar mass distribution curves to lower values and a considerable decrease in the molar mass averages of shell copolymers. As expected, the effect of molar mass reduction was manifested more significantly in the case of the weight--average and *z*-average molar masses which are strongly affected by the presence of high molar mass fractions. It is evident that a sharp drop in the molar mass occured particularly by using 0.1 and 0.75 wt. % of CTA, whereas at higher contents of CTA (1.5 and 2.5 wt. %) low molar mass copolymers were formed and the effect of molar mass regulation remained similar.

The comparison of mass recovery values from SEC and A4F separations showed (see Tables 2 and 3) that reducing the molar mass of shell copolymers using 0.75, 1.5 and 2.5 wt.% of CTA resulted in a significant drop in mass recovery in the case of the A4F separation, whereas measurements of these samples by the SEC technique were found to exhibit almost maximal values of the mass recovery. Reduction in the mass recovery in the case of A4F separation indicates the penetration of oligomeric fractions through the semi-permeable membrane. Therefore, the molar mass averages obtained by A4F-MALS for the samples exhibiting low mass recovery (L0.75, L1.5 and L2.5) are overestimated, especially Mn that reflects mainly the fractions with lower molar mass. On the other hand, A4F separation of the shell copolymers L0 (polymerized without CTA) and L0.1 (polymerized with 0.1 wt.% of CTA) exhibited a nearly maximal mass recovery in comparison with the SEC separation of these samples. It can be assumed that the shell copolymers L0 and L0.1 contain a significant amount of ultra-high molar mass fractions of branched or crosslinked macromolecules that are filtered out by SEC columns, thus lowering the value of SEC mass recovery. It can be concluded that SEC not only provides false information about the molar mass distribution, but the high molar mass fractions retained by the SEC columns deteriorate the column performance.

Fig. 1 – Comparison of cumulative molar mass distribution curves of shell copolymers obtained from SEC-MALS (top) and A4F-MALS (bottom). The content of isooctyl 3-mercaptopropionate (CTA) in the copolymer: 0 wt.% (1), 0.1 wt.% (2), 0.75 wt.% (3), 1.5 wt.% (4), 2.5 wt.% (5).

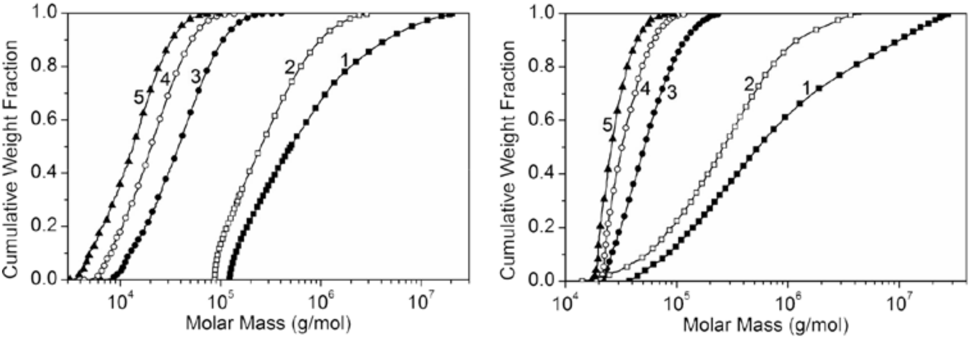

As alkyl acrylates are prone to the chain transfer to polymer, the ultra-high molar mass structures were apparently formed during the emulsion copolymerization of BA as a result of inter-molecular chain transfer to polymer. On the other hand, the chain transfer to short polymer chains does not result in complete crosslinking, therefore no structures having extremely high molar mass (~10^8 g/mol) were formed in the case of samples polymerized in the presence of higher amounts of CTA. In addition, macromolecules of very high molar mass are prone to shear degradation in SEC columns. Hence, the higher moments of molar mass (Mw, Mz) obtained from SEC-MALS for the shell copolymers L0 and L0.1, are underestimated, whereas the results of SEC-MALS analysis for low molar mass shell copolymers L0.75, L1.5 and L2.5 can be considered correct. It can be concluded that the molar mass of shell copolymer samples L0 and L0.1 is determined more precisely using A4F-MALS, while the molar masses of low molar mass shell copolymers L0.75, L1.5 and L2.5 are measured more correctly by SEC-MALS.

Tab. 2 – Effect of isooctyl 3-mercaptopropionate (CTA) content in shell copolymers on molar mass averages (M_n, M_w, M_z) of shell copolymers determined using SEC-MALS

Sample	CTA content [wt. %]	M_n [10^3 g/mol]	M_w [10^3 g/mol]	M_z [10^3 g/mol]	Mass recovery [%]
L0	0	793	3,300	12,863	83.5
L0.1	0.1	331	604	1,207	86.1
L0.75	0.75	32	57	103	97.6
L1.5	1.5	17	27	44	97.7
L2.5	2.5	12	18	27	99.7

Tab. 3 – Effect of isooctyl 3-mercaptopropionate (CTA) content in shell copolymers on molar mass averages (M_n, M_w, M_z) of shell copolymers determined using A4F-MALS

Sample	CTA content [wt. %]	M_n [10^3 g/mol]	M_w [10^3 g/mol]	M_z [10^3 g/mol]	Mass recovery [%]
L0	0	206	7,262	22,465	99.4
L0.1	0.1	125	777	2,302	98.5
L0.75	0.75	40	59	86	85.9
L1.5	1.5	28	31	38	66.7
L2.5	2.5	24	30	36	34.8

A4F analysis of core-shell microgels

It has been shown that SEC fails in case of polymer samples containing large branched macromolecules that elute abnormally or ultra-high molar mass fractions that can be degraded by shearing forces in SEC columns. As described in the previous section, SEC is unable to provide true molar mass distribution of the shell copolymers L0 and L0.1 containing high molar mass fractions. For this reason, the investigated ultra-high molar mass microgel structures were analyzed only by means of A4F-MALS as the separation in this technique is not affected by stationary phase. The results of A4F-MALS for core-shell microgels L0–L2.5 are presented in Fig. 2. The molar mass versus retention time plots of all microgel samples showed a bimodal molar mass distribution comprising of low molar mass fractions represented by soluble macromolecules of molar mass of ~ 10^5 and crosslinked microgel super-molecular structures of molar mass of the order of magnitude of 10^8 g/mol. All samples under investigation showed bimodal molar mass distribution pattern with different ratio of soluble macromolecules and crosslinked microgels. With rising content of CTA in the shell layer of microgel particles (analogously with decreasing the molar mass of the shell copolymer) the content of low molar mass fractions in microgel samples increased.

Fig. 2 – Molar mass versus retention time plots overlaid on RI fractograms for the core microgel (1) and core-shell microgels containing different amounts of CTA in the shell copolymer layer: 0 wt. % (2), 0.75 wt. % (3), and 2.5 wt. % (4).

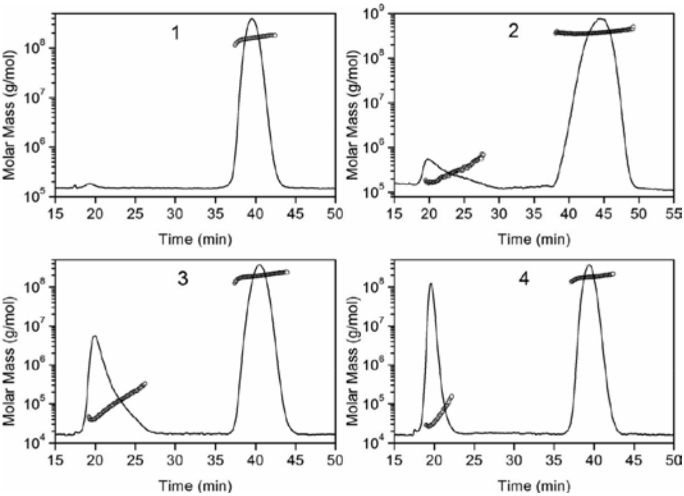

Conclusions

The object of our interest focused on self-crosslinking latexes based on keto-hydrazine crosslinking system. The structured latex particles consisted of an internally crosslinked core and a shell layer containing DAAM repeat units within the polymer chains. Molar mass of the shell copolymer was gradually reduced with different amounts of isooctyl 3-mercaptopropionate included in the synthesis of the shell layers. In the present work, we aimed demonstrate and compare the molar mass determination of the prepared structured emulsion microgels by means of SEC-MALS and A4F-MALS analytical systems. Whereas SEC-MALS was found to be convenient for the characterization of low molar mass shell copolymers without crosslinked structure, A4F-MALS was proved as a very efficient technique for the characterization of high molar mass shell copolymers and core-shell microgels.

Acknowledgements

The Technological Agency of the Czech Republic (TA02000011) is gratefully acknowledged for supporting this work.

References

[1] S.F. Zhang , F.R. Liu, Y.F. He, R.M. Wang, P.F. Song, Waterborne polyurethane-polyacrylic ester hybrid emulsion for humidity-controlling coatings. *Arab. J. Sci. Eng.*, 2014, 39, p23.

[2] Ch.G. Koukiotis, M.M. Karabela, I.D. Sideridou, Mechanical properties of films of latexes based on copolymers BA/MMA/DAAM and BA/MMA/VEOVA-10/DAAM and the corresponding self-crosslinked copolymers using the adipic acid dihydrazide as crosslinking agent. *Prog. Org. Coat.*, 2012, 75, p106.

[3] X. Zhang, Y. Liu, H. Huang, Y. Li, H. Chen, The diacetone acrylamide crosslinking reaction and its control of core-shell polyacrylate latices at ambient temperature. *J. Appl. Polym. Sci.*, 2012, 123, p1822.

[4] R.G. Joshi, T. Provder, P. Ziemer, W. Mao, W. Shen, F.N. Jones, Investigation of the effect of precoalescence or postcoalescence crosslinking on film formation, properties, and latex morphology. *J. Coat. Technol.*, 2009, 6, p47.

[5] T. Provder, R. Joshi, E. Lefevre, Ch. Patel, R. Crombez, W. Shen, F. Jones, Thermoanalytical and morphological studies of the film formation and resulting fundamental properties of precoalescence or postcoalescence crosslinked latex films. *Polym. Mater. Sci. Eng.*, 2008, 99, p139.

[6] S. Tobing, A. Klein, L.H. Sperlinh, B. Petrasko, Effect of network morphology on adhesive performance in emulsion blends of acrylic pressure sensitive adhesives. *J. Appl. Polym. Sci.*, 2001, 81, p2109.

[7] M.D. Gower, R.A. Shanks, The effect of chain transfer agent level on adhesive performance and peel master-curves for acrylic pressure sensitive adhesives. *Macromol. Chem. Phys.*, 2004, 205, p2139.

[8] J.M. Stubbs, D.C. Sundberg, The dynamics of morphology development in multiphase latex particles. *Prog. Org. Coat.*, 2008, 61, p156.

[9] Ch. Plessis, G. Arzamendi, J.M. Alberdi, M. Agnely, J.R. Leiza, J.M. Asua, Kinetics and polymer microstructure of the seeded semibatch emulsion copolymerization of n-butyl acrylate and styrene. *Macromolecules*, 2001, 34, p5147.

[10] F. Deplace, C. Carelli, A. Langenfeld, M.A. Rabjohns, A.B. Foster, P.A. Lovell, C. Creton, Controlled sparce and percolationg cross-linking in waterborne soft adhesives. *Appl. Mater. Int.*, 2009, 1, p2021.

[11] A.B. Foster, P.A. Lovell, M.A. Rabjohns, Design and synthesis of structured latex particles for enhancing the performance of water-borne pressure-sensitive adhesives. *Polym. Mater. Sci. Eng.*, 2008, 99, p788.

[12] S.D. Tobing, A. Klein, Molecular parameters and their relation to the adhesive performance of emulsion acrylic pressure-sensitive adhesives. II. Effect of crosslinking. *J. Appl. Polym. Sci.*, 2001, 79, p2558.

ANTIKOROZNÍ PIGMENTY NA BÁZI PEROVSKITŮ S POVRCHOVOU ÚPRAVOU VODIVÝM POLYMEREM PPDA

ANTICORROSIVE PIGMENTS BASED OF PEROVSKITE WITH A SURFACE LAYER OF CONDUCTIVE POLYMER PPDA

HÁJKOVÁ T., KALENDOVÁ A.

Faculty of Chemical Technology, Institute of Chemistry and Technology of Macromolecular Materials,
University of Pardubice, Studentská 573, 532 10 Pardubice, Czech Republic

Summary

The properties of protective organic coatings containing perovskites whose surface had been modified with conductive polymers were investigated, with focus on their anticorrosion effect. The perovskite type pigments (XYO_3; X = Ca Sr, Y = Ti, Mn) were synthesized by high-temperature solid-phase reaction, and their surface was modified with a conductive polymer, specifically polyparaphenylendiamine phosphate (PPDA), by chemical oxidative polymerisation.

Conductive polymers are currently attracting considerable interest in a number of sectors, among them the paint industry owing to their non-toxicity and high stability.

Paints consisting of a solvent-based epoxy-ester resin as the binder and the above-mentioned perovskite/PPDA pigments were formulated and subjected to mechanical tests in order to assess the effect of the composite pigment particles on the paints' mechanical resistance. Corrosion resistance of the coatings was tested also evaluated in dependence on the type of particle surface treatment with the conductive polymer, chemical composition of the pigment, and pigment volume concentration (PVC) in simulated corrosive atmosphere.

Keywords

Perovskites, anticorrosion pigment, organic coating, conductive polymer, epoxy-ester resin, paraphenylendiamine

Introduction

The most famoused method to protect the surfaces of metallic materials consists in coating them with paints possessing anticorrosion properties [1,2]. Paints designed to protect metals against corrosion always contain corrosion-inhibiting pigments that slow down the metal corrosion process through electrochemical and chemical reactions [3, 4]. Therefore, the possibility of developing nontoxic pigments for anticorrosion pigments that would feature efficiency at the same or even better level than the traditional toxic anticorrosion pigments is being explored. A number of papers have been devoted to protective coatings containing pigments based on oxides with the perovskite structure, which exhibit anticorrosion properties.

Chemically and electrochemically acting pigments encompass a wide range of substances of various chemical composition, mainly lead-containing compounds and chromate pigments, phosphate compounds, modified phosphates, and metal powder based pigments [5,6].

Conductive polymers start to be popular among organic corrosion inhibitors [7]. Examples of conductive polymers include polypyrrole and polyaniline (Fig. 1), involving systems of conjugated double bonds with the presence of charge carriers making possible charge transfer along the chain [8]. Owing to their properties, conductive polymers induce passivation processes on steel surfaces, in which respect they are similar to the compounds containing heavy metals. This shows promise are regards the feasibility of using conductive polymers to replace, or reduce the use of, e.g., chromate-based corrosion inhibitors [9]. They may also find application as electrochemical, or electrically active, pigments to attain passivation of the surface of a corroding steel substrate [10,11].

Fig. 1 – Pigments treated conductive polymers on the surface layer

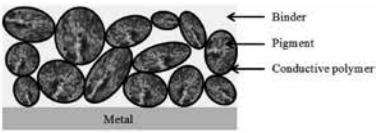

A new conductive polymer is polyphenylenediamine (PPDA), which can also be oxidized to the oligomer or polymer [12,13]. Phenylenediamine contains two primary amino groups, serving to interconnect the monomers during the oxidative polymerization process. Ammonium peroxodisulphate is used as the oxidative reagent. The two amino groups can be included in a phenazine-like ladder structure if the oxidative reagent is present in appreciable concentrations [14,15]. Polyphenylenediamine is considerably less conductive than polyaniline but many properties are similar owing to the similarity of the structures (Fig. 2). Redox activity is one of such properties [16].

Fig. 2 – Idealized structure of poly(p-phenylenediamine) produced by the oxidation of both amine groups in p-phenylenediamine [15]

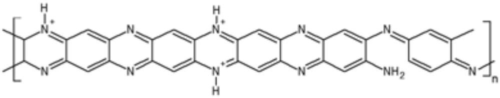

Experimental

Laboratory preparation of pigments

Perovskites with a generally isometric particle shape were synthesized to serve as the pigment cores for coating with a conductive polymers and to be added to a binder to form anticorrosion paints. Pigments possessing the simple perovskite structure: $CaTiO_3$, $SrTiO_3$, $CaMnO_3$ and $SrMnO_3$, were synthesized by calcination [17].

The anticorrosion pigment based on the zinc phosphate hydrate $Zn_3(PO_4)_2 \times H_2O$ (PVC = 15 %) was also tested as a reference material allowing us to compare the results obtained with the pigments synthesized by us with those obtained with a commercially available product.

Pigment preparation procedure

The pigments were synthesized by solid-phase reaction, viz. by high-temperature calcination of the homogenized mixtures of the starting materials by following the general principles of preparation of high-temperature inorganic pigments. The process of preparing the pigments consists of 4 operational steps: homogenization, calcination, washing with water and milling by wett process. [17].

The surface of the pigments was modified by treatment with polyparaphenylendiamine phosphate (PPDA). The anti-corrosion efficiency was evaluated both for the untreated pigments and for the pigments with surfaces modified with PPDA.

Preparation of the perovskites modified with a surface layer of polyparaphenylendiamine phosphate

This is the oxidative polymerization of phenylendiamine, which is carried out under laboratory conditions in the environment of phosphoric acid. Peroxydisulfate is the most commonly used oxidant [18]. To this reaction was added to each of the synthetised perovskite [17].

Determination of the physico-chemical properties of the perovskites with conductive polymer surface layers

The pigments' specific weight was determined by using a AccuPyc II 1340, gas pycnometer (Micromeritics, USA. Linseed oil absorption was measured by the pestle-mortar method. The outcome, called the oil number (in g 100 g^{-1}), is a prerequisite for calculation of the CPVC and for the formulation of the paints Parameters are given as arithmetic averages within 10 measured values [19].

Formulation, preparation and testing of the paints

Epoxy-ester resin-based paints were formulated for investigation of the pigments' anticorrosion properties. Description of binder: a 60 % solution of a medium high molecular weight epoxy resin esterified with a mixture of fatty acids of dehydrated ricin oil and soy oil, trade name WorléeDur D 46, acid number 4, viscosity 2.5–5.0 Pa s^{-1}, flow time (DIN 53211-4200) 250 s, solvent xylene. The pigment volume concentration (PVC) in the paints were invariably 1, 5, 10 %, and 15 %. The PVC/CPVC ratio was adjusted in all the model paints to 0.50 by means of the anticorrosion-neutral filler calcite $CaCO_3$.

The paint films were applied to the substrates by means of an applicator for steel panels (Q–panel, UK) 152 mm x 102 mm x 0.8 mm size. A total of 10 test panels were prepared for each paint. A thin cut (groove), 10 cm long, which penetrated through the paint film and reached the substrate metal, was made using a sharp blade. The samples on the test panels were allowed to dry under standard conditions (temperature 20 °C, relative humidity 50 %) in a conditioned laboratory for 6 weeks. The dry film thickness (DFT) was measured with a Minitest 110 magnetic thickness gauge fitted with a F16 type probe (Elektrophysik, Germany) in accordance with ISO 2808. A 7 mm long test cut was made on the bottom of all steel panels for the corrosion tests.

Cyclic corrosion test with salt mist and condensing moisture

In the 24-hour cyclic corrosion test in the presence of condensing water and SO_2, the test panels were exposed to condensing water containing SO_2 at 36°C ± 2°C for 8 hours (1st cycle stage) followed by drying at 23°C ± 2°C (2nd cycle stage). This test encompassed 15 cycles, i.e. it took 1400 hours in total.

Results and discussion

Structure and morphology of the composite pigment particles

The pigment particle morphology is illustrated by scanning electron micrographs Figure 3 for the perovskites and for the surface modified perovskites. The micrographs were taken in the secondary electron imaging (SEI) mode. The composite pigments had a tendency to form clusters.

Fig. 3 – Morphology of perovskite particles as observed by SEM: a) $CaTiO_3$; b) $CaTiO_3$/PPDA; c) $CaMnO_3$; d) $CaMnO_3$/PDPA; e) $SrTiO_3$; f) $SrTiO_3$/PPDA; g) $SrMnO_3$; h) $SrMnO_3$/PPDA

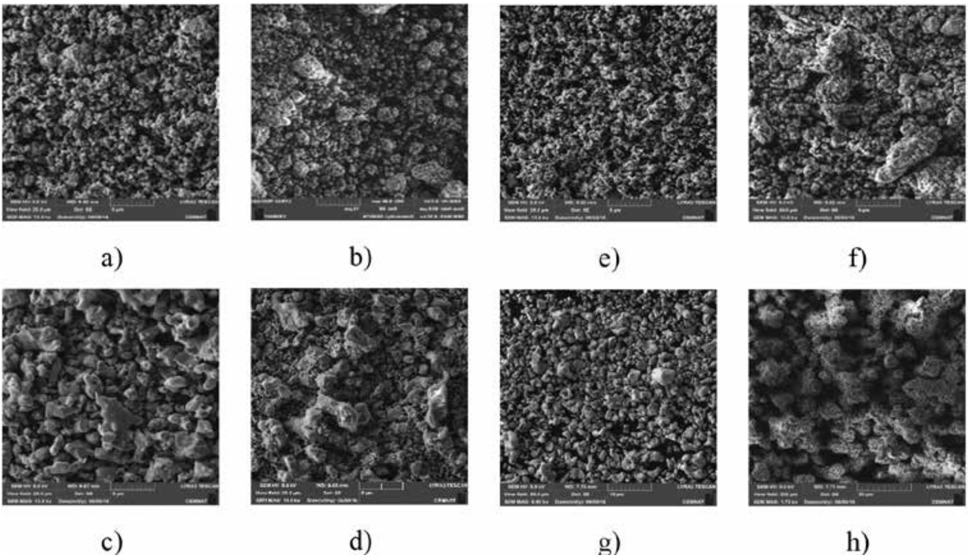

Corrosion tests

The size and frequency of blisters in the paint film were determined as per ASTM D 714-87, the fraction of substrate metal area affected by corrosion was determined as per ASTM D 610, the distance of propagation of corrosion in the cut was determined after removing the paint film as per ASTM D 1654-92, and the overall anticorrosion efficiency (E_{SO2}) was calculated as described above [20].

Corrosion test in the atmosphere with SO_2

The paints were exposed to a corrosion test in the atmosphere with SO_2 (Tab. 1) for 1400 hours. Modification with a surface layer conductive polymer improved the paints' overall anti-corrosion efficiency. Modification of particles of the perovskite $SrTiO_3$ with PPDA ($SrTiO_3$/PPDA) gave rise to a form that exhibited an anti-corrosion efficiency that was higher than that of untreated perovskite ($SrTiO_3$). The highest anticorrosion efficiency was found with $SrTiO_3$/PPDA, where the overall anticorrosion efficiency score was 99 (PVC = 10% and 15%).

Tab. 1 – Results of accelerated corrosion tests of the paints containing composite pigments in mist of a salt electrolyte (exposure 1400 hours, film thickness = 100 ± 10 µm)

Pigment	PVC/%	Blistering		Corrosion		Anticorrosion efficiency E_{SO_2}/%
		In a cut/dg	Metal base/dg	In the cut/mm	Metal base/%	
$CaTiO_3$	1	8MD	–	0–0.5	0.1	83
	5	8M	–	0–0.5	0.03	89
	10	8M	–	0–0.5	0.03	89
	15	8M	–	0–0.5	0.03	89
$SrTiO_3$	1	8F	–	0–0.5	0.1	93
	5	8F	–	0–0.5	0.3	94
	10	8F	–	0–0.5	0.1	93
	15	8F	–	0–0.5	0.1	93
$CaMnO_3$	1	6M	–	0–0.5	0.1	87
	5	6MD	–	0.5–1	0.03	80
	10	8MD	–	0.5–1	0.3	80
	15	8MD	–	0.5–1	0.03	82
$SrMnO_3$	1	8MD	–	0–0.5	0.03	84
	5	8MD	–	0.5–1	0.1	81
	10	8M	–	0–0.5		85
	15	8F	–	0–0.5	0.1	93
$CaTiO_3$/PPDA	1	8M	–	0.5–1	0.1	86
	5	8F	–	0–0.5	1	90
	10	–	–	0–0.5	0.3	98
	15	–	–	0–0.5	0.1	99
$SrTiO_3$/PPDA	1	8M	–	0.5–1	–	86
	5	–	–	0–0.5	0.3	98
	10	–	–	0–0.5	0.03	99
	15	–	–	0–0.5	0.03	99
$CaMnO_3$/PPDA	1	8F	–	0–0.5	1	90
	5	8F	–	0.5–1	3	85
	10	8F	–	0–0.5	1	90
	15	–	–	0–0.5	3	93
$SrMnO_3$/PPDA	1	–	–	0–0.5	–	99
	5	–	–	0–0.5	3	93
	10	8M	–	0.5–1	3	80
	15	8M	–	0–0.5	0.1	88
$Zn_3(PO_4)_3xH_2O$	15	2M	8M	4.0–5.0	10	59
Non-pigm. film	–	–	–	0.5–1.0	>50	73

Perovskite itself possesses a relatively low electric conductivity, which was increased to an optimum level for use in paints by modification with PPDA.

The highest anticorrosion efficiency was found with $SrTiO_3$/PPDA, where the overall anticorrosion efficiency score was 99 (PVC = 10% and 15%).

The overall conclusions from the exposure of the paints to an atmosphere with SO_2 are as follows:

- Paints with conductive polymer PPDA reduced the rate of the corrosion phenomena occurring in the steel substrate surface.
- The anti-corrosion efficiencies of paints with pigments modified with the conductive polymers were higher than those of the respective paints with the untreated pigment.
- The highest corrosion resistance showed pigment $CaTiO_3$/PPDA.
- The anti-corrosion efficiencies of paints decreased in the following order:

  $SrTiO_3$/PPDA > $CaTiO_3$/ PPDA > $SrTiO_3$ > $CaMnO_3$/PPDA > $SrMnO_3$/ PPDA > $CaTiO_3$ > $SrMnO_3$ >
  > $CaMnO_3$

Anticorrosion effect of perovskites and conductive polymers in a paint layer

In recent years, application of conductive polymer coatings such as PPDA on ferrous and non-ferrous alloys against corrosion has received much attention [21,22]. In addition to applying the physical barrier, which is the protection mechanism of most coatings, the conductive polymers are capable to anodic protection of metal surface by the healing their oxidative properties and accelerating the formation of stable metal oxides on the surface of the substrate [23,24]. In other words, the ability of the conducting polymer to oxidize the substrate metals allows potential of metals to be shifted to the passive state, in which the metals are protected by the passive oxide formed beneath the conducting polymer.

Where the pigment particle is not modified with a conductive polymer layer, the anticorrosion protection role is played by the inorganic pigment itself.

Conclusions

PPDA as the conductive polymer for pigment particle surface modification was found superior to the corrosion-inhibiting efficiency of the composite pigments. It is an advantage that a low pigment volume concentration in the epoxy-ester resin based paint is adequate to attain a high anticorrosion efficiency. For some of the pigments, their optimum concentration in the paints was as high as PVC = 10 % and 15 %, which is beneficial also from the financial aspect.

When exposed to the atmosphere with SO_2, the paint films exhibited an anticorrosion effect particularly at high PVC levels (10% and 15%).

All of the paint films exhibited a high anticorrosion resistance in this chamber; excellent results were obtained with the paints containing PPDA. Specifically, they were paints containing $SrTiO_3$/PPDA at PVC = 10% and 15%, where the overall anticorrosion efficiency score was 99%.

The surface modified pigments are promising from several aspects, particularly owing to their high anticorrosion efficiency compared to that of the reference paint, low pigment concentration in the paints adequate to attain a high anticorrosion effect, and their environmental harmlessness. The results obtained suggest that the pigments deserve further research.

Acknowledgment

Authors acknowledge SEM analysis provided by Center of Materials and Nanotechnologies with financial support by the grants LM2015082 and CZ.1.05/4.1.00/11.0251 from the Ministry of Education, Youth and Sports of the Czech Republic.

References

[1] M. Criado, I. Sobrados, J.M. Bastidas, J. Sanz, Steel corrosion in simulated carbonated concrete pore solution its protection using sol-gel coatings, *Progress in Organic Coatings*, 2015, 88, p228–236.

[2] W. Yang, Q. Li, Q. Xiao, J. Liang, Improvement of corrosion protective performance of organic coating

on low carbon steel by PEO pretreatment, *Progress in Organic Coatings*, 2015, 89, p260–266.

[3] N.M. Ahmed, M.G Mohamed, M.R. Mabrouk, A.A. ELShami, Novel anticorrosive pigments based on waste material for corrosion protection of reinforced concrete steel, *Construction and Building Materials*, 2015, 98, p388–396.

[4] H. Vakili, B. Ramezanzadeh, R. Amini, The corrosion performance and adhesion properties of the epoxy coating applied on the steel substrates treated by cerium-based conversion coatings, *Corrosion Science*, 2015, 94, p466–475.

[5] R. Naderi, S. Y. Arman, S. Fouladvand, Investigation on the inhibition synergism of new generations of phosphate-based anticorrosion pigments, *Dyes and Pigments*, 2014, 105, p23–33.

[6] C. H. Vliet, Reduction of zinc and volatile organic solvents in two-pack anti- corrosive primers, a pilot study, *Progress in Organic Coatings*, 1998, 34, p220–226.

[7] E. Armelin, C. Alemán, J.I. Iribarren, Anticorrosion performances of epoxy coatings modified with polyaniline: A comparison between the emeraldine base and salt forms, *Progress in Organic Coatings*, 2009, 65, p88–93.

[8] E. Armelin, R. Pla, F. Liesa, X. Ramis, J.I. Iribarren, C. Alemán, Corrososion protection with polyaniline and pyrrole as anticorrosive additives for epoxy paint, *Corrosion Science*, 2008, p721–728.

[9] N.S. Sangaj, V.C. Malshe, Permeability of polymers in protective organic coatings, *Progress in Organic Coating*, 2004, 50, p28–39.

[10] W. Lu, R.L. Elsenbaumer, B. Wessling, Corrosion Protection Of Miold Steel By Coatings Containing Polyaniline, *Synthetic Metals*, 1995, 71, p2163–2166.

[11] B. Wessling, J. Posdorfer, Corrosion prevention with an organic metal (polyaniline): corrosion test results, *Electrochimica Acta*, 1999, 44, p2139–2147.

[12] E.T. Kang, K.G. Neoh, K.L. Tan, Polyaniline: A polymer with many interesting intrinsic redox states. *Progress in Polymeric Science*, 1998, 23, p277–324.

[13] X.G. Li, M.R. Huang, W. Duan, Novel multifunctional polymers from aromatic diamines by oxidative polymerizations, *Chemical Reviews*, 2002, 102, p2925–3030.

[14] M.R. Huang, Q.Y. Peng, X.G. Li, Rapid and effective adsorption of lead ions on fine poly(phenylenediamine) microparticles. *Chemical European Journal*, 2006, 12, p4341–4350.

[15] J. Stejskal, Polymers of phenylenediamines, *Progress in Polymer Science*, 2015, 41, p1–31.

[16] G.M. Nascimento, R.H. Sestrem, M.L.A Temperini, Structural characterization of poly-para-phenylenediamine montmorilloniteclay nanocomposites, *Synthetic Metals*, 2010, 160, p2397–2403.

[17] A. Kalendová, D. Veselý, J. Stejskal, M. Trchová, Anticorrosion properties of inorganic pigments surface-modified with a polyaniline phosphate layer, *Progress in Organic Coatings*, 2008, 63, p209–221.

[18] I. Sapurina, J. Stejskal, The mechanism of the oxidative polymerization of aniline and the formation of supramolecular polyaniline structures, *Polymer International*, 2008, 57, p1295–1325.

[19] A. Kalendová, D. Veselý, Study of the anticorrosive efficiency of zincite and periclase-based core-shell pigments in organic coatings, *Progress in Organic Coating*, 2009, 64, p5–19.

[20] A. Kalendová, D. Veselý, P. Kalenda, Properties of paints with hematite coated muscovite and talc particles, *Applied Clay Science*, 2010, 48, p581–588.

[21] C.M. Li, C.Q. Sun, W.Chen, L. Pan, Electrochemical thin film deposition of polypyrrole on different substrates. *Surface & Coatings Technology*, 2005, 198, p474–477.

[22] A.T. Özyilmaz, T., Tüken, B., Yazici, M. Erbil, The electrochemical synthesis and corrosion performance of polypyrrole on brass and copper. *Progress in Organic Coatings*, 2004, 51, p152–160.

[23] T.D. Nguyen, T.A. Nguyen, M.C. Pham, B. Piro, B. Normand, H. Takenouti, Mechanism for protection of iron corrosion by an intrinsically electronic conducting polymer, *Journal of Electroanalytical Chemistry*, 2004, 572, p225–234.

[24] D.E. Tallman, Y. Pae, G.P. Bierwagen, Conducting Polymers and Corrosion: Polyaniline on Steel, *Corrosion*, 1999, 55, p779–786.

SYNTÉZA STYRÉN-AKRYLÁTOVÝCH KOPOLYMÉROV AKO MODIFIKÁTORY VLASTNOSTÍ NÁTEROVÝCH HMÔT METÓDOU RAFT

SYNTHESIS OF STYRENE-ACRYLATE COPOLYMERS BY RAFT, USEABLE LIKE MODIFICATIONS OF COATINGS

BOHÁČIK P.[1], PODZIMEK Š.[1,2], ŠPAČEK V.[2]

1 Institute of Chemistry and Technology of Macromolecular Substances, Faculty of Chemical Technology,
University of Pardubice, Studentská 95, Pardubice 532 10
2 Synpo a.s., S. K. Neumanna 1316, Pardubice 532 07

Summary

This work is focused on the synthesis of random and block copolymers based on styrene and acrylic acid esters. The copolymers are prepared by Reversible addition-fragmentation Chain Transfer Polymerization (RAFT) and are characterized by size ex-clusion chromatography (SEC). Coating films were cast on steel panels and were evalu-ated by standard coatings tests. Prepared coatings show bad stability in the Q-sun tests.

Key words

RAFT, styrene-acrylate copolymers, modification of coatings

Introduction

Reversible addition-fragmentation chain transfer (RAFT) polymerization has been well established in polymerization systems, such as bulk or solution polymerization. It is a novel technique for controlled / living polymerization. RAFT is one of the most often used synthetic polymerization methods for the preparation of well defined polymers with complex architecture. Synthesis of uniform macromolecules with precisely controlled size, novel topology, composition and functionality is a prerequisite for the specific application. [1,2,3] Implementing RAFT polymerization can be as simple as introducing a suitable chain transfer agent – normally thiocarbonylthio compounds into a conventional free radical polymerization system. The RAFT agents used have a significant effect on the controllability of the RAFT polymerization and thus should be carefully chosen for specific polymerization system. RAFT polymerization starts with a standard initiation step as in the conventional radical polymerization, where the homolytic bond fission of a radical initiator into primary radicals occurs. Radicals react with monomer molecules to form a propagating polymeric radical *P*n*, which subsequently adds to the C=S bond of the RAFT agent and carboncentre intermediate RAFT radical arises. Fragmentation of this intermediate gives rise to either the original reactant or polymeric RAFT compound and a new radical. The radical is able to reinitiate the polymerization and can generate its own active centre by reacting with monomer molecules, providing eventually a new polymeric radical *P*m*. Equilibrium is established between the actively growing polymeric radicals and the dormant polymeric RAFT compounds, this provides equal chance for all chains to grow and allows the production of narrowly dispersed polymers between thiocarbonylthio end group. The mechanism of the RAFT living polymerization is illustrated in Figure 1. [4]

Fig. 1 – The principle of RAFT synthesis

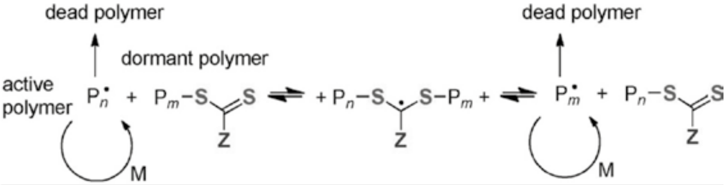

Experimental part

Polymers were synthetized of styrene (St), hydroxyethyl methacrylate (HEMA), 3-(trimethoxysilyl)propyl methacrylate (TMSMAA). All the monomers were purchased from Sigma Aldrich, the Czech Republic. Before polymerization, all monomers were purified in columns with neutral activated aluminum oxide under inert gas and stored in cold and dark place. 2,2´-Azobis(2-methylpropionitrile (AIBN, 0.05 % wt.) was used as the initiator and 2-(dodecylthiocarbonothioylthio)-2-methylpropionic acid (DDMAT, 0.095 % wt.) was utilized as the RAFT agent. All copolymers were polymerized in bulk under inert gas during 10 hours, at the tem-perature of 65 °C. After 10 hours, the prepared polymer was cooled, purified and dried in the last step.

All polymers were characterized by SEC coupled with Optilab rEX refractive index (RI) de-tector, both Wyatt Technology Corporation. The RI detector operated at 658 nm. Columns Agilent PlGel Mixed C 300x7.5 mm with particle size of 5µm were calibrated by polystyrene standards. Samples were injected as solutions in tetrahydrofuran (THF) in the amount of 100 µl, the concentra-tion was approximately 3 mg/ml. All prepared solutions were filtered with 0.45 µm filter before the injection in SEC column. Each sample was measured at 35 °C.

Results

The composition and properties of prepared polymers are listed in Table 1. The averages of molar masses M_n, M_w, and M_z (g/mol), index of polydispersity $Đ$, and % wt. of styrene and acrylic acid ester comonomers. Prepared polymer RAFT 1, RAFT 2, RAFT 4 and RAFT 5 were prepared by random polymerization in the bulk and RAFT 3 was prepared like block copolymer for compare properties between random and block copolymers. Coating were prepared with thickness apt. 80 µm on the steel panels. After 14 days were prepared coatings tested in the Q-sun for 600 hours. Coatings were containing higher part of styrene has disappeared from steel panels when test finished. Coating were contents lower part of styrene were having yellow color with some disappeared parts. But for improvement of the properties in UV light will be better add small amount of UV stabilizator. All prepared polymers have dispersity from 1.26 to 1.42. Molar mass M_n is independent on the content of St and acrylic acid esters, but on the amount of RAFT agent. If is in the reaction mixture small amount of RAFT agent, resultant polymer has higher molar mass M_n, M_w and M_z but have too high polydispersity. In the opposite, if is in the reaction mixture to much amount of the RAFT agent, the reaction will be stopped. RAFT agent and his amount has been chosen carefully for specific polymerization system. In the polymers who contents TMS-MAA will be trimethoxysilyl groups preserved. Were found no differences between stability of the block polymers and random polymers.

Tab. 1 – Averages molar masses and composition of prepared polymers

Sample	Polydispersity Đ	Molar mass of stars [g/mol]			Contents of St and ester acrylic acid		TMSMAA
		M_n	M_w	M_z			
RAFT 1	1.32	12,000	16,000	19,000	10	10	0.0
RAFT 2	1.26	20,000	25,000	31,000	15	5	0.0
RAFT 3	1.42	13,000	18,000	23,000	18	2	0.0
RAFT 4	1.34	13,000	17,000	21,000	10	0.0	10
RAFT 5	1.27	15,000	19,000	24,000	15	0.0	5

Conclusion

Before synthetized polymers by RAFT, we should found the right ratio between RAFT agent (DDMAT) and initiator (AIBN). Were prepared five polymers by RAFT polymerization. Four poly-mers were prepared by random polymerization and once polymer by block polymerization. Coatings films were cast on steel panel with thickness apt. 80 µm. When Q-sun test stopped coatings made from RAFT 2, RAFT 3 and RAFT 4 were disappearing from steel panel. Coatings made from RAFT 1 and RAFT 5 were yellow, with some parts of disappear coatings. All coatings will be for better properties stabilized by UV stabilizators.

References

[1] G. Moad, J. Chiefari, YK. Chong, J. Krstina, RTA. Mayadunne, A.Postma, et al. Living free radical polymerization with reversible addition fragmentation chain transfer (the lifo of RAFT), *Polym Int.*, 2000, 9, p993.

[2] J. Zhu, XL. Zhu, ZP. Cheng, F. Liu, JM. Lu,. Study on controlled free-radical polymeriza-tion in the presence of 2-cyanopop-2-yl 1-dithionaphtalene (CPDN,) *Polymer.*, 2002, 43, p7037.

[3] M. Levy, R. Milkovich, Polymerization initiated by electron transfer to monomer a new method of formation of block polymers, *J. Am. Chem., Soc.* 1956, 78, p2657.

[4] C. Barner-Kowollik, S. Perrier, The future of reversible addition fragmentation chain transfer polymerization. *J Polym Sci Part A: Polym Chem.*, 2008, 46, 17, p5715–5723.

POLYETHERIMIDOVÁ NANOVLÁKNA JAKO SORBENT PRO STANOVENÍ ORGANOCHLOROVÝCH PESTICIDŮ

POLYETHERIMIDE NANOFIBRES AS SORBENTS FOR ORGANOCHLORINATED PESTICIDES DETERMINATION

ANTOŠ V., HRABÁK P., KOMÁREK M., STUCHLÍK M.

Technical University of Liberec, CxI, Studentská 2, 461 17 Liberec, Czech Republic, EU

Summary

In the present work, electrospun polyetherimide (PEI) nanofibres were fixed on a steel wire solid phase microextraction (SPME) assembly. The basic properties of the prepared nanofibres were determined by thermogravimetry, differential scanning calorimetry, adsorption and SEM. The analytical performance of prepared PEI SPME fibres was compared with three commercially available SPME fibres – PDMS 7 µm / 100 µm and DVB/Carboxene/PDMS. As model water pollutants, persistent organochlorinated pesticides hexanchlorocyclohexanes (HCH) and chlorobenzenes (ClB) were chosen as model water pollutants. The fibres were compared in the headspace (HS) SPME mode of GC MS/MS instrumentation. The comparison omitted other method parameters and focused exclusively on the extraction time variability. Lab-made PEI SPME fibres showed significantly better response for the target compounds than the other tested fibres from industrial production.

Based on the results, the extraction time could be shortened from 50 to 10 min, if PEI SPME fibres were used as a modification of existing analytical protocol.

Key words

SPME, nanofibres, electrospinning, polyetherimide, hexachlorocyclohexanes, chlorobenzenes, organoglorinated pesticides

OCHRANNÉ POVLAKY NA BÁZI ALKALICKÝCH SILIKÁTŮ

PROTECTIVE COATINGS BASED ON THE ALKALI SILICATES

ANTOŠOVÁ B.[1], ANTOŠ P.[2], KALENDOVÁ A.[3]

1 Unipetrol Centre of Research and Education, a.s., Ústí nad Labem
2 Technopark Kralupy University of Chemistry and Technology in Prague, Kralupy nad Vltavou
3 Institute of Chemistry and Technology of Macromolecular Materials, FCHT, The University of Pardubice

Summary

The protective coatings based on the silicate binders prepared and filled with standard pigments and fillers were hardened by the following methods: physical procedure, zinc powder with isometric spherical particles, zinc powder with lamellar particles, blocked polyisocyanate in an organic solvent, blocked polyisocyanate in water dispersion, with condensed aluminum phosphate, hydrated aluminum phosphate, and alkoxysilyl isocyanurate. With coating compositions the physico-mechanical property tests of the coats on steel or, eventually, glass panels (adhesion by the grid method, bending strengths, cupping stability, shock resistance, and coating hardness) and corrosion resistance in a condensation chamber and salt chamber with cycles tests were performed. The results obtained were evaluated from the silicate binder type point of view, so as the used hardening system type point of view. The overall best results were obtained with a lithium-sodium water glass, the coats of which exhibit good physico-mechanical and anticorrosion properties. From the composition point of view the coating materials filled with zinc powder exhibit very good results. Zinc with lamellar particle shape exhibits a higher anticorrosion efficiency.

Key words

Protective coatings, zinc powder, silicates, lithium-sodium glass

Introduction

The soluble synthetic silicates, in the liquid form called also sodium water glass, potassium water glass, lithium water glass (eventually their combinations) are quite frequently used as binders for various systems (coating compositions, cements, forms, cores and coatings in foundries, welding electrodes, building materials, refractories, insulation materials). They give to them not only ecological harmlessness, but also e.g. acid resistivity (cements), high steam permeability (facade coating compositions), incombustibility (fire resistant coating compositions), anticorrosive protection (zinc rich paints).

The basic starting material for the products based on synthetic silicates and silicon dioxide is silica sand, which is the initial material for technologies of dry and wet processes. Various procedures can be used for processing the crystalline silicon dioxide to synthetic amorphous silicon dioxide with precisely defined properties for specific applications. The most usual product or eventually the semiproduct for further processing comprise alkaline silicates in solid and liquid forms. Sodium silicate belongs to basic inorganic chemicals and its production in Europe presents more than 500,000 t/y. Potassium silicate is used as a binder for coating compositions, refractories, cements and for the production of welding electrodes; its consumption in Europe is at a level of about 21,000 t/y. The lithium water glasses belong among chemical specialities and their usage is limited to the region of coating compositions (coating compositions, destined for heavy anticorrosion protection, rich in zinc powder filler), to the technologies of restoring the historical buildings (stabilizing means for synthetic and natural stones), and for the production of welding electrodes (application as a binder).

Theory

Properties of silicate binders

Water glasses – solutions of alkali silicates can be ordered among colloidal systems, wherein the particles are smaller than average light wavelength but larger than the average molecule size. The water glass particle size fluctuates between 1 to 500 nm and can be verified by the Tyndall effect observation or by a microscopic method. On evaluating the colloidal properties of water glass it is necessary to follow two states: water glass as a dispersion system (sol) and water glass as a transient system (gel) [1]. The sols are characterized as the systems containing particles, among which a large number of limited surfaces can be found. The sols can be distributed to phase dispersion systems and molecular colloids [2]. The water glass belongs to phase dispersion systems. The particles represent an independent phase separated by the dispersion medium. Large surface of interface is characterized by a high surface energy and thus a great thermodynamic instability. The system can be destabilized by a small impact and transformed through a transient gel form to the solid compound.

On evaluating the colloidal properties of water glass we follow three basic characteristics: solvation, size and charge. Generally the particles obtain an electric charge by the ionic adsorption or electrolytic dissociation. There takes place the formation of electric double layer. This layer is of diffusion character, on the movement of particles only the internal part of the double layer adheres on it. The particle appears on outside as electrically conductive particle. The micelle is a sol particle composed of a core and solvate layer. Water glass may be ordered among the isostable sols, the solvate layer thereof is formed as of ions, so as of the solvent molecules. The solvate layer of colloid water glass particles has two components: the inside strongly bound layer, which exhibits the Brownian motion with a particle, and the outside diffusion layer. Thus in water glass water occurs in three forms. On the one side it is a free water in an intermicallar space, further water bound at the outside lyosphere diffusion layer, and water bound strongly at the inside lyosphere layer. At the commercial sodium water glass sorts the hydration moves on the following level: inside bound water (W1) ~ 8%, outside bound water (W2) ~ 36% and free water (Wv) ~ 12%.

Fig. 1 – Schematic structure of solution of water glass

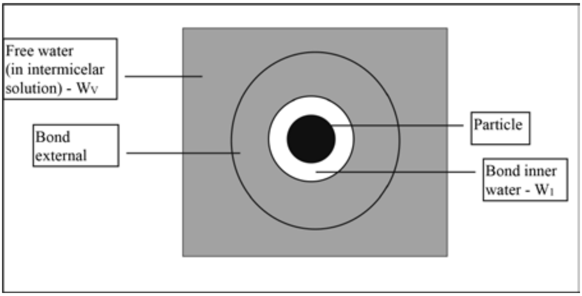

Hardening of silicate binders

The solutions of glass alkali silicates can be used as binders in coating compositions pigmented with zinc powder. In these systems the capability of zinc to form the cathodic protection on the contact with steel surface is used. As far as the conductive contact between individual zinc particles and steel surface is achieved, the electric Zn-Fe cell in which the steel is a cathode and therefore does not suffer corrosion, is formed. As far as the cell is functioning, an increase of the water pH value takes place, on diffusing through the coating film and acting on the zinc particles and also on the steel surface. Therefore it is necessary to select the binders stable in alkaline medium. Having this in mind polystyrene, chlorinated rubber, epoxy resins and vinyl copolymers were used for this purpose in the past. The silicon polymers are really suitable binders, both in the form of colloidal aqueous solutions of alkali silicates, and in the form of alkoxy silicates, soluble in organic solvents. Coating compositions pigmented with zinc powder protect the steel surfaces primarily by an electrochemical mechanism. The porous coatings of this type enable the water diffusion through the coat and thus the formation of electrolyte, which has inhibition properties (pH effect), but primarily the galvanic cell is formed. As a result of the electrochemical reaction the reaction products are formed, which seal the pores in film, and this film is gradually converted to the barrier protection mode.

In the process of hardening water-borne zinc silicate coatings the whole complex of physicochemical processes as the water evaporation on the drying of coat, the diffusion of carbon dioxide through the coating, the chemical reaction with carbon dioxide, the transport of eventually formed gaseous reaction products – hydrogen out of the coating etc., find application. At first the coating dries, which runs comparatively fast – to max. several hours in dependence on the temperature and relative humidity. The further subsequent processes are slower and take, in dependence on temperature, of the order of magnitude days to weeks. Of the proper chemical processes the following reactions make themselves useful: the reaction with atmospheric carbon dioxide, the reaction of water glass with zinc metal, and, under limitation to the adhesion interlayer, also the reactions between steel surface iron and water glass.

The hardening of water glass with inorganic salts runs by a similar mechanism as the hardening with organic esters. On the salt hydrolysis similarly as on the ester hydrolysis an inorganic acid, which hardens water glass, is freed. Therefore the salts of weak bases and strong acids are used primarily. The velocity of hardening is controlled by the dosed amount of hardening agent on the one side, and by the type of used salt on the other, as the determining reaction of the whole process is the velocity of inorganic salt hydrolysis. In the building industry fluorides and fluorosilicates were used frequently [3]. With respect to toxicity of fluorosilicate it is more suitable to use a mixture of aluminum phosphates, which are used for the hardening in the building industry (dry mortars, refractory cements and adhesives) [4]. Combinations of polyphosphates showing a low polymerization degree (3–6 structural units) and a high polymerization degree (more than 40 structural units) us used. The rate of hardening is controlled by a mutual ratio of both polyphosphate types. The phosphates showing a short chain are hardened by a higher rate than the phosphates showing a long chain [5]. The phosphates are prepared by a thermal reaction of aluminum hydroxide with ammonium phosphate in solid phase at temperatures about 400 °C [6].

The colloidal solutions of alkali silicates belong among principal inorganic chemicals with a broad spectrum of usage. One of the significant applications of water glasses is the application as a binder for foundry sand mixtures. The mixtures are hardened either by carbon dioxide or by liquid organic hardening agents mostly on the base of esters [7]. In practice the acetic acid esters and two- to five-member polyhydroxyalcohols, namely glycerol acetates, are used most frequently. Hydrolysis of glycerol triacetate leads across diacetate, monoacetate, and ends at the formation of acetic acid and glycerol. Gradually formed acetic acid reacts with water glass under the formation of sodium acetate, which disturbs the compactness of the formed silicon dioxide gel. Glycerol monoacetate is hydrolyzed most rapidly, the glycerol triacetate most slowly. By the mutual ratio of individual esters the rate of water glass hardening is controlled (elimination of the climatic summer-winter effects).

For the applications in building industries (solidification of road beds) is described hardening with esters of olefinic alcohols with carboxylic acids having a carbon atom number in the chain by 18 C (vinyl and methylvinyl esters of acetic, propionic, lauric, stearic and lactic acids) under adding further organic compounds of the halogenated hydrocarbons, ketones, aldehydes and acrylic acid ester [8] types.

For the building mortars a hardening system is described, which is based on acting mixtures of aluminum or ferric salts with organic hydroxyacids [9] (citric acid, lactic acid, glyceric acid, tartaric acid); a mole ratio of hydroxyacid/SiO_2 fluctuating between 0.05–0.3. The cements bound with sodium or potassium water glasses are hardened with organic compounds bearing free amino or amido groups, which react with water and water glass, e.g. formamide and cyanamide [10] or their compounds with bivalent metals (lead, calcium, barium) [11].

Usage of alkali silicates

The binding properties of alkali silicates are widely used in various applications and with various combinations of binders, fillers, and pigments. For the production of coating compositions, mortars and plasters the water glass is combined with burnt or hydrated limes and silicate powders. Into facade coating materials bound with acrylic dispersions the water glass additions up to 2 wt. % acting here as a conservation agent or a combination of both binder types (acrylate + silicate) is used. As a binder for the facade coating compositions primarily a potassium water glass of a suitable modulus or a potassium water glass adapted with colloidal silicon dioxide solution is used. Potassium water glass presents also a base for coating compositions on glass. Zinc silicate coatings or coats based on inorganic silicate binder together with organic coatings pigmented with zinc belong into the group of the so-called zinc coatings with a high content of zinc metal of 80–95 wt. % in the nonvolatile coating fraction (Figure 2). Dry layers of nominal thicknesses of 60–90 µm are determined to long-duration anticorrosion protection of steel structures, especially in atmospheres of the corrosion aggressivity degree C3, C4, and C5 (ČSN ISO 9223).

Fig. 2 Cathodic protection of metal substrate with zinc rich coatings

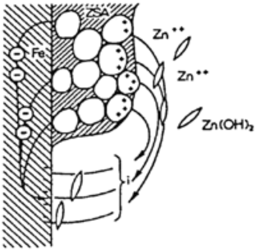

Experimental

Production of binders

Polysilicate binders based on the potassium and sodium water glasses were prepared from industrially produced semiproducts, in which the silicate modulus was adapted with colloidal silicon dioxide solution. Lithium and lithium-sodium water glasses were prepared by the sol-gel method from the colloidal silicon dioxide and appropriate hydroxides. The binder compositions are given in the following tables:

Tab. 1 – Basic composition of the prepared silicate binders

Silicate binder type	Sodium water glass	Potassium water glass	Lithium water glass	Sodium-lithium water glass
Dry matter content [wt. %]	31.39	24.48	20.84	21.39
SiO_2 content [wt. %]	25.59	18.39	19.28	18.37
Na_2O content [wt. %]	5.8	–	–	1.19
K_2O content [wt. %]	–	6.09	–	–
Li_2O content [wt. %]	–	–	1.56	1.83
Mole ratio [–]	4.55	4.74	6.16	3.82
Weight ratio [–]	4.41	3.02	12.36	6.08
Density [$g.cm^{-3}$]	1.286	1.208	1.166	1.203

Tab. 2 – Silicate binders - water distribution

Water glass type	Water distribution [wt. %]			
	W	W1	W2	Wv
Sodium water glass	69.03	5.42	49.82	13.8
Potassium water glass	75.14	3.33	41.54	30.27
Lithium water glass	79.08	2.04	44.3	32.7
Sodium-lithium water glass	76.96	2.45	65.84	8.67

Preparation of coating compositions

The coating compositions (Table 3) were prepared on the Dissolver Dispermat equipment by dispersing all the components in attritor. The coating composition dispersing was performed at 3,000 rpm for 30 minutes. To the attritor at first all the liquid system components were introduced. For reaching the better dispersing effect the dispersing bodies (ballotine having 3 mm in diam.), the volume of which amounted to about 1/3 of the coating composition volume was used. The mixture was homogenized and afterwards all the powdery components were added. On finishing the dispersion the glass balls were separated on a screen and the coating composition was applied to steel testing panels and glass plates for the corrosion and mechanical tests. Figure 3 brings morphology of zinc particles (SEM).

Tab. 3 – Composition of coatings

Starting material	**Coating**							
	1	**2**	**3**	**4**	**5**	**6**	**7**	**8**
Silicate binder	53.57	29.19	39.84	53.93	53.93	48.62	47.79	51.79
Sokrat 2431	8.93	13.47	13.6	8.93	8.93	8.62	8.85	8.93
Plastorit Micro	5.89	–	4.39	6.07	6.07	6.9	7.08	7.14
Bentone SD-2	3.21	2.74	3.74	2.86	2.86	3.1	3.18	3.21
Fepren TP 200	16.6	–	5.53	8.0	8.0	15.51	15.9	16.07
Potassium dichromate	–	0.01	0.01	–	–	–	–	–
Distilled water	10.71	9.68	9.76	10.71	10.71	13.79	10.62	10.71
Hydropalat A	0.9	0.8	0.8	0.9	0.9	0.9	0.9	0.9
Dehydran 1293	0.18	0.16	0.16	0.18	0.18	0.18	0.18	0.18
Zinc Dust VM-4P16	–	44.2	–	–	–	–	–	–
BLITZ Zinkpulver Z 2031	–	–	21.95	–	–	–	–	–
Alphos	–	–	–	8.21	–	–	–	–
Targon HS	–	–	–	–	8.21	–	–	–
Desmodur BL 4265	–	–	–	–	–	2.41	–	–
Bayhydur® BL 5140	–	–	–	–	–	–	5.13	–
Silquest® Y 11597 Silane	–	–	–	–	–	–	–	1.07
PVC [%]	38.5	51.14	44.9	36.8	37.1	39.24	39.47	39
Q [%]	*90*	*95*	*95*	*90*	*90*	*90*	*90*	*90*

Silicate binder: sodium water glass (NaWG), potassium water glass (PWG), lithium water glass (LiWG) and sodium-lithium water glass (NaLiWG).

Fig. 3 – Morphology of zinc particles (SEM)

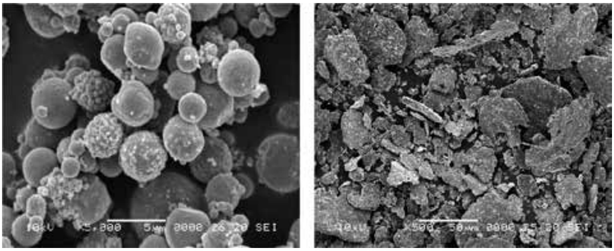

Zinc Dust VM-4P16 **BLITZ Zinkpulver Z 2031**

Used processing methods

To basic characteristics of water glass the following quantities belong: silicate modulus, water content, dry matter content, specific density, viscosity, and admixture contents. For evaluating the water glass properties especially the standard volumetric analysis was used. For determining the individual oligomers in water glass the NMR method was used. The pigments were characterized by means of electron microscopy, X-ray spectral analysis, laser granulometry, BET, and helium pycnometry methods. The physico-mechanical properties of coating films were ascertained by means of measuring the film hardness, shock resistance, cupping stability in Erichsen instrument, bending strength and adhesion by the grid method. The anticorrosion coating film properties were ascertained in a condensation chamber with a condensing humidity and SO_2 content. The test was performed by the ČSN ISO 69 88. In a testing chamber space a temperature of about 38 °C and a relative humidity of 100 % were kept during the test. Sulfur dioxide in a testing chamber was prepared by the reaction of sodium sulfite with sulfuric acid. The sample exposure was selected as a continuous for 120, 240, 480, and 720 hours. Further a corrosion cyclic test of the coatings was performed. The cyclic test resents a combination of condensation and salt chambers in dependence on the selected program. The samples fitted with a cut and placed in stands were exhibited to spraying a 5% NaCl solution, the humidity of water condensation and a subsequent drying of the sample. Individual cycles were connected to each other. The temperatures and duration times of the cycle were selected for individual cycle component separately.

- Salting: 10 hours at a temperature of 35 °C
- Condensation: 1 hour at a temperature of 55 °C
- Drying out: 1 hour at a temperature of 23 °C
- The coating films were exhibited to the individual cycle actions for 240 and 720 hours.

Results

Evaluation of the binders

The Table 4 brings a comparison of the alkali metal ion hydrations for water glass for lacquer purposes with water glass for foundry purposes (Silbond) and standard commercial glass of m = 2.4 and 3.2. At long-duration following the foundry water glass the hydration was obtained in an adsorption layer in a range of 1.1 to 1.9 mol H_2O per 1 mol Na, and in a diffusion layer in a range of 9 to 45 mol H_2O per 1 mol Na. The lacquer binders exhibit a hydration of alkali ions in an adsorption layer the same as standard silicate binders, but in a diffusion layer the hydration is much higher, which is caused by a low dry matter content, i.e. by a high water content in the water glass of interest. Table 5 brings results Si^{29} – NMR of silicate binders.

Tab. 4 – Hydration of sodium silicate binder ions

Type of binder	Hydration of alkali ions, mol H_2O/mol Me	
	Adsorption layer	Diffusion layer
Sodium water glass	1.6	–
Potassium water glass	1.76	94
Lithium water glass	1.70	65
Sodium-lithium water glass	1.37	60
Silbond CO 6.5, standard	1.9	9.7
Silbond ST L/01	1.8	11.1
Water glass 48–50	2.2	10.5
Water glass 36–38	1.6	45

Tab. 5 – Results Si^{29} – NMR of silicate binders

Binder type/wt. % of polymers	Q^0	Q^1	Q^2+$Q^3_{(cy-3)}$	Q^3	Q^4
Sodium water glass	0.7	4.4	21.3	53.8	19.8
Potassium water glass	1.1	4.6	24.6	54.1	15.6
Lithium water glass	1.4	4.8	22	53.4	18.5
Sodium-lithium water glass	0.8	4.5	25.2	53.8	15.8
Q^0 – monomer, Q^1 – dimer, Q^2 – trimer, Q^3 – octamer, Q^4 – colloidal phase Sodium water glass diluted to 24 wt. % dry matter					

Evaluation of coating compositions – Physico-mechanical properties

The best results of all the systems are exhibited by lithium-sodium water glass; especially after burning out at 150 °C for a time of 2 hours the results obtained in all the formulations are very balanced (Table 6). Additional burning out of the coating exhibits an advantageous effect on the mechanical coating properties, which undergo about 10% improving and are more balanced than in case of nonburnt out coatings. The result allow to order the tested binders from the best one to the worst one: lithium-sodium water glass, potassium water glass, sodium water glass, lithium water glass. Especially the results obtained with lithium water glass as a binder are really nonbalanced and the types of coating compositions hardened with aluminum phosphates could not be prepared at all in applicable form (no mixture lifetime), which is caused by a high reactivity of lithium water glass.

From the composition of coating material point of view (hardener type) it is possible on the basis of the mechanical test results to order the individual hardening systems from the best one to the worst one: system hardened by the reaction with solvent isocyanate type (coating 6), system hardened by the reaction with isometric particle zinc (coating 2), system hardened by the reaction with alkoxysilyl isocyanurate (coating 8), system without active components (coating 1), system hardened by the reaction with lamellar particles zinc (coating 3), system hardened by the reaction with aqueous isocyanate dispersion (coating 7), system hardened by the reaction with condensed aluminum phosphate (coating 5) and system hardened by the reaction with hydrated aluminum phosphate (coating 4).

Figures 4 and 5 show morphology of zinc pigmented coatings at various PVC (isometric and lamellar particlers).

Tab. 6 – Average values of coating hardness for individual binder types

Binder type in coating	Average hardness prior to burning out [%]	Average hardness after burning out [%]
Lithium-sodium water glass	38.4	40.5
Sodium water glass	36.4	39.1
Potassium water glass	39.9	38.7
Lithium water glass	45.6	44.6

Fig. 4 – Morphology of zinc pigmented coatings at various PVC (isometric particles)

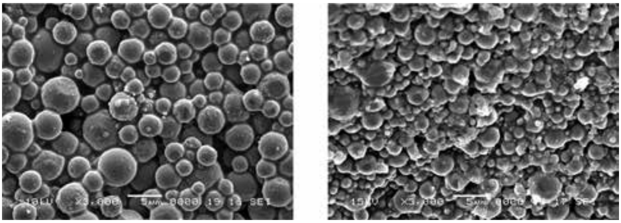

Spherical particles: PVC70%>CPVC (3000x) **Spherical particles: PVC60% ~CPVC (3000x)**

Fig. 5 – Morphology of zinc pigmented coatings at various PVC (lamellar particles)

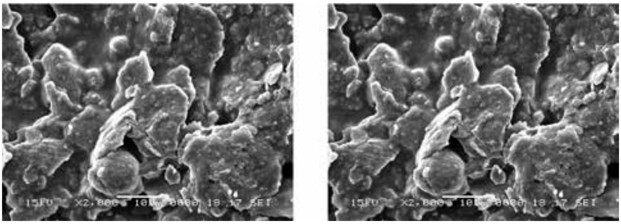

Lamellar zinc: PVC50% =CPVC (2000x) **Lamellar zinc: PVC50% =CPVC (2000x)**

Test in a condensation chamber

The tested samples of steel panels with deposited coating films were exposed to condensation chamber conditions for 120, 240, 480, and 720 hours. With samples the corrosion of substrate was evaluated after 120, 240, 480, and 720 hour exposure. The corrosion in cut was evaluated only after 720 hour exposure. No formation of osmotic blisters was observed with the samples. The order of individual silicate binder is as follows: lithium-sodium water glass, lithium water glass, sodium water glass and potassium water glass. The results obtained with the sodium and lithium water glass are at an almost same level (Table 7). With the lithium water glass it was not possible to prepare coating compositions hardened by aluminum phosphates owing to too rapid reaction with the hardener. The worst result were obtained with potassium water glass.

In Table 8 the overall anticorrosion efficiency in the condensation chamber after 720 hour exposure is given. The results are affected by a considerable substrate corrosion after this exposure. The lowest anticorrosion efficiency and thus the highest corrosion was observed in the system, which contained besides the silicate binder only inert pigments, fillers and additives. The results of system without active components are after 720 hour exposure identical for all binder types, but the course of corrosion phenomena is suppressed in the highest degree in lithium-sodim water glass. The best results of anticorrosion protection were observed in the systems filled with zinc particles, the systems filled with lamellar zinc particles exhibiting better results than the systems filled with isometrical zinc particles (Figure 6).

In the systems hardened with aluminum phosphates the inhibition action of aluminum phosphate manifests itself as anticorrosive pigment, yet better results being obtained with condensed aluminum phosphate, probably owing to lower solubility compared to hydrated aluminum phosphate. The blocked polyisocyanates give better results with isocyanate dissolved in an organic solvent than with isocyanate in water dispersion. Of actively hardened systems the worst results from the anticorrosion protection point of view are offered by the system hardened with alkoxysilyl isocyanurate, which does not contain any active pigment and the content of hardening agent is the lowest one.

The overall worst results are observed in the system, which does not contain any active anticorrosion component, either a component which could cross-link silicate binder, and the coating film protects the metal surface only by the barrier mechanism. The order of anticorrosion efficiency of individual systems in the condensation chamber is as follows: system hardened with zinc powder with lamellar particle shape, system hardened with zinc powder with spherical particle shape, system hardened with condensed aluminum phosphate, system hardened with hydrated aluminum phosphate, system hardened with isocyanate in an organic solvent, system hardened with an aqueous isocyanate dispersion, system hardened by the reaction with alkoxysilyl isocyanurate and system without any hardener and active components.

Tab. 7 – Effect of the binder type on substrate corrosion with individual coatings

Order[A]	Coating 1	Coating 2	Coating 3	Coating 4	Coating 5	Coating 6	Coating 7	Coating 8
1	NaLiWG	NaLiWG	NaLiWG	NaWG	NaWG	NaLiWG	NaWG	NaWG
2	PWG	LiWG	LiWG	NaLiWG	NaLiWG	NaWG	LiWG	PWG
3		PWG	PWG	PWG	PWG	LiWG	NaLiWG	LiWG
4	NaWG	NaWG	NaWG	–	–	PWG	PWG	NaLiWG
[A] 1– the lowest substrate corrosion, 4 – the highest substrate corrosion								

Tab. 8 – Overall anticorrosion efficiency [%] in the condensation chamber after 720 hours

Coating	Lithium water glass	Sodium water glass	Potassium water glass	Lithium-sodium water glass
1	56.25	56.25	56.25	56.25
2	62.5	56.25	62.5	70
3	67.5	67.5	62.5	72.5
4	–	72.5	62.5	62.5
5	–	77.5	62.5	70
6	65	75	56.25	72.5
7	67.5	72.5	56.25	57.5
8	61.25	56.25	56.25	56.25

Test in the salt chamber with cycles

The tested samples of steel panels with deposited coating films were exposed to a salt chamber medium with cycles of 240 hours. In samples after 240 exposure hours the corrosion of substrate and the corrosion in cut were evaluated. In no samples the formation of osmotic blisters was observed. The overall anticorrosion efficiency is given in the following Table 9. The corrosions of samples was considerable after 240 exposure hours, so that it is not possible to follow the effect of silicate binder type on the efficiency of coating film. The substrate corrosion fluctuated at 100% except the systems filled with zinc, failure at the cut exhibited 2–3 mm. The anticorrosion efficiency was shown in the coating compositions filled with zinc, which only showed a higher anticorrosion efficiency and in which the substrate corrosion was about one third compared to other samples, and failure in the cut fluctuated at 1–2 mm. Again better results were given by the system filled with zinc powder with lamellar particles than a system filed with zinc powder consisting of spherical particle shapes.

Tab. 9 – Overall anticorrosion efficiency [%] in a salt chamber with cycles

Coating	Lithium water glass	Sodium water glass	Potassium water glass	Lithium-sodium water glass
1	66.25	73.75	82.5	66.25
2	72.5	70	66.25	70
3	70	75	72.5	77.5
4	not evaluated	66.25	66.25	66.25
5	not evaluated	66.25	66.25	66.25
6	66.25	66.25	66.25	66.25
7	66.25	66.25	66.25	66.25
8	66.25	66.25	72.5	66.25

Fig. 6 – Photos of experimental steel panels fitted with a cut after the 500 h exposure to a condensation chamber medium and after the coating removal

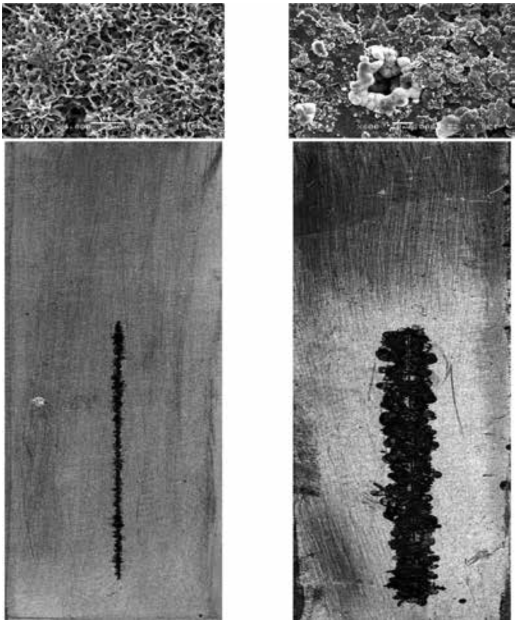

a) spherical Zn particles **b) lamellar Zn particles**

Conclusions

For the coating compositions based on alkali silicates the sodium, potassium, lithium, and lithium-sodium water glass of a high SiO_2/M_2O mole ratio and suitable physico-chemical properties for the preparation of coating compositions were prepared or produced. The silicate coats based on the prepared binders and filled with standard pigments and fillers were hardened by the following methods: a physical mode, a zinc powder with isometrical spherical particles, a zinc powder with lamellar particles, a blocked polyisocyanate in an organic solvent, a blocked polyisocyanate in the water dispersion, a condensed aluminum phosphate, a hydrated aluminum phosphate, and alkoxysilyl isocyanurate.

In coating compositions the tests of physico-mechanical properties of the coats on steel, or, eventually, glass panels, especially the adhesion by the grid method, the bending strength, the cupping stability, the shock resistance and the hardness value of coating, and tests of corrosion stability in a condensation chamber and a salt chamber with cycles.

The results achieved were evaluated as from the effect of silicate binder type point of view, so as the type of used hardening system type point of view. According to the physico-mechanical properties of coats it is possible to order the tested binders from the best one to the worst one: lithium-sodium water glass, potassium water glass, sodium water glass and lithium water glass. According to the composition of coating material and the type of hardener points of view it is possible on the basis of the mechanical testing results to order individual hardening systems from the best one to the worst one: system hardened by the reaction with solvent isocyanate type, system hardened by the reaction with isometric particle zinc, system hardened by the reaction with alkoxysilyl isocyanurate, system without hardener and active components, system hardened by the reaction with lamellar particle zinc, system hardened by the reaction with aqueous isocyanate dispersion, system hardened by the reaction with condensed aluminum phosphate and system hardened by the reaction with hydrated aluminum phosphate.

The order of silicate binders according to the anticorrosion efficiency in a condensation chamber is as follows: lithium-sodium water glass, lithium water glass, sodium water glass and potassium water glass. The order of anticorrosion efficiency of individual systems in a condensation chamber is as follows: system hardened with zinc powder with lamellar particle shapes, system hardened with zinc powder with spherical particle shapes, system hardened with condensed aluminum phosphate, system hardened with hydrated aluminum phosphate, system hardened with isocyanate in an organic solvent, system hardened with aqueous isocyanate dispersion, system hardened by the reaction with alkoxysilyl isocyanurate, system without any hardener and active components.

The overall best results were achieved with lithium-sodium water glass, the coats of which have exhibit good physico-mechanical and also anticorrosion properties. From the composition of coating material point of view are exhibited very good results by the coating materials filled with zinc. Zinc with lamellar particle shapes exhibits a higher anticorrosion efficiency.

Acknowledgement

The project was being carried out with financial support of the Ministry of Industry and Trade of the Czech Republic by Institutional support for long-term conceptual development of research organizations. The project has been integrated into the National Programme for Sustainability I of the Ministry of Education, Youth and Sports of the Czech Republic through the project Development of the UniCRE Centre, project code LO1606.

References

[1] BURIAN, A., KŘÍSTEK, J. *Slévárenství,* 1977, roč. 25, č. 3/4, s. 125–128.

[2] POUCHLÝ J., VAVROUCH I. *Fyzikální chemie koloidních soustav*, SNTL Praha, 1960.

[3] HOECHST AG. GB902935. 1962-08-09. C04B28/26. *Self-hardening water glass cement composition*.

[4] HOECHST AG. US 344525777. Inventors: MEDIC, N. et al. 1969-05-20. *Hardener for water glass cements*. C04B22/16.

[5] HOECHST AG. US 4138261. Inventors: ADRIAN, R. et al. 1979-02-06. *Hardeners for use in water glass cement compositions and process for making them*, C01B25/40, C04B22/16.

[6] PENNWALT Corp. US 4395387. 1983-07-26.inventors: GOLTZ, K., WEST, W. *Method for manufacturing water glass cement hardeners.*

[7] HOECHST AG. GB 737554. 1955-09-28. C04B28/26. *Self-hardening water glass compositions yielding acid-resistant masses and process for making such compositions*.

[8] HUSTINX, E. US 3016358. 1962-02-09. *Modified water glass for casting and its preparing process.*

[9] TAKI CHEM Co Ltd. JP 11116956. 1999-04-27. Inventor: MATSUDA, J. C09K17/46, C04B28/26, C09K17/48 *Hardening of water glass for grout*.

[10] HOECHST AG. GB 891488. *Self-hardening water glass cement compositions* 1962-03-14. C04B28/26.

[11] HOECHST AG. GB865860. 1961-04-19. C04B28/26. *Self-hardening alkali-and acid-resistant water glass cements capable of swelling.*

SYNTÉZA BIODEGRADABILNÍHO POLYMERNÍHO SYSTÉMU NA BÁZI POLYVINYLACETÁTU A JEDNODUCHÝCH CUKRŮ

SYNTHESIS OF BIODEGRADABLE POLYMER SYSTEM BASED ON POLYVINYL ACETATE AND SIMPLE SACCHARIDES

PUKOVÁ K.[1], MACHOTOVÁ J.[2], MIKULÁŠEK P.[1], RÜCKEROVÁ A.[2], BAYEROVÁ P.[2]

1 Ústav environmentálního a chemického inženýrství FChT, Univerzita Pardubice,
Studentská 573, 532 10 Pardubice, Česká republika

2 Ústav chemie a technologie makromolekulárních látek FChT, Univerzita Pardubice,
Studentská 573, 532 10 Pardubice, Česká republika

Summary

The aim of the research is to find the ideal balance and process for polymerizing sugar units in the chain of polyvinyl acetate and thus improve biodegradation, primarily in the soil environment. The product is in the form of an aqueous dispersion which can be applied as biodegradable glue or as a micro-container for gradually releasing fertilizers.

Key words

Polyvinyl acetate, simple sugars, biodegradable polymer

Introduction

The consumption of polymeric materials is constantly growing, therefore their production emphasizes on the use of ecological materials and also on recyclability and biodegradability of the final polymer product. This work is focused on completely biodegradable latex, based on polyvinyl acetate and saccharides [1]. Its potential application may be e.g. the encapsulation [2] of controlled released fertilizers, environmentally friendly paper glues and others. The preparation of lattices is carried out using the technique of emulsion polymerization [3] in an aqueous medium with the addition of sodium carbonate to provide an alkaline pH. Thanks to the basicity of the medium, the sugars are transferred to endiol reactive form (Fig. 1) that is able to participate in a radical polymerization with the vinyl acetate monomers. During the polymerization, alkaline hydrolysis of the acetate groups also occurs resulting in vinyl alcohol units in the polyvinyl acetate chain (Fig. 2).

Fig. 1 – Scheme showing the creation of endiol form of glucose

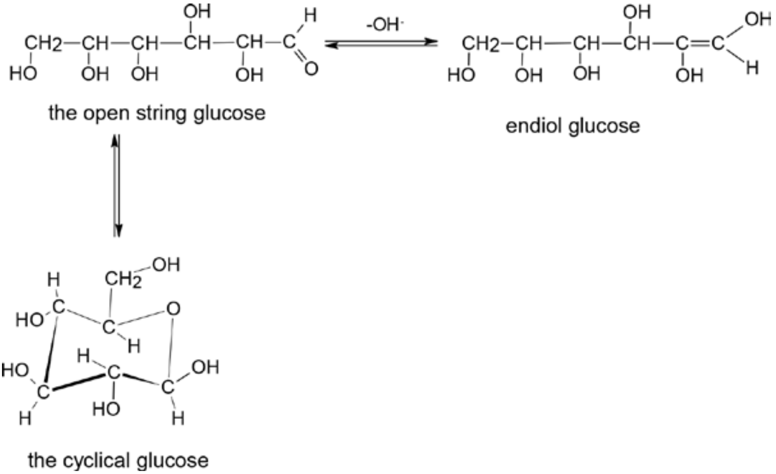

Fig. 2 – Alkaline hydrolysis of polyvinyl acetate

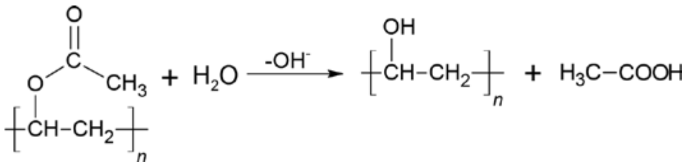

Experimental methods

The emulsion polymerization of vinyl acetate is usually carried out at temperatures around 80 °C. Two series of latexes using two types of saccharides, namely D-glucose and sucrose were prepared. The concentration of the saccharides in the reaction mixture was 100, 50, 25 and 10 wt. % based on the initial amount of vinyl acetate. As the protective colloid, polyvinyl alcohol was used in the amount of 15 wt. % based on the initial amount of vinyl acetate. To prevent degradation of saccharide molecule during the polymerization, the redox initiator [4] based on ammonium persulfate and sodium bisulfite was used. In this case, the polymerization was carried out at 35 °C for a total time of 6.5 hours. In another series of experiments, hydrogen peroxide was used as the initiator. In this case, the polymerization was conducted at 50 °C for a total time of 4.5 hours. To ensure the environment is alkaline, liquid sodium carbonate was added at the beginning and also during the polymerization. In the presence of both types of saccharides, a saponification of the acetate groups is significant as well as a decrease in the molecular weight, leading to the formation of low molecular weight polymers or even oligomer products (Fig. 3). This phenomenon was well described by Takasu et al.[1] who discussed the biodegradability of emulsion copolymers based on polyvinyl acetate and saccharide derivatives. In the case the series of polymerizations initiated by the redox initiator system, a significant decrease in conversion occurred. For this reason, a thorough attention was focused on the series of lattices based on the initiation by means of hydrogen peroxide in later studies.

Fig. 3 – The attachment of glucose in a polymer chain composed of vinyl acetate and vinyl alcohol units

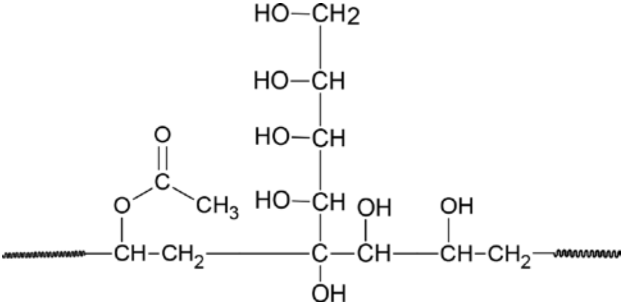

Results and Discussion

To prove the appearance of the saccharide units in the polyvinyl acetate chains, the infrared spectroscopy using the FTIR Nicolet 6700 instrument with a spectral resolution of 0.09 cm^{-1} with unlimited use in distant, intermediate and near infrared region of wave numbers length of 27,000 to 10 cm^{-1} was used. For separating the water-dissolved saccharide and lower-molar-mass polyvinyl alcohol (protective colloid) and thus ensuring the proper measurements of the prepared polyvinyl acetate polymer bearing saccharide units, the samples were precipitated in tetrahydrofuran and washed repeatedly with distilled water to give the polyvinyl acetate polymer portion which was analyzed by the aforementioned method.

Figure 4 is IR spectrum for the polyvinyl acetate sample containing sucrose. As indicated in the spectrum, saccharide units are located in the region of 1,000–1,100 cm^{-1}. Furthermore, absorption peaks of acetate groups and hydroxyl groups can be seen as well. Due to the alkaline hydrolysis of the acetate groups, not only alcohol, but also sodium acetate arises during the polymerization, which was also detected in the spectrum. For the comparison, Figure 5 shows an infrared spectrum of the polyvinyl acetate sample containing no saccharide units. This can be seen in the region of 1,000–1,100 cm^{-1} where no absorption peak was recorded. The spectrum shows the presence of vinyl acetate and vinyl alcohol units.

Fig. 4 – The infrared spectrum of a resulting polymer produced via the hydrogen peroxide-initiated polymerization of vinyl acetate and sucrose (the starting ratio of vinyl acetate and sucrose was 1/1)

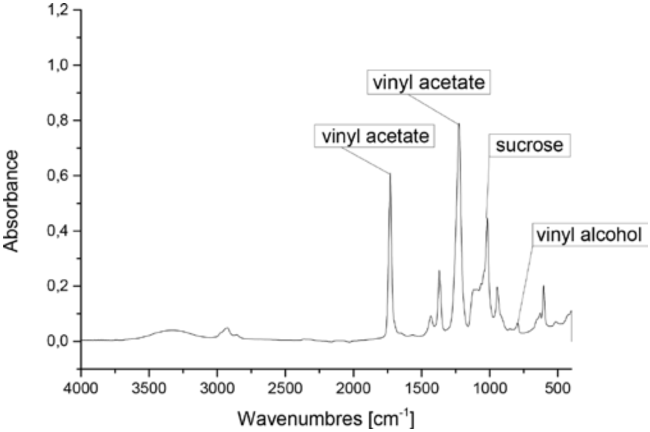

Fig. 5 – The infrared spectrum of a resulting polymer produced via the hydrogen peroxide-initiated polymerization of vinyl acetate

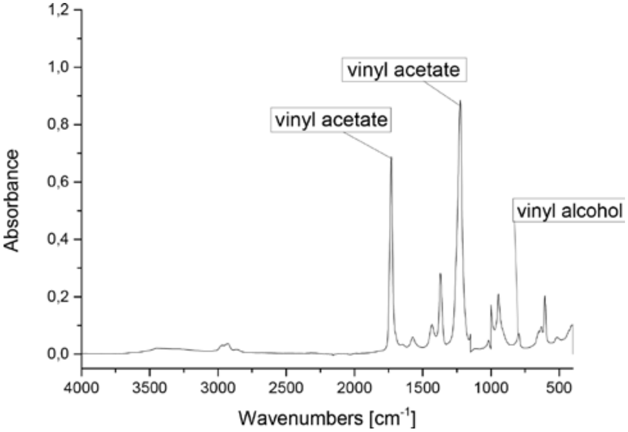

Conclusion

Currently, the biodegradability of the prepared materials is being tested according to CSN EN ISO 14855-1 based on the monitoring of CO_2 evolution measured by means of gas chromatography. This standard method is aimed to be confronted with the results of the degradability testing from the point of view of bacterial decomposition of inoculum (compost). The results of the latter test will be compared with international standards, the Organization for Economic Cooperation and Development (OECD). The tests are divided into two parts, the biological decomposition in the ground aerobic and anaerobic disintegration and a section of the substance in aqueous medium.

Reference

[1] A. Takasu, M. Baba, T. Hirabayashi; Preparation and biodegradation of sugar-containing poly(vinyl acetate) emulsions, *Macromolecular Bioscience* 2008, 8, p193–198

[2] A. K. Patra, S. Dahiya; *Microencapsulation – technique and applications*, Man-made in India, 2009, 52, p224–232

[3] J. Machotová, J. Šňupárek, L. Prokůpek, T. Rychlý, P. Vlasák; Effect of functionalized core-shell microgels prepared by emulsion polymerization on acrylic coatings properties, *Progress in Organic Coatings* 2008, 63, p175–181

[4] I. D. Sideridou, D. S. Achilias, O. Karava; Reactivity of benzoyl peroxide/amine system as an initiator for the free radical polymerization of dental and orthopaedic dimethacrylate monomers: effect of the amine and monomer chemical structure, *Macromolecules* 2006, 39, p2072–2080

VLASTNOSTI NÁTĚRŮ NA BÁZI SAMOSÍŤUJÍCÍCH LATEXŮ OBSAHUJÍCÍ NANOČÁSTICE OXIDU ZINEČNATÉHO

PROPERTIES OF COATINGS BASED ON SELF-CROSSLINKING LATEXES CONTAINING NANOPARTICLES OF ZINC OXIDE

RÜCKEROVÁ A., MACHOTOVÁ J., PUKOVÁ K.

Institute of Chemistry and Technology of Macromolecular Materials, University of Pardubice,
Studentská 95, 532 10, Pardubice

Summary

The paper deals with the synthesis and properties of water polymer dispersions. Latexes were prepared by emulsion polymerization with adding zinc oxide during the polymerization in the amount from 0 to 6 wt.%. The paper describes preparation and characterization of latex coatings as well. The real amount of zinc oxide in the prepared water-borne coatings is correlated with optical properties of the coatings. The creation of flash rust was shown to be inhibited by the application of the coatings on steel substrates.

Key words

Anticorrosive coatings, emulsion polymerization, latex, zinc oxide

Water dispersions of copolymer microgel particles were prepared by emulsion polymerization. Composition of copolymer microgel particles consisted of methyl methacrylate (MMA), butyl acrylate (BA), methacrylic acid (KMA) and diacetone acrylamide (DAAM) as starting main monomers. Microgel particles are structured as core-shell particles, wherein the shell of microgel particles was crosslinked by adding hexaallylamino-*cyclo*-triphosphazene. [1–2] Additionally, an interparticle crosslinking called keto-hydrazide crosslinking was performed after draw-downing the coating films. [3] Nanoparticles of zinc oxide were added in various amounts to the polymer system during the synthesis, specifically to the emulsion of monomers comprising the shell structure of microgel particles. The zinc oxide was added to the polymer system in order to inhibit the creation of flash rust. Creation of flash rust after the application of water based coatings on steel substrates is a frequently referred phenomenon. [4–7]

Synthesis and characterization of latexes

Emulsion consisting of water, acrylic monomers mixture, initiator and emulsifier was added into a heated reactor. This emulsion formed the core of core-shell microgel particles. After 15 minutes of post-polymerization, the emulsion of monomers creating the shell of microgel particles was added dropwise. First, water with the emulsifying agent and nano-powder of zinc oxide was allowed to the exposure of ultrasonic waves for 20 minutes, then the mixture was mechanically dispersed using a disperser for 15 minutes. After that, the aqueous phase containing zinc oxide was stirred with a mixture of monomers and the initiator. The resulting zinc oxide-containing monomer emulsion was added dropwise to the reactor and the polymerization of shell layer of polymer particles proceeded. After cooling the polymer dispersion at 23 °C, latexes were characterized in terms of the amount of coagulum formed during the polymerization. The amount of coagulum indicates the stability of polymer system. Besides, the Brookfield viscosity, pH and the minimal film-forming temperature were measured.

Characterization of coating films

The prepared latexes were casted on glass-, steel- and silicone substrates. Monitored properties of the coatings were investigated after 30 days of drying at 23 °C. The coatings applied on glass substrates were evaluated in terms of their appearance, gloss and surface hardness using pendulum damping by Persoz. The hardness was measured after 24, 48 and 72 hours of drying and after 30 days. The dried films formed on silicone substrates were tested from the point of view of their noncombustible share. By this method, the real content of solid zinc oxide in polymer film was examined. Coating films prepared on silicone substrates were removed from the substrate and weighed in porcelain cups which were burned at 600 °C before. Prepared samples were combusted in an oven at 600 °C up to achieving constant weight of incombustible residues. After weighing of incombustible residues the real content of zinc oxide in the coating film was calculated.

Discussion

The amount of coagulum shows the stability during the emulsion polymerization. The lowest amount of coagulum was reached by using 0.5 wt.% of hexaallylamino-*cyclo*-triphosphazene in the shell structure of microgel particles and also in the case of 5 wt.% of diacetone acrylamide relative to the amount of monomers. Structure of hexaallylamino-*cyclo*-triphosphazene is shown in Figure 1.

Fig. 1 – Structure of hexaallylamino-cyclo-triphosphazene

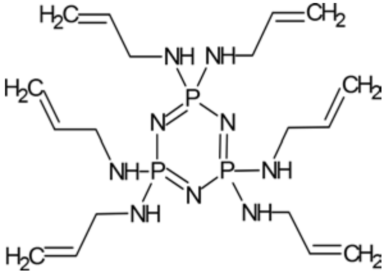

Therefore, the formulation with 0.5 wt.% of hexaallylamino-*cyclo*-triphosphazene was chosen as the most appropriate microgel composition and latexes containing this amount of hexaallylamino-*cyclo*-triphosphazene with various concentration of zinc oxide ranging from 0,5 wt.% to 6 wt.% were synthesized with the particle size of 40–100 nm. It was found that the amount of coagulum increased with increased amount of zinc oxide that was added to the polymer system. The coagulum contained a certain amount of zinc oxide, so the actual amount of zinc oxide within the latex is not consistent with the quantity added during the synthesis. The quantity of coagulum in various polymer systems is shown in Figure 2. For determining the real amount of zinc oxide, the amount of incombustible residues in the coating film without zinc oxide was deducted.

Fig. 2 – Amount of coagulum depending on the theoretical zinc oxide concentration in latex

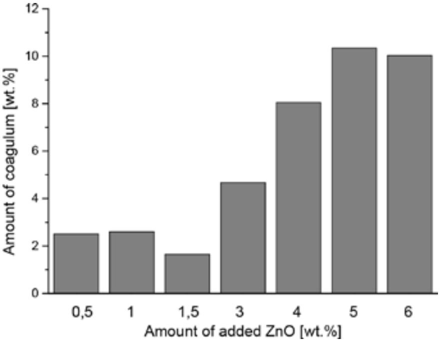

In the case of the prepared self-crosslinking latexes, the film formation is achieved by two simultaneous processes: the coalescence of microgel particles and interparticle crosslinking via diacetone acrylamide and adipic acid dihydrazide reaction. Also the formation of ionic bonds between Zn^{2+} ions and COO^{-} groups belonging to methacrylic acid takes place there. This kind of bonds affects the film forming and also coating properties. The highest amount of zinc oxide in the coating film was achieved by preparing the latex with 4 wt.% of zinc oxide, as shown in Figure 3. It was shown that higher amount of added zinc oxide does not affect properties of the coatings, because the major amount of zinc oxide was excluded from the polymeric system with the coagulum.

Fig. 3 – Amount of incombustible residues depending on the theoretical zinc oxide concentration in the coating film

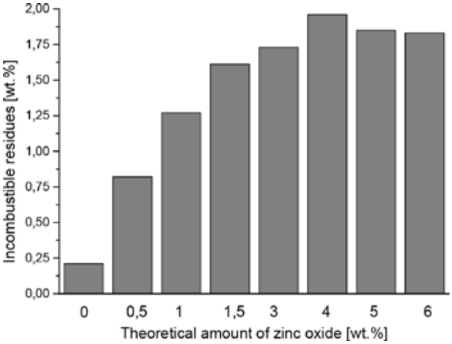

The prepared coatings were evaluated for their l appearance. The coating films were transparent and clear, without any surface defects. Only the coating prepared with 4 wt.% of zinc oxide exhibited surface cracks and haze. This phenomenon could be caused by a higher minimum film-forming temperature of this coating related to the high amount of zinc oxide nanoparticles. This phenomenon was confirmed by measuring the minimum film-forming temperature. The value of minimum film-forming temperature depended on the concentration of the added zinc oxide, as shown in Figure 4. It is evident that the coating system prepared with 4 wt.% of zinc oxide reached the highest value of 14.9 °C.

Considering the inadequate appearance of coating films based on latexes prepared with 4 wt.% of zinc oxide, this coating system is not very convenient for practical use. This polymeric system exhibited also the highest amount of coagulum and the highest value of minimum film-forming temperature. Hence, it would be appropriate to use maximum 3 wt.% of zinc oxide for coatings for further research.

Fig. 4 – Value of minimum film-forming temperature depending on the theoretical zinc oxide concentration in the coating film

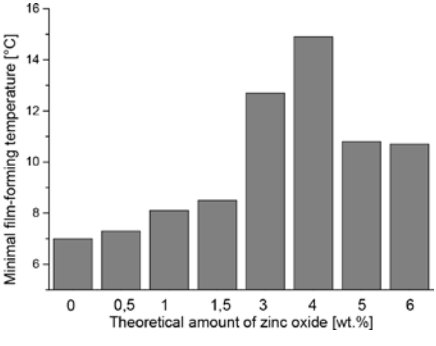

Conclusion

Latex coatings were prepared by emulsion polymerization that was altered by a simultaneous addition of zinc oxide to the polymeric system during the polymerization. The amount of coagulum formed during polymerization increased with the increasing amount of zinc oxide added to the polymeric system. Therefore, it is appropriate from an economical viewpoint to use maximal 3 wt.% of zinc oxide (related to monomers) during the polymerization. This claim was supported by optical properties of coating films. Higher amount of zinc oxide than 3 wt.% caused turbidity of coating films and mechanical defects of coatings.

References

[1] A.B. Foster, P.A. Lovell, M.A. Rabjohns, Design and synthesis of structured latex particles for enhancing the performance of water-borne pressure-sensitive adhesives, *Polym. Mat. Sci. Eng.*, 2008, 99:788–789

[2] X. Zhang, Y. Liu, H. Huang, Y.Li, H. Chen, The diacetone acrylamide crosslinking reaction and ist control of core-shell polyacrylate latices at ambient temperature, *J. Appl. Polym. Sci.*, 2012, 123, 1822–1832

[3] F. Buckmann, A. Overbeek, T. Nabuurs, Self-crosslinking surfactant free acrylic dispersions, *Eur. Coat. J.*, 2001, 6:53–60

[4] J.Auvinen, L. Wirtanen, The influence of photocatalytic interior paints on indoor air quality, *Atmospheric Environment*, 2008,42,4101–4112

[5] D. Raoufi, T.Raoufi, The effect of heat treatment on the physical properties of sol-gel derived ZnO thin films, *Applied Surface Science* 2009, 225, 5812–5817

[6] J.Chen, Ch. Poon, Photocatalytic construction and building materials: From fundamentals to application, *Building and Environment*, 2009, 44, 1899–1906

[7] S.K. Dhoke, A.S. Khana, T. Sinha, Effect of nano-ZnO particles on the corrosion behavior of alkyd-based waterborne coatings, *Progress in Organic Coatings*, 2009, 64, 371–382

TRYSKANIE – VHODNÁ VOĽBA PREDÚPRAVY POVRCHOV POD POVLAKY

BLASTING – SUITABLE CHOICE OF THE SURFACE TREATMENT BEFORE COATINGS APPLICATION

BREZINOVÁ J., DRAGANOVSKÁ D., GUZANOVÁ A.

Katedra strojárskych technológií a materiálov, Strojnícka fakulta, Technická univerzita v Košiciach

Summary

The article deals with still attractive technology of cleaning and roughening of engineering surfaces – abrasive grit blasting. It refers to the various types of primary blasting effects in cleaned surface – plastic deformation, work hardening, heat affection with possible changes in structure of the base material. Blasting abrasive, however, has secondary, sometimes negative effects on base material – residual stress, secondary pollution of cleaned surface by notched fragments of abrasive and changes in activity of cleaned surfaces.

Key words

Mechanical pre-treatment, blasting, blasting media, coating

V súčasnej dobe stúpa náročnosť na akosť, životnosť, technickú úroveň a čoraz viac na vzhľadovú stálosť strojárskych výrobkov. Z hľadiska spoľahlivej funkcie a životnosti každej súčiastky má zvláštny význam jej povrch. Vlastnosti povrchovej vrstvy a základného materiálu sú obvykle rôzne a tieto časti sú rôzne namáhané. Povrchové vrstvy sú často zdrojom porúch, ktoré sa šíria do celého objemu. Procesy, ktoré prebiehajú na povrchu súčiastky a v jej povrchovej vrstve, určujú aj jej interakciu s inými súčiastkami a prostredím.

Z celého radu spôsobov predúpravy povrchu, či už chemickou alebo mechanickou cestou, vystupuje do popredia tryskanie ako vhodná technológia, ktorou je možné pripraviť povrch požadovanej akosti, čím sa rozumie okrem očistenia povrchu základného materiálu aj dosiahnutie vhodnej mikrogeometrie a fyzikálnych resp. fyzikálno – chemických vlastností povrchu.

Technológia tryskania patrí do skupiny mechanického opracovania povrchu základného materiálu, ktorého nástroj – tryskací prostriedok (ďalej len TP), vyvoláva pri dopade v jeho povrchových vrstvách kvalitatívne zmeny, pričom vzniká charakteristická morfológia povrchu. Pri dopade TP na otryskávaný základný materiál vznikajú kvalitatívne premeny oboch zúčastnených subjektov.

V praxi sa technológia tryskania využíva v širokom rozsahu. Typickými aplikáciami tryskania sú odokovinenie, odhrdzavenie, zdrsnenie povrchu prípadne vyhladenie povrchu, tvorba vhodnej morfológie povrchu, predúprava povrchu pod rôzne typy povlakov, dekoratívna úprava povrchu, odstraňovanie starých náterov, spevňovanie povrchu, zvýšenie únavovej a korózno-únavovej pevnosti, úprava zvarov a ich okolia a ďalšie.

Povrchové zmeny dosahované po aplikácii tryskania

Povrch, vytvorený tryskaním, pri opakovanom zaťažení akumuluje plastickú deformáciu. Pod vplyvom opakovaného zaťaženia povrchu materiálu povrchové vrstvy menia rozmery, geometrické charakteristiky, štruktúrne vlastnosti, stav napätosti, tepelné ovplyvnenie materiálu a iné. Tryskaním sa dosahuje zvýšenie niektorých mechanických a technologických vlastností (napr. húževnatosti, odolnosti proti únave a opotrebeniu) a iné.

Z aspektu účinku tryskania na základný materiál, treba tryskanie chápať ako proces plastickej deformácie povrchu, resp. proces elasticko-plastickej deformácie kovu v celom jeho objeme. Úhrnná energia pri tryskaní, ako pri každom procese plastickej deformácie za studena sa spotrebuje na:

1. vlastnú plastickú deformáciu doprevádzanú:
    a) spevnením základného materiálu,
    b) tepelným efektom,
    c) štruktúrnymi zmenami,
    d) zmenou mechanických a technologických vlastností,

2. vyvolanie sekundárnych javov a to:
    - a) zvyškové napätia,
    - b) zmeny charakteru povrchu / zdrsnenie a zväčšenie povrchu /.

Vlastná plastická deformácia povrchu po tryskaní

V procese tryskania tryskací prostriedok naráža na povrch a v mieste dopadu ho plasticky deformuje, obr.1. Pri náraze na povrch sa premení časť energie na teplo a odvedie sa povrchom súčiastky a časť na prácu spotrebovanú na plastickú deformáciu.

Obr. 1 – Zmeny povrchu pri dopade granulátu. Oblasť elastických -1 a plastických -2 deformácií

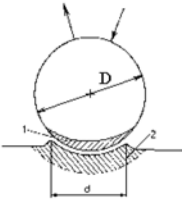

Proces plastickej deformácie sa uskutočňuje pohybom dislokácií jedným z dvoch jednoduchých mechanizmov: sklzom alebo dvojčatením. Mechanizmus je závislý na kryštalografickej stavbe kovov a podmienkach plastickej deformácie. že tryskanie spôsobuje plastickú deformáciu povrchových vrstiev, v ktorých sa vytvárajú tlakové zvyškové napätia.

Spevnenie materiálu je dôsledok plastickej deformácie, je sprevádzané zmenou vlastností materiálu po plastickej deformácii. Súvisí s obtiažnejším vznikom dislokácií alebo ich obmedzeným pohybom a prejavuje sa zvýšením pevnosti materiálu v povrchovej vrstve alebo v celom objeme materiálu. Charakteristické pre tryskané povrchy sú tlakové zvyškové napätia a extrémne vysoké hustoty dislokácií v povrchových vrstvách. Základnú myšlienku v teórii spevnenia formuloval Taylor r. 1934, ktorý vyslovil hypotézu, že ak plastická deformácia prebieha pohybom dislokácií, spevnenie je spôsobené obtiažnejším pohybom dislokácií, alebo tým, že dislokácie ťažšie vznikajú. Krivka spevnenia závisí od štruktúry kryštálu, od orientácie, čistoty a stavu povrchu .

Priebeh mikrotvrdosti povrchu po tryskaní je znázornený na obr. 2. Krivka mikrotvrdosti je rozdelená na tri oblasti:

I. – oblasť spevnenia (hĺbka spevnenia),

II. – oblasť zasiahnutá plastickou deformáciou,

III. – neovplyvnená oblasť.

Obr. 2 – Schematické znázornenie zmeny mikrotvrdosti po otryskaní

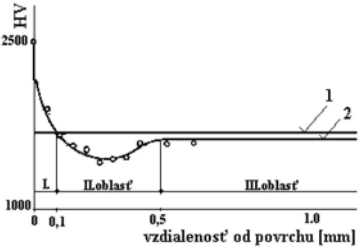

1-priebeh mikrotvrdosti pred tryskaním, 2-priebeh mikrotvrdosti po tryskaní

Tepelný efekt. Energia, vynaložená na uskutočnenie procesu plastickej deformácie, určitou svojou časťou, podľa podmienok deformácie, sa podieľa na vývine tepla. Teplo v mieste kontaktu tryskacieho prostriedku a povrchu základného materiálu vzniká transformáciou deformačnej energie pri plastickej deformácii a v dôsledku trecej práce vynaloženej pri danom procese. Schematické znázornenie tepelného ovplyvnenia TP a základného materiálu je na obr. 3. Teplo v medznej zóne nástroj (tryskací prostriedok) – materiál významne ovplyvňuje procesy trenia a pomery v oblasti plastickej deformácie. Výška teploty, teda aj pomery pri plastickej deformácii, sú ovplyvnené podmienkami deformácie. Rozhodujúci je vplyv rýchlosti deformácie, resp. stupňa deformácie.

Obr. 3 – Schematické znázornenie tepelného ovplyvnenia TP a základného materiálu pri tryskaní

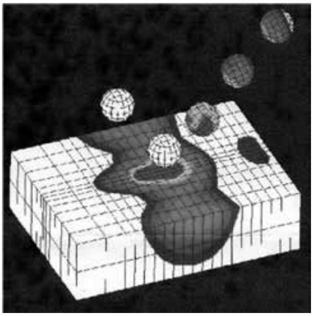

Štruktúrne zmeny po tryskaní. Štruktúrne zmeny sú vyvolané spolupôsobením plastickej deformácie a tepelného efektu. Na povrchu substrátu v otryskanom materiáli dochádza k rekryštalizácií, čoho dôkazom je aj výskyt dvojčiat ako dôsledok rekryštalizačného žíhania.

Zmeny mechanických a technologických vlastností. Každý proces plastickej deformácie, teda aj tryskanie, je sprevádzaný zmenou mechanických a technologických vlastností materiálov súčiastok a polotovarov. Na základe vykonaných experimentálnych prác je možné konštatovať, že:

– lineárne stúpa medza pevnosti, medza klzu a ich pomer,

– klesá ťažnosť,

– vrubová húževnatosť sa otryskaním takmer nemení,

– rastie medza únavy,

– pri narastaní rozmeru zrna TP a zmenšovaní hrúbky plechu hlbokoťažnosť klesá.

2 Sekundárne javy sprevádzajúce proces tryskania

Okrem primárnych dôsledkov tryskania na základný materiál sa stretávame aj s jeho sekundárnymi vplyvmi, medzi ktoré je možné zaradiť zvyškové napätia vznikajúce v závislosti na plastickej deformácii otryskaného povrchu, zmenu mikrogeometrie povrchu ako aj čistotu a aktivitu otryskaného povrchu. Dôsledky tryskania na povrchu základného materiálu závisia na kinetickej energii letiaceho zrna.

Zvyškové napätia sú dôsledkom porušenia rovnovážnych síl na povrchu materiálu, čo vedie k jeho deformácii. V procese tryskania po dopade TP je materiál podrobený plastickej deformácii. V určitej hĺbke napätie v materiáli nie je vyššie ako medza pružnosti a po odľahčení sa pružne deformovaná oblasť odpruží. V plasticky deformovanej (neodpruženej povrchovej vrstve vznikajú zvyškové tlakové napätia.

Zmeny charakteru povrchu. Tryskanie je okrem vyššie spomínaných javov doprevádzané zmenou charakteru povrchu, ktorý sa podstatne líši od povrchov získaných trieskovým obrábaním. Dopadom súboru zŕn TP na povrch základného materiálu, z ktorých každé sa zúčastňuje na lokálnom plastickom pretvorení povrchu, vzniká členitý povrch, ktorého charakter je závislý na viacerých činiteľoch.

Hlavnými faktormi, ktoré ovplyvňujú charakter otryskaného povrchu sú: tvar a rozmer zrna TP, stupeň pokrytia povrchu, režim tryskania a materiálové charakteristiky základného materiálu a materiálu TP. Otryskaný povrch patrí medzi neorientované (izotropné) povrchy, čo znamená, že drsnosť a rozstup vrcholkov v navzájom kolmých smeroch sa výrazne nelíšia. Vzhľady povrchov sú na obr. 5.

Čistota a aktivita povrchu po tryskaní – Povrch sa vo všeobecnosti chápe ako rozhranie dvoch fáz, kde sa odohrávajú rozmanité procesy, ako je adsorpcia cudzích látok, korózia a pod. Zvlášť dôležité je definovať povrch, ktorý vzniká pri technológiách predúprav. Tu totiž je tento povrch určujúcim faktorom kvality následne aplikovaného povlaku, resp. povlakovacieho systému.

V mieste úderu častice sa základný materiál porušuje a odkrýva sa nový, tzv. juvenilný povrch materiálu. Juvenilný povrch sa vyznačuje veľmi vysokou aktivitou. Ak je tento povrch vytváraný v čistom vákuu, potom jeho aktivita klesá veľmi pomaly. Avšak v reálnych podmienkach to neplatí a aktivita povrchu základného materiálu sa veľmi rýchlo znižuje (chemická adsorpcia plynov z atmosféry a oxidácia).

Povrch je okrem chemického znečistenia, orientácie a pnutí zmenený aj fyzikálne. Fyzikálne zmeny povrchu vznikajú najmä v dôsledku mechanického opracovania a to najmä mäkkých materiálov. Vznik vrstiev na kovovo čistom povrchu materiálu s mechanicky opracovaným povrchom pri styku s okolitým prostredím je znázornený na obr. 4.

Obr. 4 – Vznik vrstiev na kovovo čistom povrchu mechanicky opracovanom

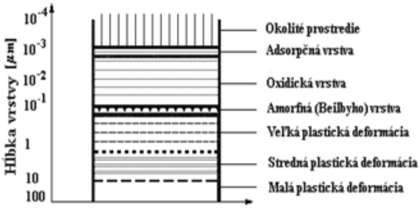

Aktivita je charakterizovaná schopnosťou korózneho roztoku rozpúšťať hydroxid kovu, ktorý pri anódovom rozpúšťaní vzniká. Opakom je pasivita, ktorá je z hľadiska ochrany veľmi výhodná, nakoľko zabezpečí spomalenie alebo úplné zastavenie korózie v agresívnych prostrediach. Za pasívny je považovaný taký stav povrchu kovu, pri ktorom na mieste predpokladanej intenzívnej korózie v určitom prostredí sa kov stal korózne odolným a jeho potenciál sa posunul k ušľachtilejším hodnotám. Príčiny účinného zníženia korózie pri prechode do pasívneho stavu sa vysvetľujú vytvorením bariéry – medznej vrstvy medzi kovom a prostredím, ktorá spomaľuje ich vzájomnú reakciu. Pasivita nastane vytvorením bariéry buď adsorpciou niektorých látok (prevažne kyslíka z roztoku na povrchu kovu) alebo existenciou tenkej vrstvy zlúčeniny (zvlášť oxidov na povrchu kovu) .

3 Typy tryskacích prostriedkov

Veľmi dôležitou úlohou pri tryskaní je voľba vhodného druhu TP. Použité TP vyvolávajú na povrchu také zmeny, ktoré zodpovedajú jeho charakteru, t.j. materiálu, tvaru a veľkosti zŕn. Voľbu druhu TP značne ovplyvňujú ekonomické činitele, určujúcim činiteľom je však účel, pre ktorý má byť tryskanie použité (čistenie, úprava povrchu, spevnenie atď.). Tam, kde sa vyžaduje recyklácia TP sa používajú TP s dlhou životnosťou (predovšetkým **kovové TP**) a kde ide o viac-menej jednorázové použitie uprednostňujú sa **nekovové TP** minerálneho pôvodu. Je žiadúce, aby bolo v symbióze ekonomické a ekologické hľadisko.

Pod pojmom tryskací prostriedok rozumieme nástroj tryskania, ktorý je charakteru zrnitého (polydisperzného), tvaru určeného výrobnou technológiou. Podľa výrobnej histórie sa TP delia na:

– **guľovitý TP** (granulát), obr. 5a. Účinkom guľovitého TP sa vytvorí povrch so zaguľateným reliéfom. Používa v prevažnej miere na spevnenie povrchových vrstiev otryskávaného materiálu.

– **ostrohranný TP** (drvina), obr. 5b. Povrch je charakterizovaný ostrými hlbokými zásekmi. Používa sa hlavne pre získanie požadovanej drsnosti pri predúprave ako aj na čistenie povrchu.

– **sekaný drôt**, obr. 5c, tvaru valčekov, vyrobený z patentovaného oceľového drôtu s pevnosťou 1600–2200 MPa.

Obr. 5 – Vzhľad tryskacích prostriedkov a povrchov po ich aplikácii

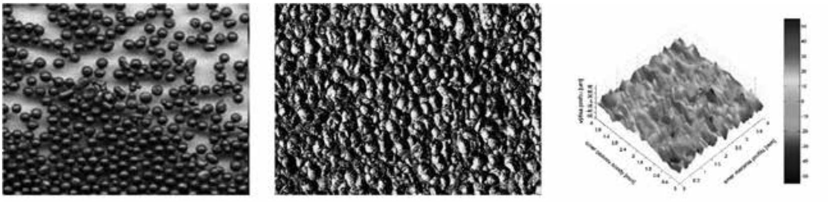

a) granulát

b) drvina

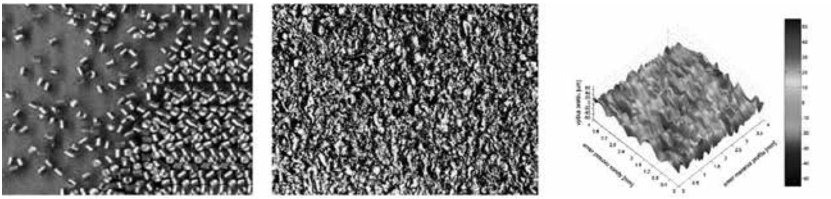

c) sekaný drôt

Najrozšírenejšie kovové TP sú vyrobené na báze železa, prípadne zušľachtené legovaním alebo tepelným spracovaním. Popri týchto materiáloch používajú sa aj iné kovové TP pre tryskanie neželezných kovových výrobkov. Najintenzívnejšie rozšírenie zaznamenali štyri druhy kovových TP. Sú to liatinová a oceľová drvina, oceľový granulát a sekaný drôt. Z nekovových TP najväčšie rozšírenie zaznamenali prostriedky minerálneho pôvodu, či už prirodzené alebo umelé (korundová drvina, sklo, meďná troska, demetalizovaná oceliarenská troska atď.).

Záver

Na základe uvedeného je možné konštatovať, že tryskanie je technológia so značným uplatnením v praxi. Aby sa však tryskanie mohlo technicky správne a ekonomicky výhodne použiť, t.j. aby sa dosiahla žiadaná kvalita povrchu pri ekonomicky prijateľných nákladoch, nestačí tryskanie len mechanicky aplikovať, ale je nutné neustále hľadať najvhodnejšie technické parametre pre túto technológiu, a to tak z aspektu nových tryskacích prostriedkov, režimu tryskania ako aj zariadení.

Poďakovanie

Príspevok je riešený v rámci grantového projektu VEGA č. 1/0600/13.

Literatúra

[1] Brezinová J., Guzanová A., Draganovská D. *Abrasive Blast Cleaning and Its Application*. 1st ed. 2015. 107 p. ISBN 978-3-03835-995-1.

[2] Guzanová A., Brezinová J., Koncz J., Draganovská D., Landová M., Sekundárne znečistenie povrchov po mechanickej predúprave tryskaním., in: *Pigmenty a pojiva 2015*, Pardubice, p129–131.

[3] Draganovská D., Ižaríková G., Brezinová J., Guzanová A., The study of parameters of surface roughness by the correlation analysis, *Materials Science Forum*, Trans Tech Publications, 2015, 818, p15–18.

[4] Brezinová J., Guzanová A., Draganovská D., Koncz J., Electrochemical Characteristics of Mechanically Treated Metallic Surfaces, *Material Science Forum*, 205, 818, p145–148.

[5] Guzanová A., Brezinová J., Draganovská D., Jaš F., A study of the effect of surface pre-treatment on the adhesion of coatings, *Journal of Adhesion Science and Technology*, 2014, 28, 17, p1–18.

[6] Hadzima B., Bukovina M., Škublová L., Brezinová J., Vplyv tryskania na elektrochemické charakteristiky povrchu horčíkovej zliatiny AE21, *Chemické listy*, 2011, 105, 16, p455–458.

[7] Momber A., *Blast cleaning technology*, Springer-Verlag Berlin Heidelberg, 2008, p.540.

[8] Novák Z., Prostorová charakteristika textury povrchu, *MM Průmyslové spectrum*, 2009, 10, 10, p.64.

SAMOSÍŤUJÍCÍ LATEXY OBSAHUJÍCÍ RETARDÉR HOŘENÍ

SELF-CROSSLINKING LATEXES CONTAINING A FLAME RETARDANT

ZÁRYBNICKÁ L., MACHOTOVÁ J.

Institute of Chemistry and Technology of Macromolecular Materials, Faculty of Chemical Technology, University of Pardubice, Studentska 573, 532 10 Pardubice, Czech Republic

Summary

The paper describes the development of transparent one-component coating systems based on the core-shell acrylic aqueous dispersions prepared using emulsion polymerization technique. Latexes of functionalized core-shell particles bearing in the structure a covalently linked hexachloro-cyclo-triphosphazene were prepared by the semi-continuous non-seeded emulsion polymerization of methyl methacrylate, butyl acrylate and methacrylic acid as main monomers. For interfacial crosslinking, diacetone acrylamide was copolymerized into the shell layer of latex particles to provide sites for subsequent reaction with adipic acid dihydrazide. The presence of the flame retardant increased the flame stability of coatings in terms of total heat release, amount of released smoke and maximum average rate of heat emission which indicates a slower flame spread during the material combustion.

Key words

Phosphazene, flame retardant, emulsion polymerization, acrylic monomers

Introduction

Currently, an increasing interest in exploiting of waterborne polymer coatings is related to the growing pressure on environmental protection, especially the need to comply with legislation restricting the volatile compounds (VOC) and emissions related to the use of solvent-based polymer coating systems. The aqueous colloidal polymer dispersions, i.e. latexes are used in many applications such as adhesives, additives for paper, paints and cosmetics, synthetic rubbers, floor polishes and sealants. The colloidal polymeric particles can be prepared to exhibit a desired morphology, composition, particle size distribution, surface groups and a molecular weight [1].

For special applications, increased flame stability of utilized coating materials may be appreciated. Several authors investigated derivatives of halogeno-*cyclo*-phosphazenes linked into the structure of the film-forming polymers. Hexahalogeno-*cyclo*-triphosphazenes contain alternating phosphorus and nitrogen atoms in the cycle with two substituents attached to the phosphorus atoms. These compounds exhibit unusual thermal properties, such as flame retarding and self-extinguish ability [2,3].

In the present work, we focused on the synthesis of a flame retardant based on hexachloro-*cyclo*-triphosphazene (HCCTP) and its incorporation into self-crosslinking latexes based on DAAM and ADH crosslinking system. The flame retardant was synthesized using nucleophilic substitution of HCCTP with allylamine resulting in hexaallylamino-*cyclo*-triphosphazene (HACTP). The latexes bearing in the polymeric structure covalently linked molecules of HACTP were further were investigated with respect to their potential application as transparent binders with improved flame stability.

Experimental

Synthesis of HACTP

The synthesis of HACTP was performed under anhydrous conditions in an inert argon atmosphere using Schlenk containers. The synthesis reaction of the phosphazene derivative is shown in Fig. 1. A Schlenk flask was filled in with 0.0014 mol of HCCTP and 20 mL of THF under an inert atmosphere. 0.0073 mol of allylamine was slowly added dropwise into the stirred reaction mixture at the boiling point of THF. The reaction was terminated after 72 h followed by filtration of resulting salts. Three times washing with THF was followed by vacuum distillation to remove THF from the product. The preparation of HACTP was monitored during the synthesis by means of thin layer chromatography and the identity of the prepared derivative was confirmed also by measuring the melting point.

Fig. 1 – The structure of hexaallylamino-cyclo-triphosphazene

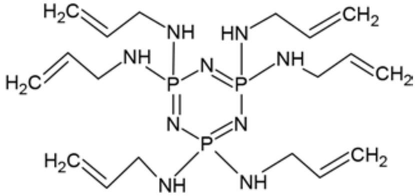

Preparation and characterization of self-crosslinking latexes with copolymerized HACTP

Self-crosslinking latexes of core-shell particles containing various levels of HACTP were synthesized by the semi-continuous non-seeded emulsion polymerization comprising a variable content of acrylic monomers. The latexes were produced in a 700 ml glass reactor under nitrogen atmosphere at 85 °C. The reactor charge was put into the reactor and heated to the polymerization temperature. Then the monomer emulsion was fed into the stirred reactor at the feeding rate about 2 ml/min in two steps (1. core preparation, 2. shell preparation). After that, during 2 hours of hold period the polymerization was completed. The recipe of emulsion polymerization is described in the reference [4. The pH was adjusted to 8.5 with ammonia solution. To produce the self-crosslinking latexes, a 10 wt.% aqueous solution of ADH, in the amount corresponding to the molar ratio ADH:DAAM = 1:2, was added to the latex under agitation. The minimum film-forming temperature (MFFT) was measured using the MFFT-60 instrument (Rhopoint Instruments, UK) according to ISO 2115. For the glass transition temperature (T_g) and gel content measurements, specimen were prepared by pouring the self-crosslinking latexes into a silicone mould. Films were formed by water evaporation at room temperature for a month. T_g values were determined by means of differential scanning calorimetry using a Pyris 1 DSC instrument (Perkin-Elmer, USA). The gel content was determined according to CSN EN ISO 6427 using a 24-hr extraction with THF in a Soxhlet extractor. The presence of the copolymerized HACTP in the emulsion copolymers was investigated by means of ^{31}P NMR using a Bruker Advance DRX 300 instrument (Bruker Corp., Germany) at the frequency of ^{31}P: 202.46 MHz and 85 % H_3PO_4 (as the external standard).

Discussion and result analysis

Characterization of latex copolymers

Latexes were synthesized by the semi-continuous non-seeded emulsion polymerization process with varying amount and location of HACTP molecules in core-shell compositions. All the prepared self-crosslinking latexes (after ADH addition) were stable for over 12 months. MFFT values were shown not to be influenced by presence of HACTP in latex particles. All the synthesized self-crosslinking latexes exhibited low values of MFFT suggesting good application and film-forming properties. The prepared latex copolymers were studied from the point of view of glass transition temperature and gel content with respect to HACTP concentration and location inside the latex particles. T_g and gel content values were shown to be influenced markedly by the content of HACTP in latex particles. When comparing the results of the gel content for the emulsion copolymers before and after post-crosslinking using ADH, the ADH-crosslinked copolymers exhibited increased T_g and gel content values as a result of increasing the network density owing to keto-hydrazide crosslinking.

The presence of the copolymerized HACTP in the synthesized emulsion copolymers was tested using ^{31}P NMR. It was found that almost the identical ^{31}P NMR spectra were obtained in the case of gel fractions of the investigated emulsion copolymers; a singlet at a chemical shift δ (S) = 21.63 ppm occurred in the spectrum of the high-molar mass polymer fraction, which indicated the presence of HACTP molecules (Fig 2). Hence, it can be stated that HACTP was successfully incorporated into the macromolecular structure of acrylic polymers via the emulsion polymerization technique proceeding at standard conditions.

Fig. 2 – ^{31}P NMR spectrum for the gel fraction of the $C_{0.4}S_0$ copolymer containing theoretically 0.4 wt.% of HACTP in the core structure of latex particles

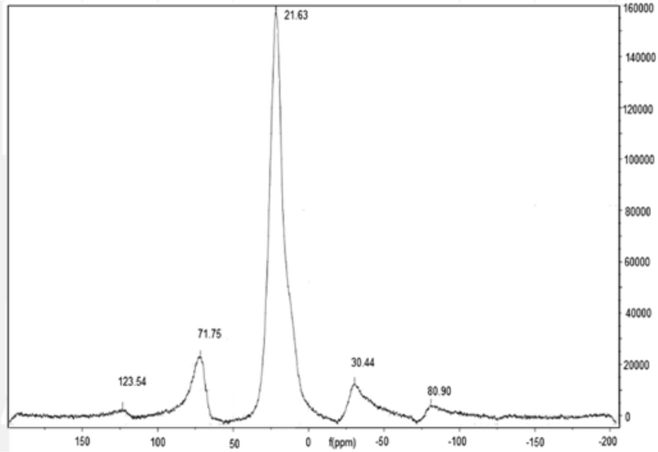

Characterizatition of latex coatings

As our system of interest was focused primarily on the evaluation of flame retardancy of the prepared phosphazene derivative in the resulting coatings, the effect of HACTP amount and location inside latex particles on combustion of coating films was studied in particular. The results obtained from measurements using dual cone calorimeter. The coating material containing HACTP (C_0-$S_{0.4}$) ignited later than the coating based on microgels without phosphazene derivative (C_0S_0). The other coatings containing the phosphazene derivative exhibited a similar behavior. The coatings comprising HACTP exhibited lower values of mean heat release rate, mean effective heat of combustion and total heat release. This phenomenon is more pronounced with increasing HACTP content, which indicates a slower flame spread due to incorporated HACTP. Decreased values of total smoke release during combustion of samples containing HACTP may reflect a more efficient oxidation of hydrocarbon chains in the presence of the phosphorus compound. It is assumed that the phosphorus atom reacts in the gas phase where the PO• radical is playing the main role. In the case of values of total oxygen consumed, no significant effect of HACTP presence was proved. Nevertheless, one of the most important criterions of the flammability evaluation is the maximum average rate of heat emission (MARHE) that decreased markedly by the growing content of HACTP in the tested coating materials. These results lead us to conclude that HACTP did act as a flame retardant in the investigated coating materials. The flame stability was influenced mainly by the HACTP content while the HACTP location inside emulsion microgels was not proved to be of great importance.

Conclusion

HACTP was successfully prepared by nucleophilic substitution of HCCTP with allyl amine using the one-step synthesis. The prepared phosphazene derivative was incorporated into the macromolecular structure of acrylic polymers via the emulsion polymerization technique proceeding at standard conditions, which was evidenced by ^{31}P NMR. During the emulsion polymerization of acrylic comonomers, HACTP performed the function of an efficient crosslinker leading to the formation of latex particles of microgel structure. In addition to that, the basic objective of this work was to evaluate the flame retardancy of the prepared phosphazene derivative in the keto-hydrazide self-crosslinking aqueous coatings based on the HACTP-modified emulsion microgels. The presence of HACTP was found to cause decreased amount of produced smoke and a slower flame spread during the material combustion without affecting transparency, flexibility and adhesive properties of resulting coatings. Moreover, water sensitivity of the coating films comprising the novel phosphazene derivative was decreased. Thus, it can be concluded that HACTP acted as a flame retardant and one-package thermosetting transparent coating systems with increased flame stability and enhanced water resistance were developed, having a potential application as primer as well as topcoats.

Acknowledgement

The Technological Agency of the Czech Republic (TA02000011) is gratefully acknowledged for supporting this work.

References

[1] Kessel N., Illsley D.R., Keddie J.L., *J. Coat. Technol. Res.* 5, 285 (2008)

[2] Zarybnicka L., Bacovska R., Vecera M., Snuparek J., Alberti M., Rychly J., Kalenda P., *J. Appl. Polym. Sci.*, 133, 42917 (2016).

[3] Allen C.W., *Chem. Rev.*, 91, 119 (1991).

[4] Machotová J., Šňupárek J., Prokůpek L., Rychlý T., Vlasák P., *Prog. Org. Coat.*, 63, 175 (2008).

SEZNAM ÚČASTNÍKŮ

LIST OF PARTICIPANTS

Platný k 8.11.2016 / Valid to 08/11/2016

Antoš	Vojtěch	Technická Univerzita v Liberci
Antoš	Petr	CHEMAGAZÍN / Technopark Kralupy, VŠCHT Praha
Antošová	Barbora	Unipetrol výzkumně vzdělávací centrum, a.s.
Bajer	Miroslav	Severochema, družstvo pro chemickou výrobu, Liberec
Bandžuch	Jan	SYNPO, a.s.
Bartošek	Ivo	Precheza a.s.
Baudys	Michal	Technopark Kralupy, VŠCHT Praha
Belavá	Adriana	Slovlak Košeca, a.s.
Bendáková	Nela	Synpo, akciová společnost
Beran	František	STACHEMA CZ s.r.o.
Bezkočka	Karel	Lučební závody a.s. Kolín
Blahušiaková	Alexandra	3U s. r. o.
Blažek	Petr	BlaVo Chemicals s.r.o.
Boháčik	Peter	Univerzita Pardubice, Fakulta chemicko-technologická
Borýsek	Petr	Synthesia, a.s.
Botlík	Robert	Polychem composite CS
Brož	Michal	STACHEMA CZ s.r.o.
Brůna	Petr	3P-Chem s.r.o.
Burešová	Blanka	SBLCore s. r. o.
Cagan	Peter	Pointner & Rothschädl Ges.m.b.H.
Canev	Michal	Omya s.r.o.
Cibulka	Ladislav	POLYMER COLOR, s.r.o.
Cornick	Marc	Vencorex
Čáp	Vladislav	BIOPOL paints s.r.o.
Černý	Michal	HET spol. s r. o.
Čihák	Martin	Radka s.r.o. Pardubice
Čvanda	David	STOMIX, spol. s r.o.
Dalecký	Jiří	Pragolab s.r.o.
Denk	Karel	Pragochema s.r.o.
Draganovská	Dagmar	Strojnícka fakulta, Technická univerzita v Košiciach
Drápela	Jiří	Viton s.r.o
Drdová-Škodová	Jana	HET spol. s r. o.
Dudák	Michal	ANAMET s.r.o.
Duroň	Jaroslav	Colorlak a.s.
Dušek	Michal	Safic-Alcan Česko, s.r.o.
Dvořák	Milan	Ravago Chemicals Czech Republic s.r.o.
Dygrýnová	Květa	STACHEMA CZ s.r.o.
Eichler	Jiří	HET spol. s r. o.
Emingerová	Radka	STACHEMA CZ s.r.o.
Fialová	Veronika	LAKOVNA HAJDÍK s.r.o.
Florián	Štěpán	Ústav polymérov SAV
Fojtík	Jaroslav	Detecha, chemické výrobní družstvo
Frošová	Dana	Radka s.r.o. Pardubice

Fryauf	Vladimír	Fryauf FilMix s.r.o.
Gergel	Peter	Lanxess Central Eastern Europe s.r.o.
Giba	Josef	Preciosa a.s.
Goebel	Adolf	Precheza a.s.
Gubová	Jarmila	KORA a.s.
Hajdík	Milan	LAKOVNA HAJDÍK s.r.o.
Hájková	Tereza	Univerzita Pardubice, Fakulta chemicko-technologická
Hájková	Mária	SYNPO, akciová společnost
Háková	Monika	Viton s.r.o
Hanka	Pavel	Radka s.r.o. Pardubice
Havránek	Jiří	Stachema CZ s.r.o.
Hlaváček	Petr	EURO-Šarm spol. s r.o.
Holas	Stanislav	BARVY A LAKY TELURIA s.r.o.
Holec	Petr	LAKOVNA HAJDÍK s.r.o.
Holeček	Jaroslav	Wacker-Chemie, s.r.o.
Hortenská	Martina	Synthesia, a.s.
Hozák	Kamil	CHEMAP, spol. s r.o.
Hrdina	Radim	Univerzita Pardubice, Fakulta chemicko-technologická
Hrubý	Martin	HSH-Chemie spol. s r.o.
Hynčica	Pavel	LAKOVNA HAJDÍK s.r.o.
Chlostová	Lenka	Synthesia, a.s.
Chvojka	René	JO&JO Kolín s.r.o.
Izák	Jan	Synthesia, a.s.
Jakeš	Petr	Momentive Performance Materials
Janda	Pavel	Ace Trade, s.r.o.
Janhuba	Filip	Urdiamant, s.r.o.
Javoreková	Daniela	CHEMOLAK a.s.
Jehlářová	Eva	Precheza a.s.
Jelínek	Bohdan	KORA a.s.
Kalendová	Andréa	Univerzita Pardubice, Fakulta chemicko-technologická
Kantorová	Marika	Synthesia, a.s.
Kavečanský	Ľubor	Slovlak Košeca, a.s.
Kavka	Arnošt	Profilabor s.r.o.
Kluz	Daniel	ZVU Strojírny a.s.
Kohl	Miroslav	Univerzita Pardubice, Fakulta chemicko-technologická
Kolářová	Eva	
Konvička	Zdeněk	Precheza a.s.
Košíková	Helena	Brenntag Slovakia s.r.o.
Košová	Martina	STACHEMA CZ s.r.o.
Kozinová	Lenka	STACHEMA CZ s.r.o
Krejčíková	Štěpánka	Radka s.r.o. Pardubice
Křivánek	Jiří	THORSON CHEMICAL Praha, s.r.o.
Křižan	Martin	Lučební závody a.s. Kolín
Kubíček	Petr	BIOPOL paints s.r.o.
Kubiňák	Rastislav	Azelis Slovakia, s.r.o.
Kumm	Rotraut	Grolman s.r.o.
Kusyn	Daniel	Radka s.r.o. Pardubice
Kutlík	Jozef	Radka s.r.o. Pardubice

Kysučan	Petr	Ravago Chemicals Czech Republic s.r.o.
Lejdar	Erhard	Preciosa a.s.
Lipiec	Leszek	Wacker Chemia Polska Sp. z o.o.
Loučka	Pavel	Radka Pardubice a.s.
Machačka	Vladislav	Preciosa a.s.
Machotová	Jana	Univerzita Pardubice, Fakulta chemicko-technologická
Mareček	Petr	LANIK s.r.o.
Martínek	Josef	Azelis Czech Republic s.r.o.
Miksa	Daniel	Habich Pigments GmbH
Mikula	Radek	LAKOVNA HAJDÍK s.r.o.
Milič	Richard	SYNPO, a.s.
Mindoš	Lubomír	SVÚOM s.r.o.
Mlateček	Martin	Synthesia, a.s.
Motyčka	Aleš	Ace Trade, s.r.o.
Mudroňová	Kateřina	Nicolet CZ s.r.o.
Nechvílová	Kateřina	Univerzita Pardubice, Fakulta chemicko-technologická
Nejezchlebová	Ladislava	Azelis Czech Republic s.r.o
Němcová	Dana	STACHEMA CZ s.r.o
Némethová	Viera	CHEMOLAK a.s.
Nováček	Michal	Viton s.r.o
Novák	Jiří	Detecha, chemické výrobní družstvo
Novák	Petr	Biesterfeld Silcom
Novák	Igor	Ústav polymérov SAV
Novotný	Petr	JO&JO Kolín s.r.o.
Otáhal	Roman	Brenntag CR s.r.o.
Pallich	Martin	Brenntag CR s.r.o.
Paška	Pavel	BKP Group a.s.
Patrovský	Josef	KORA a.s.
Perdoch	Jakub	LAKOVNA HAJDÍK s.r.o.
Peterková	Viktorie	Preciosa a.s.
Pikal	Petr	Precheza a.s.
Pinková	Blanka	Precheza a.s.
Plášek	Petr	IMCD Czech Republic s.r.o.
Pokorný	Jiří	Technopark Kralupy, VŠCHT Praha
Poledno	Michal	Nordmann, Rassmann Czech Republic s.r.o.
Pospíšilová	Michaela	Gamin s.r.o.
Pražák	Milan	Labimex CZ s.r.o.
Procházka	Jan	Advanced Materials - JTJ s.r.o.
Prokop	Jakub	Polz Instruments s.r.o.
Průcha	Zbyněk	HSH-Chemie spol. s r.o.
Přikryl	Jan	Precheza a.s.
Přikrylová	Romana	UNIPETROL RPA s.r.o. - POLYMER INSTITUTE BRNO
Putna	Pavel	LB Cemix, s.r.o.
Rády	Andrej	COLOR Company s.r.o.
Resch	Petr	Fryauf FilMix s.r.o.
Rot	Jan	MB Sving s.r.o.
Rozhon	Martin	AUSTIS výroba s.r.o.
Rückerová	Adéla	Univerzita Pardubice, Fakulta chemicko-technologická

Rybová	Anna	Azelis Czech Republic s.r.o
Sedlář	Jiří	Colorlak a.s.
Schoalert	Thomas	UMICORE Bruggy
Sibilak	Dawid	Dow Poland Sp. z o.o.
Slapnička	David	Estrella Es-Press spol. s r.o.
Sliž	Jaroslav	Lankwitzer CR, Spol. s.r.o.
Sokola	Lubomír	STOMIX, spol. s r.o.
Souček	Martin	Bochemie a.s.
Suč	Jiří	Urdiamant, s.r.o.
Suda	Eduard	MANEKO, spol. s r.o.
Sznapka	Partik	BASF
Šec	Karel	Nicolet CZ s.r.o.
Šefl	Pavel	Advanced Materials - JTJ s.r.o.
Šindelář	Jan	European Coatings Laboratory, spol. s r.o.
Škrabana	Michal	Colorlak a.s.
Šmejkalová	Darina	SBLCore s. r. o.
Šmitberský	Jiří	POLYMER COLOR, s.r.o.
Šostý	Radomír	BARVY A LAKY TELURIA s.r.o.
Šrubař	Radim	EURO-Šarm spol. s r.o.
Švrček	Jiří	Bochemie a.s.
Tomanicová	Darina	Slovlak Košeca, a.s.
Torma	Petr	3P-Chem s.r.o.
Tůma	Zdeněk	COLORLAK, a.s.
Urban	Christian	3U s. r. o.
Valášek	Pavel	Precheza a.s.
Válek	Jaroslav	Severochema, družstvo pro chemickou výrobu, Liberec
Válek	Lukáš	ANAMET s.r.o.
Vařeková	Irena	UNIPETROL RPA s.r.o. - POLYMER INSTITUTE BRNO
Vavřík	Tomáš	Colorlak a.s.
Večeřa	Jan	Precheza a.s.
Veselý	Pavel	Lučební závody a.s. Kolín
Vidláková	Kateřina	Precheza a.s.
Vichta	Zbyšek	LABtechnik s.r.o.
Vlasáková	Jarmila	Synpo, a.s.
Volfová	Petra	Pragolab s.r.o.
Vorlovský	František	Krkonošské vápenky Kunčice, a.s.
Vraštilová	Andrea	Synpo, a.s.
Vrba	Pavel	Estrella Es-Press spol. s r.o.
Vykypělová	Alice	Synthesia, a.s.
Výmolová	Petra	Moravia Cans a.s.
Výmolová	Eliška	BKP Group a.s.
Widzisz	Richard	Azelis Czech Republic s.r.o
Zdráhala	Ondřej	Profilabor s.r.o.
Zouhar	David	Grolman s.r.o.
Zsigo	Martin	Brenntag Slovakia s.r.o.
Žouželka	Radek	Advanced Materials - JTJ s.r.o./ ÚFCH J. Heyrovského AV ČR

Ravago Chemicals

Founded in 2012, initially as a joint-venture, to bundle 60 years of expertise and to distribute speciality chemicals for major suppliers across EMEA.

With offices and warehouses in most of the European countries, Turkey, Dubai and Africa, Ravago Chemicals established a commercial network with local presence to serve its customers and suppliers in the best possible way. We offer a comprehensive product portfolio of speciality additives and chemical materials.

COATINGS & CONSTRUCTION	PERFORMANCE CHEMICALS	PU & POLYMERS	LIFE SCIENCE
Construction & civil engineering	Care Chemicals Personal, Home & Industrial	Polymer manufacturing & processing	Food
Coatings & inks	Chemical specialities	PU components flex & rigid	Feed
Adhesives & sealants	Paper & cardboard		Pharma
	Water treatment		

Asociace výrobců nátěrových hmot České republiky

Association of Paint Manufacturers of the Czech Republic

AVNH ČR byla založena v roce 1994 jako dobrovolné profesní sdružení výrobců, výzkumných ústavů, distributorů nátěrových hmot a surovin pro jejich výrobu. Na základě stanov nabízí všem členům možnost využít široké nabídky spolupráce v hájení jejich specifických společných a individuálních zájmů pokud nejsou v rozporu se společnými zájmy Asociace.

AVNH ČR je od r. 1995 kolektivním členem Svazu chemického průmyslu ČR.

Řádnými členy Asociace je celkem 16 firem, z toho 12 výrobců a dodavatelů nátěrových hmot, 1 výzkumná společnost, 3 dodavatelé surovin, resp. obalů. Přidruženými členy jsou 1 vydavatel odborného časopisu, 2 chemické univerzity, 1 ústav chemické univerzity, Cech malířů a tapetářů a 2 asociace z příbuzných oborů.

Členská základna představuje cca 70%ní podíl na trhu nátěrových hmot vyrobených v České republice a cca 30%ní podíl na celkově prodaných NH v ČR včetně dovozu.

Sídlo

Učňovská 1 **,190 00 Praha 9**

www.avnh.cz

mail: avnh@avnh.cz

tel: 266 106 421

IČO: 60459727

Řádní členové

ARDAGH METAL PACKAGING CZECH a.s.

AUSTIS, a.s.

BARVY A LAKY HOSTIVAŘ, a.s.

BARVY A LAKY TELURIA, s.r.o.

BUILDING PLAST, s.r.o.

COLORLAK, a.s.

DCH SINCOLOR, s.r.o.

DRUCHEMA, družstvo pro chemickou výrobu a služby

HEXION a.s.

KM PLUS spol. s r.o.

MANKIEWICZ PRŮMYSLOVÉ BARVY A LAKY, **k.s.**

NÁTĚROVÉ HMOTY, s.r.o.

PPG DECO CZECH a.s.

PRECHEZA a.s.

SEVEROCHEMA, družstvo pro chemickou výrobu

SYNPO, a.s.

Aeration

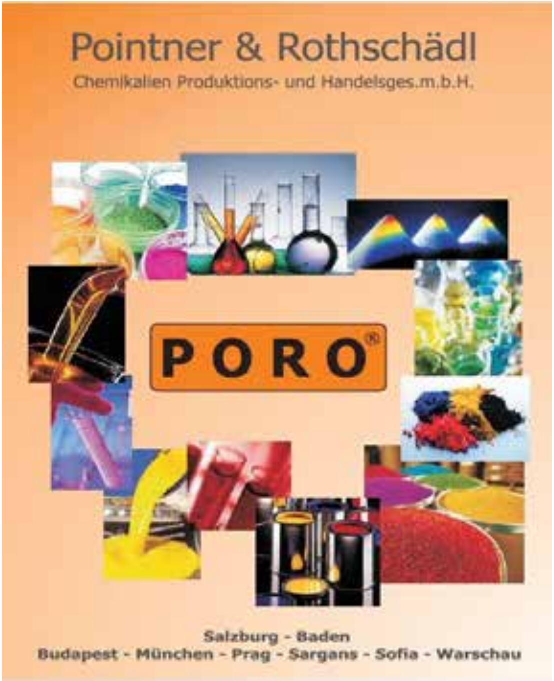

Pointner & Rothschädl

Chemikalien Produktions- und Handelsges.m.b.H.

PORO®

Salzburg - Baden

Budapest - München - Prag - Sargans - Sofia - Warschau

KONTAKT:

- PETER CAGAN

Office: 2500 Baden / Wienerstrasse 89

☎: +43 (0)664-4340265
☎: +43 (0)2252-82870-14

✉: Peter.Cagan@poro.eu

- ELISABETH O’CONNOR

Office: 5020 Salzburg / Münchner Bundestrasse 121

☎: +43 (0)662-431 541-119
☎: +43 (0)662-431541-20

✉: elisabeth.oconnor@poro.eu

SYSTÉMY PRO KONTINUÁLNÍ MĚŘENÍ PROCESNÍCH VELIČIN

KONTAKTNÍ A BEZKONTAKTNÍ MIKROVLNNÉ MĚŘENÍ VLHKOSTI

Harrer&Kassen
Široké použití ve dvousložkových systémech, z nichž jedním je voda. Vlhkost, Koncentrace, Sušina, Hustota, Konzistence, TS.

M-Sens2
Pro kontinuální měření vlhkosti-šnekové dopravníky.

BEZKONTAKTNÍ ON-LINE MĚŘENÍ NIR

Harrer&Kassen
NIR spektrofotometr pro přesné měření obsahu vody, bílkovin, tuků a dalších organických látek. Možné detekovat až čtyři látky najednou.

URČENÍ PRŮTOKU SYPKÝCH MATERIÁLŮ

SolidFlow, MaxxFlow, DensFlow, SlideControl
Měření průtoku tuhých hmot dopravovaných v kovových potrubích.

MĚŘENÍ RYCHLOSTI PEVNÝCH ČÁSTIC V POTRUBÍ

SpeedFlow
Kontinuální měření rychlosti pevných částic.

DETEKCE PRACHU

ProSens, Dusty
Použitelný ve všech kovových potrubích. Detekce protržených filtračních vaků, měření koncentrace prášků v plynu.

DETEKCE POHYBU MATERIÁLU V POTRUBÍ

FlowJam
Bezdotykový systém detekuje pohyb pevných materiálů v potrubí.

MĚŘÍCÍ SKENOVACÍ RÁMY VYUŽÍVAJÍCÍ RADIAČNÍ, LASEROVÁ A OPTICKÁ ČIDLA

ProControl
Systémy schopné měřit plošnou hmotnost, tloušťku, pórovitost, vlhkost, detekovat otvory v materiálech.

DETEKCE VAD A NEČISTOT MATERIÁLU PLOŠNÝCH MATERIÁLŮ

Dr.Schenk
Kamerový systém na detekci optických vad a nečistot materiálu.

DETEKCE VAD A NEČISTOT MATERIÁLU

OCS
Kamerové systémy na sledování příměsí, vad a nečistot materiálu.

MĚŘENÍ RYCHLOSTI, DÉLKY, PRŮTAHU

Elovis
Bezkontaktní laserové či mechanické měření rychlosti, délky a průtahu na principu Dopplerova jevu.

BEZKONTAKTNÍ MĚŘENÍ TLOUŠŤKY PRŮSVITNÝCH MATERIÁLŮ

Lumetrics
Rychlé a přesné měření tloušťky průsvitných materiálů (fólie, sklo, trubičky, hadičky). Určení tloušťky jednotlivých vrstev materiálu.

Fuchs
Měření tloušťky průsvitných materiálů.

OBJEKTIVNÍ MĚŘENÍ BAREVNOSTI

Hunterlab
Bezkontaktní měření barevnosti materiálu pevných látek i kapalin, laboratorní i on-line. Měření remisní a transmisní.

SPEKTRORADIOMETRY, MĚŘENÍ RETROREFLEXE

Photoresearch
Spektroradiometry, fotometry a video fotometry.

LMT
vysoce přesné fotometry, kolorimetry a goniometry.

KONTROLA VLASTNOSTÍ NÁTĚROVÝCH HMOT

Zehntner TI
Mnoho zajímavých přístrojů a nástrojů pro kontrolu mechanických vlastností nátěrových hmot. Leskoměry, grindometry, nanášecí pravítka, tloušťkoměry, retroreflektometry.

DETEKCE ÚROVNĚ HLADINY V NÁSYPKÁCH

ProGap
Snímač flexibilně použitelný jako bodový spínač úrovně hladiny materiálu. Skládá se z vysílače a přijímače na bázi mikrovlnné technologie.

IZOTOPICKÉ MĚŘENÍ ÚROVNĚ HLADINY A HUSTOTY

RGI
Systémy využívající radiačních vlastností Cs a Kr ke zjišťování úrovně hladiny a hustoty v nepřístupných ocelových nádržích nebo v potrubích.

MĚŘENÍ OBJEMOVÉ HMOTNOSTI SYPKÝCH MATERIÁLŮ

Dens M
Kontinuální určení objemové hmotnosti prášku nebo granulí.

ZJIŠŤOVÁNÍ CHEMICKÉ A MECHANICKÉ ČISTOTY VODY

Process Instruments - kontinuální měření a analýza vody
Analýza volného chlóru, monitorování celkového chlóru, analýza chlordioxidu, monitorování ozónu, měření rozpuštěného kyslíku, monitorování nerozpuštěných látek, měření zákalu, analýza pH, analýza ORP, řízení dávkování polymeru, monitorování biofilmu, online vodivost, měření počtu částic, monitorování filtru, monitorování usazenin.

PRŮTOKOMĚRY, MĚŘENÍ ÚROVNĚ HLADINY

BM
Radarové a ultrazvukové měření výšky hladiny kapalin v nádržích a pevných látek v silech. Příložné ultrazvukové průtokoměry.

Goerlich
Magnetickoindukční průtokoměry do potrubí, žlabů a kanálů.

DETEKCE KOVŮ

Fortress Technology
Detektory železných, neželezných a nerezových kovů a nečistot.

PROPUSTNOST MATERIÁLŮ

Mocon
Propustnost materiálů vodní páry, CO_2.

SpeedMixer™
GermanEngineering
by Hauschild

Made for mixing.

Rychle I Efektivně I Bez bublin

- Obarvení vysoce viskózního silikonu
  za 30 sekund / 100% homogenní
- Vysoká všestrannost, od výroby laků až po výrobu lepidel
- Míchání v uzavřeném systému:
  – rychlé, vysoce efektivní, bez bublin a prachu
  – bez nutnosti čištění
  – vysoce bezpečné, nehrozí žádné nebezpečí zranění
- Enormní výhody z hlediska kontroly kvality:
  – velmi vysoká reprodukovatelnost
  – šetří čas a náklady

Hauschild
Engineering

SpeedMixer v České a Slovenské Republice:
Mgr. Ondřej Zdráhala · Výhradní zastoupení SpeedMixer™ pro ČR a SR
Tel. CZ: +420 604 614913 · E-mail info@speedmixer.cz · www.speedmixer.cz
Hauschild Co. KG · Waterkamp 1 · 59075 Hamm/Germany · Tel. DE: +49 1577 6005050




SBLCore®
by GRACILIS

www.sblcore.cz

SOFTWARE PRO TVORBU BEZPEČNOSTNÍCH LISTŮ

VÝRAZNÁ ÚSPORA ČASU

DOKONALÝ PŘEHLED

LEGISLATIVNÍ JISTOTA

ŠKOLENÍ A PODPORA

Software SBLCore je určen ke **zpracování, evidenci, revizím a tisku bezpečnostních listů a etiket**. Je **velmi vhodným nástrojem pro firmy**, díky kterému je správa a tvorba těchto dokumentů **výrazně rychlejší a eliminuje se chybovost**.

Velice významnou funkcí je **automatická klasifikace směsi**. Na základě procentuálního zastoupení jednotlivých látek ve směsi a jejich toxikologických a ekotoxikologických informací program vypočítá výslednou klasifikaci směsi a výpočet zobrazí v klasifikační rozvaze.

Řada povinných informací podle platných právních předpisů je v softwaru SBLCore již předdefinována a generuje se automaticky výběrem z databází, které jsou přímo součástí softwaru.

Díky intuitivnímu ovládání a **vstupnímu školení** zvládnou práci se softwarem ve velmi krátkém čase nejen zkušení specialisté, ale i proškolený personál.

Hlavní funkce programu:

- Vytváření bezpečnostních listů
- Automatická klasifikace
- Klasifikační rozvaha
- Předdefinované texty
- Návrhy a tisk etiket
- Export dokumentů do PDF, Wordu a dalších formátů
- Databáze závazně klasifikovaných chemických látek
- Hromadný export bezpečnostních listů do systému CHLaP
- Tvorba datových listů k detergentům
- Archivace

V softwaru SBLCore je možné vytvářet bezpečnostní listy také v dalších jazycích. Seznam aktuálně dostupných jazyků najdete na **www.sblcore.cz**

✉ sblcore@sblcore.cz ☎ +420 702 170 168

Dry Fine Grinding

NETZSCH High-Density Bed Jet Mill ConJet®

- Spiral jet mill with patented dynamic air classifier for exact limitation of the particle range, free of oversized product
- Product fineness is independent of the load of the gas flow which increases the efficiency and economy of the mill
- Different executions available depending on the product requirements, e.g. stainless steel or wear-protected
- Compact construction enables a rapid and complete cleaning of the machine

NETZSCH

www.netzsch.com/gd

3P-CHEM s.r.o.
Areál Správa a údržba komunikací
P.O. BOX 31
267 01 Králův Dvůr - Popovice

tel.: +420 311 638 028 - 029
fax: +420 311 637 132
e-mail: 3p-chem@3p-chem.cz

Váš spolehlivý partner v oblasti dodávek chemických specialit pro výrobu nátěrových hmot, výrobu tmelů, lepidel a plastikářský průmysl.
Vše důležité najdete na:

www.3p-chem.cz

Firma 3P-CHEM s.r.o. byla založena v roce 2004. Od začátku existence se firma zaměřuje na prodej a distribuci surovin pro zpracovatelský průmysl. Nedílnou součástí naší firmy je nabídka technických obalů (kovové, plastové a skleněné obaly). Hlavními obchodními partnery a dodavateli surovin jsou přední evropští výrobci z Německa, Francie, Španělska, Belgie, Rakouska, Itálie, Chorvatska, Maďarska a dalších evropských zemí .

Naše nabídka surovin se zaměřuje hlavně na výrobce nátěrových hmot a lepidel, výrobce stavební chemie a plastikářský průmysl.

Struktura sortimentu nabízených surovin:

Pojiva – rozpouštědlové, vodouředitelné – kompletní sortiment: alkydy, akryláty, disperze, emulze, epoxidy a speciální pojiva • Pigmenty – práškové, metalitické pigmenty, saze • Plniva – vápence, talky, baryty, slídy, břidlice, mica • Additiva – dispergační prostředky, odpěňovače, rozlivová činidla, inhibitory koroze, akrylátové záhustky • Sušidla – do rozpouštědlových a vodouředitelných systémů • Matovací a zahušťovací prostředky prostředky na bázi oxidu křemičitého • Vosky – práškové typy, voskové emulze a disperze • Vzorkovnice – RAL systémy

Struktura sortimentu technických obalů:

Kovové obaly – lakovky, kovové láhve, kanystry, vědra, hoboky a sudy • Plastové obaly – kanystry, soudky, dózy • Skleněné obaly – lékovky, lahve pro potravinářský průmysl

Pro více informací prosím pište na:
bruna@3p-chem.cz, torma@3p-chem.cz, sidlo@3p-chem.cz

Více na našich internetových stránkách WWW.3P-CHEM.CZ

CHEMAGAZÍN

ČASOPIS PRO CHEMICKO-TECHNOLOGICKOU
A LABORATORNÍ PRAXI

AKTUÁLNÍ INFORMACE Z CHEMICKÉHO PRŮMYSLU A LABORATORNÍ PRAXE – WWW.CHEMAGAZIN.CZ

CHEMAGAZÍN 4

ROČNÍK XXVI (2016)

TÉMA VYDÁNÍ: PEVNÉ LÁTKY

Základní koncepty **charakterizace částic**

Chemické a fyzikální faktory ovlivňující **přípravu vzorků pro granulometrii**

Recyklace použitých baterií

Odstraňování platinových kovů **z monolitních katalyzátorů**

Nové senzorové technologie ze silikonové fólie

Kontrola povrchů digitálním mikroskopem Leica

Rychlost skluzu sypké látky v rotační peci

Chemický průmysl ČR v roce 2015

MERCI laboratoř jak má být

Laboratorní nábytek a digestoře MERCI®

Vaše laboratoř dle evropského standardu

www.merci.cz

ZASÍLANÝ **ZDARMA** V ČR A SR

VÍCE NEŽ **4 000 ČTENÁŘŮ**

ON-LINE VERZE NA INTERNETU

WWW.CHEMAGAZIN.CZ

Sborník/Conference proceedings

IX. KONFERENCE PIGMENTY A POJIVA
9TH CONFERENCE ON PIGMENTS AND BINDERS

Vydavatel/Editor:

CHEMAGAZÍN s.r.o.
Gorkého 2573, 530 02 Pardubice, Česká republika
IČO: 28785886

Vydání/Issue:

I.

Vydáno/Published:

11/2016

Tisk/Print:

Tiskárna Rentis s.r.o., Pardubice

ISBN 978-80-906269-1-1

ISBN 978-80-906269-1-1